Changes in nuclear structure during wheat endosperm development

Promotor:
Prof. Dr. Ir. M. Koornneef, Persoonlijk Hoogleraar bij het Laboratorium voor Genetica

Co-promotoren:
Dr. J.H. de Jong – Universitair hoofddocent, Laboratorium voor Genetica
Prof. Peter J. Shaw – Associate Head of the Department of Cell and Developmental Biology, John Innes Centre, Norwich

Promotiecommissie:
Prof. Dr. Ir. E. Jacobsen –Wageningen Universiteit
Prof.dr. W.J. Stiekema – Wageningen Universiteit
Dr. P.F. Fransz – Universiteit van Amsterdam
Dr. R. Dirks – Rijk Zwaan Breeding Company, Fijnaart

Eva Wegel

Changes in nuclear structure during wheat endosperm development

Proefschrift
ter verkrijging von de graad van doctor
op gezag van de rector magnificus
van Wageningen Universiteit,
Prof. Dr . M. J. Kropff,
in het openbaar te verdedigen
op dinsdag 6 december 2005
des namiddags te vier uur in de Aula.

Eva Wegel (2005)

Changes in nuclear structure during wheat endosperm development

Thesis Wageningen University – with references – with summaries in Dutch and English

ISBN 90-8504-300-X

Was lange währt, wird endlich gut.

Contents

Chapter 1
GENERAL INTRODUCTION

The origin and commercial importance of wheat

Hexaploid wheat (*Triticum aestivum*, genus *Poaceae*) originates from a corridor extending from Armenia in Transcaucasia to the southwest coastal areas of the Caspian Sea in Iran (Gill and Friebe, 2002). Its three genomes A, B and D are derived from three progenitor species, *Triticum urartu*, *Aegilops speltoides* and *Aegilops tauschii* (Gill and Friebe, 2002). Each haploid chromosome set of the progenitors contributed seven chromosomes and hexaploid wheat therefore contains forty-two chromosomes.

More wheat is produced in the world than any other crop (Curtis, 2002). Wheat is the most important food grain source for humans and is mainly used for bread-making. Bread-making quality depends largely on the viscoelastic properties of the dough, which in turn are determined by glutens, structural proteins present in wheat endosperm, which form a mesh-like polymer that allows dough to trap bubbles of carbon dioxide during fermentation. A major factor in bread quality are the high molecular weight (HMW) subunits of the glutenins, which account for up to 12% of the total grain protein content (for a review see Shewry et al., 2003). HMW glutenin genes are located on the long arms of chromosomes 1A, 1B and 1D. Each locus contains two genes. One of the six genes is always silenced and cultivated wheat expresses three to five genes depending on the variety (Shewry et al., 2003). At present 27 HMW subunit homologues are known, which have different effects on overall baking quality and the numbers are still rising (Shewry et al., 2003). HMW glutenin genes have been transformed into wheat varieties in order to improve baking quality but transgenic varieties are not commercially used at present.

Post-transcriptional and transcriptional gene silencing

In some cases, the introduction of transgenes leads to silencing of the transgenes themselves and of homologous endogenous genes. The introduction of transgenes can cause two types of silencing: transcriptional gene silencing (TGS) and post-transcriptional gene silencing (PTGS) also known as RNA interference (RNAi). TGS usually occurs via cytosine methylation of promoter sequences, which causes transcription to cease. PTGS is characterized by ongoing transcription, subsequent transcript degradation, and the appearance of small interfering RNAs (siRNAs) of 21–25 bp lengths (Hamilton and Baulcombe, 1999; Zamore et al., 2000), which are produced by a double-stranded RNA-specific endonuclease (Dicer) that was first detected in *Drosophila* (Bernstein et al., 2001). PTGS can be caused by highly transcribed transgenes, which are the template for an RNA-dependent RNA polymerase, or by an inverted transgene repeat, in both cases leading to the production of a double-stranded transcript that is the substrate for Dicer and

causes silencing (Béclin et al., 2002; Fagard and Vaucheret, 2000; Ketting et al., 2001) To complicate matters siRNAs can also guide heterochromatin formation and thus cause transcription to cease (resulting in TGS) through RNA-directed methylation of homologous DNA and through methylation of histone H3 at lysine 9 (Finnegan and Matzke, 2003; Matzke et al., 2001; Schramke and Allshire, 2003). It is hypothesised that these epigenetic marks are established through recognition of an RNA-DNA hybrid by the DNA methylation machinery followed by recruitment of chromatin-modifiying enzymes to establish a repressive chromatin structure (Matzke et al., 2004).

Development of wheat endosperm

The endosperm of wheat originates from the fusion of the two haploid polar nuclei of the central cell in the embryo sac with one haploid sperm nucleus. The other sperm nucleus fertilises the egg cell to form the zygote. Subsequent divisions lead to the formation of the embryo and the suspensor. The first division of the triploid primary endoperm nucleus occurs ca. 5 hours after pollination (Bennett et al., 1973). From then on synchronous nuclear divisions without the formation of cell walls lead to a syncytium lining the walls of the central (Bennett et al., 1973; Brenchley, 1909; Huber and Grabe, 1987a; Mares et al., 1975; Percival, 1921). Wheat therefore follows the so-called nuclear type of endosperm development, which is characterised by a limited or permanent phase of free-nuclear division and is found in cereals and Arabidopsis (Olsen, 2004; Olsen et al., 1992), as well in other plants. For the bulk of wheat endosperm cell wall formation starts from the periphery at day four after pollination via the formation of open-ended alveoli, which grow towards the centre of the endosperm, and is completed by day seven (van Lammeren, 1988). Around the time when cellularisation is complete at 7 to 8 days post anthesis (dpa) HMW glutenin transcription starts in the endosperm. Cell divisions in the endosperm of wheat continue until 12-14 days post anthesis (dpa) (Huber and Grabe, 1987b). Some nuclei in the central starchy endosperm undergo

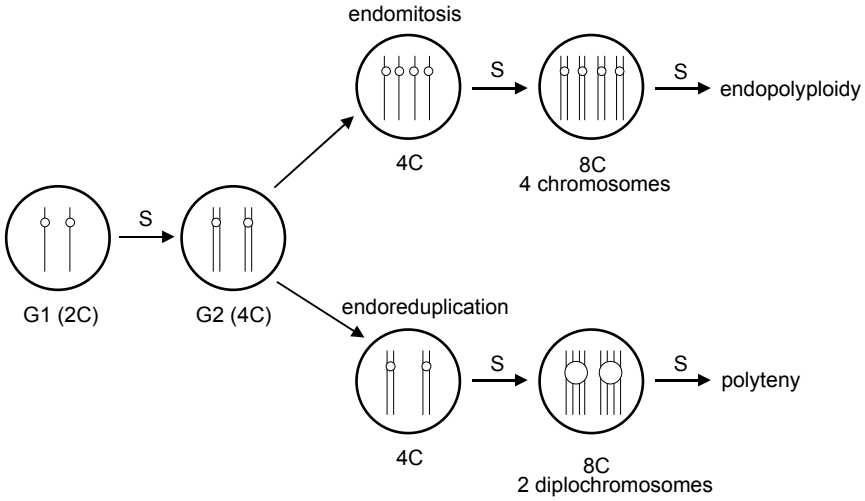

Figure 1. Endomitosis and endoreduplication (after D'Amato, 1984)

two or three rounds of DNA replication taking the DNA content up to 12C or 24C (Brunori et al., 1989). An increase in DNA content outside the mitotic cycle can lead to polyteny (through endoreduplication, where the number of chromosomes remains constant while the number of chromatids increases) or polyploidy (an increase in number of chromosome sets) or both.

Scope and outline of this thesis

This thesis analyses the structure of wheat endosperm nuclei at different levels. Chapter 2 introduces the subject with a general overview of chromatin structure in the nucleus. In chapter 3 we describe a method for modelling nuclear distribution during early endosperm development and for modelling changes within endosperm nuclei during polyploidisation. At the level of the whole endosperm we show that syncytium formation starts generally with a dorsal plate of nuclei which is connected to the zygote. This is followed or in some cases preceded by the formation of a ventral plate either side of the antipodals. By 2 dpa further synchronous divisions connect the plates to form a complete syncytium by 4 dpa, where no nuclear divisions are visible. At the nuclear level we show that with increasing C content, nuclei become disc-shaped. In the majority of 3C and 6C nuclei and in all 12C nuclei, centromeres and telomeres are located on opposite, flat sides. Chromosomes are aligned in a Rabl configuration in 3C nuclei and are positioned more randomly in nuclei of higher ploidy. In chaper 4 we investigate non-homologous centromere and telomere associations through the developmental increases in ploidy. We show that these increases in ploidy occur both through polyploidisation and polytenisation.

Chapter 5 investigates how three-dimensional chromatin structure is altered through transcription. These changes are more easily observed in multi-copy transgene loci and before this project started it had been shown in mammalian systems that complex transgene loci decondense when they become transcriptionally active but no studies had been carried out on plants. We therefore decided to analyse transgene loci in wheat. The two lines we chose contain HMW glutenin subunits under the control of their own promoters and are developmentally activated during endosperm development. In the analysed lines the HMW glutenin genes were also subject to partial silencing. We show that in non-expressing tissue each transgene locus consists of one or two highly condensed sites, which decondense into many foci upon activation of transcription. Detailed analysis of one of the lines reveals that the start of transcription precedes decondensation and the loci remain decondensed and transcriptionally active until cell death. Cytoplasmic transcript levels are high after onset of transcription, but disappear by 14 dpa, while siRNAs, indicative of post-transcriptional gene silencing (PTGS), are detected at this stage. Finally chapter 6 discusses the special characteristics of endosperm nuclei.

Chapter 2
GENERAL OVERVIEW

Gene activation and deactivation related changes in the three-dimensional structure of chromatin

Eva Wegel [a,b] and Peter Shaw [b]

[a] The Sainsbury Laboratory, John Innes Centre, Norwich Research Park, Colney Lane, Norwich NR4 7UH, UK
[b] Department of Cell and Developmental Biology, John Innes Centre, Norwich Research Park, Colney Lane, Norwich NR4 7UH, UK

Published in Chromosoma (2005) Aug 2, 1-7

Abstract
Chromatin in the interphase nucleus is dynamic, decondensing where genes are activated and condensing where they are silenced. Local chromatin remodelling to a more open structure during gene activation is followed by changes in nucleosome distribution through the action of the transcriptional machinery. This leads to chromatin expansion and looping out of whole genomic regions. Such chromatin loops can extend beyond the chromosome territory. As several studies point to the location of transcription sites inside chromosome territories as well as at their periphery, extra-territorial loops cannot simply be a mechanism for making transcribed genes accessible to the transcriptional machinery and must occur for other reasons. The level of decondensation within an activated region varies greatly and probably depends on the density of activated genes and the number of engaged RNA polymerases. Genes that are silenced during development form a more closed chromatin structure. Specific histone modifications are correlated with gene activation and silencing and silenced genes may become associated with heterochromatin protein 1 homologues or with Polycomb group complexes. Several levels of chromatin packaging are found in the nucleus relating to the different functions of and performed by active genes, euchromatic and heterochromatic regions and the models explaining higher order chromatin structure are still disputed.

Unravelling higher-order chromatin structure

In eukaryotes, DNA is complexed with histones. 146 bp of DNA are wound in 1.75 turns around an octamer of the core histones H2A, H2B, H3 and H4 in the nucleosome core particle. The interaction of a linker histone (H1) with the DNA between two core nucleosomes (linker DNA) increases the number of base pairs to 165 corresponding to two turns (Bednar et al., 1998). The addition of linker histone therefore contributes to chromatin condensation (Horn and Peterson, 2002). Short linker DNA also contributes to DNA compaction, while longer linker DNA has the opposite effect. Thus, the primary level of chromatin structure is represented by the 10 nm chromatin fibre or beads-on-a-string conformation of extended arrays of

nucleosomes (Woodcock and Dimitrov, 2001) (Fig. 1). Naked B-DNA has a length of 2.9 Kb μm^{-1} and becomes about seven-fold compacted in a 10-nm fibre (Goodrich and Tweedie, 2002; Watson and Crick, 1953). Secondary chromatin structure is formed by nucleosome interactions, the most prominent of which is a 30-nm diameter fibre with a compaction of forty to fifty fold (Woodcock and Dimitrov, 2001). The 30-nm fibre is thought to consist of a nucleosome helix, but its exact structure is still being debated (Dorigo et al., 2004). Still higher levels of chromatin structure are formed by long-range interactions between 30-nm fibres. A classical model of such higher order structure is the chromonema fibre in which thinner fibres are folded to yield thicker ones with a diameter of 100 to 130 nm and ca. 500 fold compaction (Belmont and Bruce, 1994). Other models propose radial 30-nm-fibre loops of various lengths connected to a central protein scaffold (Cremer and Cremer, 2001). The nucleosome affinity, random chain model dispenses with 30-nm fibres altogether and assumes random chains of nucleosomes exploring a given space (Müller et al., 2004). None of these models have been proven yet and all are consistent with the observation that decondensed chromatin forms a series of adjacent beads, and that active transcription is required for the maintenance of decondensed chromatin, an observation that has been made repeatedly in different organisms (Müller et al., 2004; Müller et al., 2001; Tsukamoto et al., 2000; Wegel et al., 2005, see chapter 5).

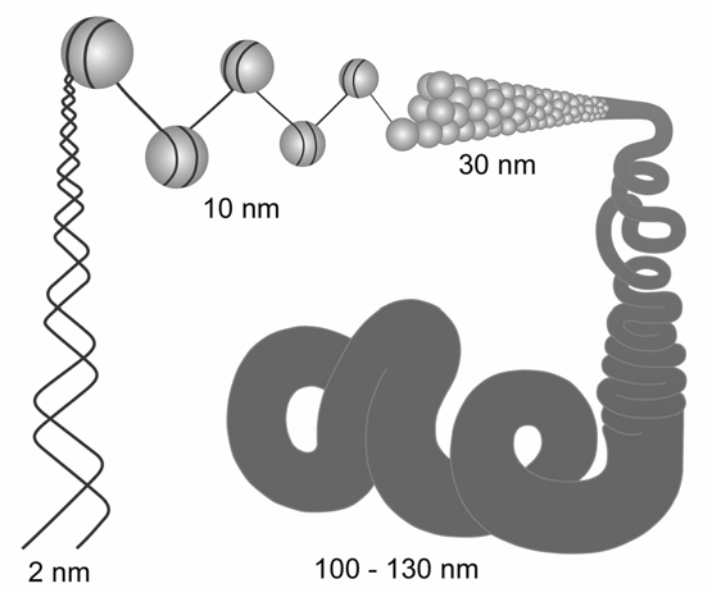

Figure 1. Progressive chromatin condensation
The DNA helix with a diameter of 2 nm is wrapped around nucleosomes to yield the beads-on-a-string conformation of the 10 nm chromatin fibre. The latter condenses to a helical stucture, the 30-nm fibre, which can compact into chromonema fibres with a diameter of 100 - 130 nm.

Histones are subject to a variety of post-translational modifications, principally in their conformationally flexible N-terminal tails. Modifications of specific residues include phosphorylation, ubiquitination, acetylation and mono-, di- or tri-methylation. The number of possible permutations of the various modifications is extremely large, and has been proposed to constitute a 'histone code' - an epigenetic mechanism for conferring differing degrees of transcribability on different regions of chromatin (Jenuwein and Allis, 2001).

Chromosome territories and the distribution of transcription sites

Each chromosome occupies a distinct space, its own territory, in interphase nuclei (Cremer et al., 1982; Cremer et al., 1988). Chromosome territories have been visualised using chromosome-specific *in situ* paints or by genomic *in situ* hybridisation (GISH) detecting alien chromosomes in addition lines (Abranches et al., 1998; Cremer and Cremer, 2001; Hochstrasser et al., 1986; Jin et al., 2000). These studies have shown variability in shape and positioning of chromosome territories. In yeast, *Drosophila* and wheat, chromosomes span the width of the nucleus in rod-like structures with the two arms of each chromosome close together and centromeres and telomeres located at opposite poles in a Rabl configuration (Abranches et al., 1998). In contrast, mammalian chromosomes are usually have a radial distribution where chromosomes are either peripherally or centrally positioned and have an irregular territory shape (Cremer and Cremer, 2001). Selective labelling of individual chromosomes has suggested that chromosome territories are mostly separated into non-overlapping spaces (Visser and Aten, 1999; Visser et al., 2000) although definitive proof of this will be hard to obtain.

Incorporation of Bromo-UTP in run-on transcription, followed by immunofluorescence detection of the incorporated BrUTP has shown that transcription occurs in many distinct small foci. In wheat, these transcription sites are uniformly distributed throughout the nucleoplasm, while the nucleoli contain a much higher concentration of transcription sites and are more intensely labelled by BrUTP (Abranches et al., 1998). No evidence has been found for a preferential localisation of transcription sites near the chromosome territorial boundaries or exclusion from the interior of chromosome territories. For mammalian nuclei, a study using BrUTP labelling of nascent transcripts in a cell line expressing green fluorescent protein (GFP)-tagged histone H2B showed that except for nucleoli and speckles, almost all nascent RNA co-localises with chromatin domains and that there is no preferential localisation in chromatin depleted areas (Sadoni and Zink, 2004). However, another study analysing Bromo-UTP incorporation at the electron microscope level found newly synthesised RNA mainly at the periphery of condensed chromatin regions in perichromatin fibrils (Cmarko et al., 1999), which might be transcription sites on chromatin loops outside the chromosome territory.

Heterochromatin and euchromatin

Heterochromatin was originally cytologically defined as highly condensed chromatin (Heitz, 1928). In *Arabidposis* for example, the heterochromatic knob on

chromosome 4 shows ca. 350 fold condensation (1Mb μm^{-1}) while an adjacent euchromatic region has a condensation rate of ca. 60 fold (180 Kb μm^{-1}) (Fransz et al., 2002). Heterochromatin is thought to consist of regular nucleosomal arrays, which impede access by nucleases and contain a high proportion of transcriptionally inactive repetitive sequences interspersed by relatively few genes (Elgin and Grewal, 2003; Grewal and Moazed, 2003). Heterochromatin has traditionally been sub-divided into constitutive heterochromatin, chromatin that is always condensed, and facultative heterochromatin, which may decondense in some circumstances. Chromosomal regions around the centromeres and telomeres are examples of constitutive heterochromatin, while genes silenced from a certain point in development onwards can form facultative heterochromatin interspersed along chromosome arms. In organisms with large genomes constitutively heterochromatic regions are also found along chromosome arms. Euchromatin is considered to be decondensed because of irregular nucleosome spacing, is relatively gene rich and is potentially transcriptionally active (Elgin and Grewal, 2003). However, these differences are not always clear-cut as a recent analysis of the human genome showed that some pericentromeric regions are decondensed and that some euchromatic regions are condensed (Gilbert et al., 2004). Epigenetic marks of silent chromatin in higher eukaryotes are histone hypoacetylation, di- or trimethylation of lysine 9 at histone H3 (H3K9 di- or trimethylation) as well as cytosine methylation (Fischle et al., 2003; Grewal and Moazed, 2003; Wu et al., 2005). Euchromatin is characterised by histone hyperacetylation and dimethylation of lysine 4 at histone H3 (H3K4 dimethylation) (Fischle et al., 2003).

Large-scale chromatin decondensation

Transcription related chromatin decondensation was first observed when specific transcriptional activators were directed to multi-transgene loci labelled in vivo by GFP and its variants in mammalian cells (Tsukamoto et al., 2000; Tumbar et al., 1999). While considerable chromatin decompaction was detected by in vivo labelling and confirmed by fluorescence *in situ* hybridisation, the loci in these studies were highly artificial since they used heterologous sequences and promoters. However, chromatin decondensation was also seen in the developmentally activated, murine *HoxB* gene cluster (Chambeyron and Bickmore, 2004). In addition, the active genes in the *HoxB* cluster as well as the major histocompatibility complex and other gene-rich regions on mammalian chromosomes were found in loops emanating from the chromosome territory (Chambeyron and Bickmore, 2004; Mahy et al., 2002; Volpi et al., 2000). In all cases the frequency with which a genomic region was detected on an external chromatin loop appeared to be related to the number of active genes in that region. In plants few studies on transcription-related chromatin decondensation have been published so far. The Arabidopsis gene *ddm1* encodes a SWI2/SNF2-like chromatin remodelling factor. In the *ddm1* mutant background transcriptional gene silencing of a transgenic locus is released, the transgenes are transcribed and the locus is decondensed (Probst et al., 2003). In wheat, transgene loci containing developmentally regulated endogenous genes for the seed storage protein glutenin

under the control of their own promoters decondense upon transcriptional activation during seed development (chapter 5). Based on their size and shape the decondensed transgene loci appeared to extend beyond the confines of the wheat chromosome territory.

Chromatin has been shown to be transcriptionally active at various degrees of compaction. A highly amplified heterochromatic transgene locus in a mammalian cell line spanning 90 Mb and containing multiple repeats of the lac operator decondensed from a ca. 30,000 fold compaction to 1,000 fold after activation (Tumbar et al., 1999). A 375 Kb region of the human major histocompatibility complex (MHC) showed a packing order of ca. 100 fold before induction with interferon and ca. 60 fold after induction (Müller et al., 2004). A higher decondensation rate than in the mammalian systems can be calculated for the transgene locus in wheat mentioned above (chapter 5). This locus consists of about 20 transgene copies of 10 Kb each. Fibre spreads of the locus suggested that there are short genomic regions interspersed with the repeated transgenes (EW and PJS, unpublished). The entire locus, transgene copies and interspersed genomic sequences is probably less than 500 Kb and the vast majority of the genes are transcriptionally active. Given the locus sizes visualized by FISH (chapter 5) this would correspond to a compaction of about 100-fold before activation and of about 11-fold in its most decondensed form after activation. These values would mean that transcription takes place with the chromatin dispersed almost to the level of the 10 nm fibre. Possibly the highest degree of decondensation has been found in the active 75S RNA genes in the Balbiani rings of dipterian chromosomes showing a DNA compaction rate of 3.6, i.e. below the histone-coated 10 nm fibre (Daneholt et al., 1982). The last example illustrates the degree of decondensation in a highly transcribed gene with few nucleosomes left on the chromatin during transcription (Daneholt et al., 1982). Likewise, active rRNA genes each have many engaged RNA polymerases and are decondensed to similar compaction ratios (González-Melendi et al., 2001). An explanation for this is that in order for the RNA polymerase to gain access to the template 30-nm fibres have to uncoil locally followed by histone displacement where the polymerase moves through. How far a gene decondenses then depends on the number of engaged RNA polymerases at any given moment and packing ratios at transcribed loci reflect the amount chromatin that is transcriptionally activated in a sequence.

Effectors of chromatin decondensation during gene activation

There is good evidence that during transcriptional activation chromatin expands in three stages: first the initial factor (activator) gets access to the nucleosomal DNA, second chromatin opens locally mediated by an activator/coactivator and third the transcription machinery causes extensive chromatin opening (for extensive reviews see Lemon and Tjian, 2000; Li et al., 2004). Once gene-specific transcriptional activators occupy their binding sites on promoters or enhancers, local chromatin decondensation is mediated by the recruitment of two types of coactivators: an adenosine-5′-triphosphate (ATP)-dependent, SWI/SNF-like chromatin

remodelling complex and a histone acetyltransferase (HAT) (Horn and Peterson, 2002; Lemon and Tjian, 2000; Li et al., 2004). Both HATs and SWI/SNF seem to disrupt higher-order folding of nucleosomal arrays and SWI-SNF enzymes can also weaken the nucleosome-DNA interaction (Horn and Peterson, 2002). The above mentioned heterochromatic transgene locus spanning 90 Mb and containing multiple repeats of the lac operator decondensed within minutes upon induction with the transcriptional activator (Tumbar et al., 1999). Elevated levels of histone acetylation (acetylated H3K9) were observed early in the activation of the *HoxB* locus at both *hoxb1* and *hoxb9*, several days before activation of the latter (Chambeyron and Bickmore, 2004). Recruitment of a chromatin remodelling enzyme and two HATs was shown during the induction of a tandem array of the mouse mammary tumour virus promoter (Müller et al., 2001). This study also showed a role for RNA polymerase II in producing and maintaining decondensed chromatin, since decondensation was blocked by two transcription elongation inhibiting drugs, DRB and α-amanitin. Equally, the frequency of extraterritorial decondensed loops of human genomic regions was reduced when transcription elongation was inhibited by DRB or actinomycin D (Mahy et al., 2002). However, the recruitment of the transcriptional machinery seemed to suffice and ongoing transcription was not necessary for decondensation of the highly amplified heterochromatic transgene locus mentioned above (Tumbar et al., 1999). Since the transgene contruct used in this study contained a high number of activator binding sites their decondensation upon activator binding may well have drowned out any visible effects of transcription triggered decondensation. Two more studies have addressed the question of whether decondensation precedes gene expression or is the consequence of it, one in animals and one in plants (Janicki et al., 2004; Wegel et al., 2005, see chapter 5). In both, nascent RNA was first detected before visible decondensation at the transgene loci. This may argue against the idea that local decondensation is a prerequisite for transcriptional initiation. However, in both cases it seems that only a subset of genes in the arrays is activated initially and that large scale decondensation visible by microscopy does not occur until later when a large proportion of the genes have become activated (Janicki et al., 2004; Wegel et al., 2005, see chapter 5).

Enhancers are cis-acting elements that increase transcription in an orientation- and distance-independent manner. They play a role in chromatin opening by relocating the target gene locus away from heterochromatin (Francastel et al., 1999; Ragoczy et al., 2003), by affecting histone modifications (Chua et al., 2003) or by initiating intergenic transcription (Li et al., 2004). It has been suggested that intergenic and LCR (locus control region) transcription play a role in maintaining an open chromatin structure and through this mechanism affect globin gene expression (Gribnau et al., 2000; Plant et al., 2001). The LCR of the β-globin locus acts as an enhancer and the current model of its action is the formation of a loop bringing the distant LCR and the promoter into close proximity (de Laat and Grosveld, 2003), which could actually be described as condensation rather than decondensation. This might also explain that the frequency of looping from the chromosome

territory is increased before activation and is reduced during transcription of the locus (Ragoczy et al., 2003). Cis-acting elements may therefore open chromatin locally and at the same time produce a more closed higher order structure through loop formation. A more detailed analysis of their involvement in gene activation may result in more instances where transcriptional activation does not equal visible chromatin decondensation because of this effect.

Effectors of chromatin condensation during gene specific silencing

There is accumulating evidence that RNA interference (RNAi) is a pathway by which centromeric heterochromatin is formed in fission yeast, Drosophila, mammals and plants (Matzke and Birchler, 2005). In this pathway the repetitive sequences in pericentromeric regions generate transcripts that form double stranded RNAs. These are processed into short interfering (si) RNAs, which in turn trigger silencing of homologous sequences through H3K9 methylation and DNA methylation (Craig, 2005; Finnegan and Matzke, 2003; Matzke and Birchler, 2005). Gene silencing during development is generally initiated by DNA sequence-specific transcription factors that act as transcriptional repressors and bind to gene promoters, recruit histone deacetylases and interact with DNA-methyltransferases and histone methyltransferases (Craig, 2005). In some cases silenced genes are moved into the vicinity of heterochromatin. One example is the *brown* locus in *Drosophila* (Dernburg et al., 1996). Another is the mouse terminal transferase gene (*Dntt*), which becomes silenced during thymocyte (immature lymphocyte) maturation. Silencing starts at the promoter with H3K9 deacetylation, loss of H3K4 methylation and methylation of H3K9, followed by bidirectional spreading of each event (Su et al., 2004). Coincidentally with deacetylation of histone 3 the gene is repositioned to pericentromeric heterochromatin (Su et al., 2004). One factor implicated in repositioning and permanent silencing of genes during lymphocyte development is the Ikaros DNA-binding protein. Ikaros has been shown to interact with chromatin-remodelling components such as histone deacetylases, it co-localises with many inactive genes in lymphocytes, can bind to specific sequences in the promoters of many lymphoid-specific genes as well as the repetitive DNA that surrounds mouse centromeres (Fisher and Merkenschlager, 2002). It has been suggested that Ikaros might function as a transcriptional repressor and mediate the permanent inactivation of genes through recruitment to heterochromatin domains (Fisher and Merkenschlager, 2002).

Several chromosomal proteins have been shown to mediate heterochromatin formation by binding to histones and condensing nucleosomal arrays. Heterochromatin Protein 1 (HP1) in *Drosophila* and mammals is a structural component of silent chromatin at telomeres and centromeres. It was first discovered as a modifier of position effect variation (PEV), the variable expression of heterochromatic and euchromatic genes that have been relocated to the vicinity of a novel breakpoint between heterochromatin and euchromatin created by the relocation (Weiler and Wakimoto, 1995). HP1 recognises H3 methylated at lysine 9 by the *Drosophila* histone methyltransferase SU(VAR)3-9 (Bannister et al., 2001).

According to a model proposed by the same authors to explain subsequent heterochromatin spreading HP1 binds to methylated K9H3 and recruits SU(VAR)3-9. SU(VAR3-9 then methylates adjacent histones which allows HP1 to spread linearly along the chromatin fibre. It has recently been shown for *Drosophila* and mammalian cells that HP1 tethered to a *lac* operator array causes silencing of downstream reporter genes and local chromatin condensation (Danzer and Wallrath, 2004; Verschure et al., 2005). However, HP1 also seems to play a role as transcriptional activator (De Lucia et al., 2005 and references therein). HP1 and SU(VAR)3-9 have homologues in fission yeast, Swi6 and Clr4 (Schramke and Allshire, 2003). HP1 also has an *Arabidopsis* homologue, TFL2 (LHP1), which is involved in amongst others the repression of several floral homoeotic genes but does not seem to be responsible for the assembly of constitutive pericentromeric heterochromatin (Gaudin et al., 2001; Kim et al., 2004; Kotake et al., 2003; Lindroth et al., 2004). Polycomb group (PcG) proteins are thought to form several distinct complexes that silence genes responsible for developmental regulation in *Drosophila* and mammals. They contain another protein with similarity to HP1, polycomb. Like HP1 it binds methylated histones and the histone methyltransferases responsible for their methylation (Craig, 2005). It has recently been shown that core components of one of theses complexes compact nucleosomal arrays in vitro and do not require histone tails for their action (Francis et al., 2004).

Models of higher order chromatin structure in a functional context

It is possible that different models of higher order chromatin structure simply describe different nuclear environments and particular stages in the regulation of genes. The nucleosome affinity, random chain model might be correct for euchromatic regions with very low heterochromatin content and low compaction, where nucleosomal chains can freely explore nuclear space. Chromonema type fibres might occur in heterochromatic regions through HP1 dimerisation and the ability of HP1 to bring distant chromosomal sites into proximity (Li et al., 2003). The latter could also involve loop formation. As mentioned above for the β-globin locus the formation of loops of less than 100 Kb seems to play a role in bringing cis-regulatory elements into proximity with the genes they control (de Laat and Grosveld, 2003; Kato and Sasaki, 2005). Loops could also be formed through the Ikaros mediated recruitment of silenced genes to heterochromatin. It has been shown that gene-rich euchromatic loops with a length of 0.2 to 2 Mbp emanate from a condensed chromocentre that comprises the few heterochromatic regions on chromosome 4, i.e. the pericentromeric regions and the nucleolus organising region (Fransz et al., 2002). This led van Driel and Fransz (2004) to suggest that interphase chromosomes are organised into transcriptionally active loops around heterochromatic centres. Since transcription occurs throughout the chromosome territory extraterritorial loops of active chromosomal regions might have little functional significance. They are only seen in a proportion of nuclei (Mahy et al., 2002) and could simply be a consequence of decondensation per se while the position of the loop with respect to the territory might not matter. The direction of

loops might, however, be influenced by the number, position, availability and mode of assembly of transcription sites throughout the nucleus. If transcription sites turn out to be relatively stationary, preassembled and bound to the nuclear matrix, a protein scaffold present in the nucleus, then chromatin needs to be reeled in and passed through the polymerase (Bode et al., 2003; Cook, 1999; Szentirmay and Sawadogo, 2000). In this case, chromatin will have to be guided to transcription sites and decondensation will be directed. Matrix attachment regions (MARs) are AT-rich sequences that act as anchors to the nuclear matrix. MARs can either form selective and transient or permanent anchors and have been proposed among other functions to facilitate transcription by positioning adjacent genes in the vicinity of the transcriptional machinery (Bode et al., 2003; Heng et al., 2004). It might be the myriad of regulatory and often transient chromatin interactions within a chromosome in addition to MARs-matrix interactions that hold the territory together (Bode et al., 2003; Taddei et al., 2004) (Fig. 2).

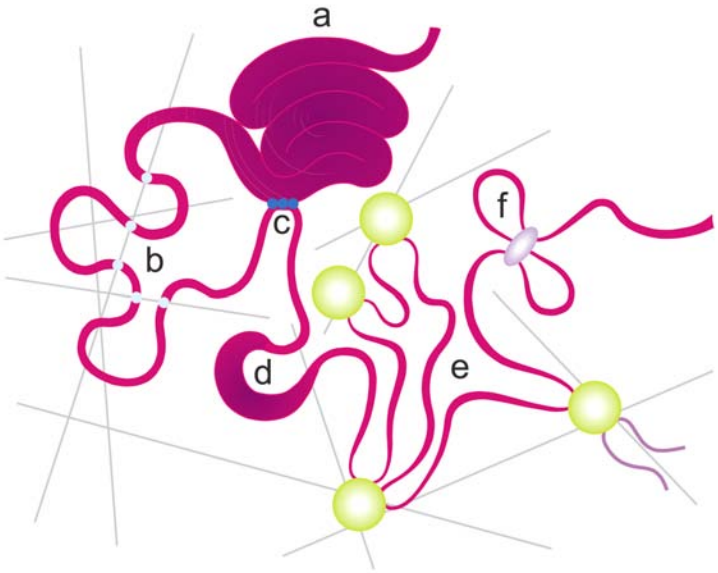

Figure 2. Model of interactions that keep the chromosome territory together
The model depicts part of a chromosome arm starting with centromeric heterochromatin. (a) Centromeric heterochromatin made up of chromonema fibres and associated with heterochromatin protein 1. (b) Chromatin loops anchored to the protein structure of the nuclear matrix (grey) via matrix attachment regions (MARs, light blue). (c) Translocation of silenced genes to centromeric heterochromatin via the Ikaros protein (dark blue). (d) Interstitial heterochromatin associated with polycomb. (e) Highly transcribed region with several transcription factories (green). Transcription factories are assumed to be attached to the nuclear matrix and transcribe to a large extent genes belonging to the same chromosome arm, dark purple gene belonging to a different chromosome (Osborne et al., 2004). (f) Active chromatin hub where positive cis-regulatory elements are in close proximity to the transcriptionally active gene while intervening inactive genes loop out.

Outlook

Clear differences between heterochromatin and euchromatin are disappearing. There is some evidence that HP1 plays a role in silencing in a euchromatic context which is currently investigated (Danzer and Wallrath, 2004). The importance of the RNAi machinery in silencing of euchromatic genes and heterochromatin will probably only increase. The nature and function of nuclear matrix anchors is still debated (Heng et al., 2004). Final proof of the importance of such anchors and of which enzyme complexes are bound to the matrix may give us a better understanding of functional and structural chromatin loops. Some progress has been made towards elucidating the structure of the 30 nm fibre but the nature of higher order chromatin folding is still debated and explained by several very different models without conclusive evidence for any of them. The discovery of histone-binding proteins such as MENT and PcG complexes that contribute to chromatin condensation and in vitro studies of their mode of action may be the clue to chromatin structure within the interphase nucleus (Francis et al., 2004; Springhetti et al., 2003).

Acknowledgements

Eva Wegel and Peter Shaw were supported by funding from the UK Biotechnology and Biological Science Research Council (BBSRC). We thank Hans de Jong, Paul Fransz, Anne Osbourn and Silvia Costa for critical reading of the manuscript.

Chapter 3

3D modelling of wheat endosperm development

Eva Wegel [1], Emma Pilling [1], Grant Calder, Sinéad Drea, John Doonan, Liam Dolan and Peter Shaw

Department of Cell and Developmental Biology, John Innes Centre, Norwich Research Park, Colney Lane, Norwich NR4 7UH, UK
[1] These authors contributed equally to the publication.

Published in New Phytologist (2005) 168(1), 253-262

Summary
- We have developed methods based on confocal microscopy and 3D modelling for the analysis of complex tissues and individual nuclei. These methods were used to study the development of early wheat (*Triticum aestivum*) endosperm as a whole and of endosperm nuclei undergoing polyploidisation.
- Fixed sections of immature caryopses were either stained with SYTOX Green or used for fluorescence *in situ* hybridisation (FISH) to visualise centromeres, telomeres and a rye chromosome arm substitution. Each section was imaged as a confocal image stack. Using Amira 3.0 for computer image processing rendered models were produced of the whole endosperm and of individual nuclei.
- We followed endosperm development up to the formation of a complete syncytium, which develops via a dorsal and a ventral plate of nuclei in the central cell. Modelling of nuclei showed that wheat chromosomes are not anchored to the nuclear membrane and become more randomly positioned in endoreduplicated nuclei.
- This analysis produced a precise description of the positioning of nuclei throughout the developing endosperm and of chromosomal domains in single nuclei.

Key words: endosperm, 3D modelling, wheat (*Triticum aestivum*), telomere, centromere

Introduction
The endosperm of wheat (*Triticum aestivum*) originates from the fusion of the two haploid polar nuclei of the central cell in the embryo sac with one haploid sperm nucleus. The first division of the resulting triploid nucleus occurs ca. 5 hours after pollination (Bennett et al., 1973). From then on synchronous nuclear divisions without the formation of cell walls lead to a syncytium lining the walls of the central cell (Bennett et al., 1973; Brenchley, 1909; Huber and Grabe, 1987a; Mares et al., 1975; Percival, 1921). For the bulk of the endosperm cell wall formation starts from the periphery at day four after pollination via the formation of open-ended

alveoli, which grow towards the centre of the endosperm, and is completed by day seven (van Lammeren, 1988). Cell divisions continue until 12-14 days post anthesis (dpa) (Huber and Grabe, 1987b). This so-called nuclear type of endosperm development, which is characterised by a limited or permanent phase of free-nuclear division, is found in cereals and *Arabidopsis* (Olsen, 2004; Olsen et al., 1992), as well in other plants.

Other than in maize no detailed cytological analysis has been undertaken to understand the steps leading to the development of the complete syncytium in cereals and even there the available evidence is based on single thin sections through the endosperm (Randolph, 1936). For *Arabidopsis*, whole-mount techniques have been developed to analyse endosperm development (Boisnard-Lorig et al., 2001; Brown et al., 2003; Garcia et al., 2005). Cereal endosperm, however, is too large and too deeply embedded in a complex caryopsis for a similar approach. To fully understand the development of cereal endosperm, and ultimately the genes controlling it, we have developed methods that allow a detailed analysis of this tissue at the cellular level using confocal microscopy and computer aided 3D modelling. From studies of the early stages of wheat endosperm development we conclude that endosperm nuclei first form a dorsal and a ventral plate in the periphery of the central cell. By 2 dpa synchronous divisions connect the plates to form a complete syncytium by 4 dpa.

After cellularisation, some nuclei in the central starchy endosperm undergo two or three rounds of DNA replication taking the DNA content up to 12C or 24C. This leads to increases in the number of chromosome arms (polyteny) and of complete chromosome sets (polyploidy) (Brunori et al., 1989; Wegel and Shaw, 2005, see chapter 4). Chromosome arms in wheat nuclei are arranged in a Rabl configuration spanning the nucleus with telomeres and centromeres at opposite poles (Abranches et al., 1998; Martínez-Pérez et al., 2001; Martínez-Pérez et al., 1999; Wegel and Shaw, 2005, see chapter 4). *In situ* hybridization and confocal imaging combined with 3D modelling allowed us to track changes in nuclear shape and chromosome positioning during endosperm development, which were not detected without the modelling step.

Materials and Methods

Plant material

Wheat (*Triticum aestivum* L cv. Savannah) was used for the analysis of endosperm development. Plants were grown from seed in a controlled environment room under the following conditions: 16 h light/8 h darkness, 18 ^{o}C and 70% relative humidity. After four to five weeks, seedlings were vernalised for six to eight weeks at 10 ^{o}C, with an 8 hr photoperiod, and then returned to the controlled environment room. For the *in situ* hybridisation experiments, cv. Pro INTA Federal with a 1RS (Secale cereale) chromosome arm substitution for the 1BS wheat

chromosome arm ($1B^l/1R^s$) was used. Plants were grown under the same conditions as Savannah but without vernalisation.

Seed sections

To maximise reproducibility, only the outer caryopses in spikes in the centre of the ear were used, since these develop earliest and become the biggest ones in the spike. Individual flowers were checked twice daily for anthesis. Flowers and immature caryopses were harvested before anthesis, and 0.5, 1, 2, 3 and 4 days post anthesis (dpa) for the study of whole endosperm development and at 7 and 16 dpa for the analysis of individual nuclei. The material was fixed for 6h or overnight in 4% (w/v) formaldehyde, freshly made from paraformaldehyde, in PEM (50 mM PIPES, 5 mM EGTA, 5 mM $MgSO_4$ pH 6.9) with or without 5% DMSO. Fixed seeds were dehydrated through an ethanol:water series (10%, 20%, 40%, 60%, 80% and 100% for 4 to 12h per step) and stored in 100% ethanol at 4 ^oC. 100 and 200 μm sections for in situ hybridisation and endosperm modelling respectively were prepared under 100% ethanol using a Vibratome Series 1000plus (TAAB Laboratories Equipment Ltd., Aldermarston, UK) and rehydrated in water. Consecutive sections were allowed to dry on poly-lysine-coated slides (BDH, Poole, UK). In initial studies, seeds were wax-embedded before sectioning but the wax could not be completely removed from the sections, which hampered subsequent staining and labelling. We observed no differences in structural preservation between wax-embedded and non-embedded material.

Nuclear staining for endosperm modelling

Slides were treated with RNase A (Sigma, 10 mg mL^{-1}) for 2h at 37 ^oC, washed in water and stained with 5 nM SYTOX Green (Molecular Probes, Leiden, The Netherlands) for 20 min. After a further wash in water, they were mounted in Vectashield (Vector Laboratories) and stored at 4 ^oC.

Pretreatments for in situ hybridisation

Sections were incubated with 1% (w/v) driselase (Sigma, Poole, UK), 0.5% (w/v) Onozuka R10 cellulase (Yakult Pharmaceutical Ind. Co. Ltd., Tokyo, Japan), 0.025% pectolyase Y23 (Kikkoman, Tokyo, Japan) in PBS (1.6 mM NaH_2PO_4, 15 mM Na_2HPO_4, 150 mM NaCl pH 7.4) for 1 h at room temperature and washed in TBS (10 mM Tris, 140 mM NaCl pH 7.4) for 10 min. They were then treated with RNase A (Sigma, 100 μg mL^{-1} in 2x SSC (300 mM NaCl, 30 mM sodium citrate pH 7.0)) for 1h at 37 ^oC, washed in TBS for 10 min, dehydrated in an ethanol:water series (70% and 100% ethanol) and air-dried.

Probes and *in situ* hybridisation

Total rye genomic DNA was partly digested with Taq1 and the fragments were then labelled with biotin-16-dUTP (Roche) by nick translation. Telomeric probes labelled with biotin-16-dUTP (Roche, Lewes, UK) were prepared according to Cox et al. (1993). Centromeric probes labelled with digoxigenin-11-dUTP (Roche) were prepared according to Aragón-Alcaide et al. (1996) using the following primers for

the CCS1 repeat fragment: 5'CGCAATATCTTGATTGCATCTATATTC3' (positions 17 to 43) and 5'GCTGGTAGTGAAAAGGTGCCCGATCTT3' (positions 249 to 223). Sections were first treated with the avidin/biotin blocking kit (Vector Laboratories, Burlingame, California, US) according to the manufacturer's instructions using a biotin blocking step followed by avidin and biotin, respectively, to block biotin binding sites in the tissue. After a final wash in PBS, FISH was performed in a slightly modified version of Abranches et al. (2000) using 200 ng of each probe in a total volume of 30 μL per slide in a hybridisation buffer containing 20x excess salmon sperm DNA in 50% formamide, 10% dextran sulfate, 2x SSC and 0.1% SDS. The probe was denatured in the hybridisation mixture for 5 min at 95 ^{o}C. Sections were denatured at 75 ^{o}C for 8 min in a modified thermocycler (Omnislide, Hybaid, Ashford, UK), and hybridisation carried out overnight at 37 ^{o}C. Post-hybridisation washes were carried out in 0.1x SSC, 20% formamide at 42 ^{o}C.

Immunodetection

Biotin-labelled probes were detected with Extravidin-Cy3 (Sigma). Probe labelled with digoxigenin was detected with a mouse anti-digoxin antibody (Sigma) followed by a secondary goat anti mouse antibody conjugated to Alexa Fluor® 488 (Molecular Probes, Leiden, The Netherlands). Antibodies were diluted in 4x SSC, 0.2% Tween 20 according to the manufacturer's instructions. Antibody incubation was performed in a humid chamber for 1 h at 37 ^{o}C followed by 3x 5 min washes in 4x SSC, 0.2% Tween 20 at room temperature. Sections were counterstained in 1 μg mL^{-1} DAPI for 10 min. Slides were mounted in Vectashield (Vector Laboratories).

Image acquisition and analysis

Sections were imaged on a Leica TCS SP2 confocal microscope (Leica Microsystems GmbH, Heidelberg, Germany). DAPI was excited with the 363 and 351 nm lines from a high powered Argon ion laser in early experiments. Later this was replaced with a blue diode laser (405 nm). Alexa-488 and SYTOX Green were excited at 488 nm from an Argon ion laser, and Cy3 was excited at 543 nm from a Helium/Neon laser. SYTOX Green fluorescence was collected using a x10/0.4 Imm objective, which allowed us to focus through tissue with a thickness of 200 μm. Triple fluorescent images of nuclei after in situ hybridisation were collected using a x40/1.25 oil objective with a working distance of ca. 100 μm. For the in situ hybridisation experiments confocal sections were collected at increments of 0.6 μm. For endosperm modelling confocal sections were collected at increments of 5 μm, which ensured that every nucleus was visible in at least two consecutive sections.

For endosperm modelling, each vibratome section was scanned through from top to bottom as one stack or, where the whole endosperm did not fit in the field of view, as multiple stacks overlapping in x and y with identical z positions. The overlapping stacks were combined and aligned in x and y using the merge tool of the Leica confocal software to create a single stack encompassing all the endosperm and surrounding cells. This process was repeated for as many consecutive vibratome sections as were needed to cover the entire depth of the

endosperm. All the confocal stacks for the entire endosperm were then combined in one file, and exported as a single multiple image (export volume) TIFF file. The confocal sections from different physical vibratome sections were not aligned with each other at this stage, and a final alignment of all slices of the stack in x and y was carried out using the AlignSlices module of Amira 3.0. An aligned data set of a 4 dpa central cell comprised 1701 x 1134 x 97 pixels and 150 – 200 Mb. The LabelVoxel module in Amira was used to threshold nuclear fluorescence. In the image segmentation editor, different tissues - seed coat, endosperm, embryo and antipodals - were defined and colour-coded by outlining the nuclei (endosperm, embryo, antipodals) or the whole tissue (seed coat). Surfaces for each nucleus were generated by resampling and triangulation (SurfaceGen module in Amira).

For the analysis of individual nuclei, confocal stacks were cropped to single nuclei and channels were aligned in z in ImageJ (a public domain program by W. Rasband available from http://rsb.info.nih.gov/ij/). Z alignment between the UV/far blue and visible green/red channels was necessary due to the chromatic aberration inherent in the objective used for this study. It was done by adding or removing sections at the beginning and end of each stack. In the Amira 3.0 software, channels were combined in a MultiChannelField and displayed using the Voltex module. The positions of centromeres and telomeres were analysed in orthogonal sections through nuclei using the Orthoslice module. C values were estimated for individual nuclei from nuclear volume measurements using the TissueStatistics module after thresholding in the LabelVoxel module. Figures were composed using Adobe Photoshop 7.0 (Adobe Systems Inc., Mountain View, CA).

Results

3D modelling of early endosperm development

We analysed 157 seeds aged from just before anthesis to 4 dpa. Figure 1 shows the plane of sectioning through the embryo sac and defines the terms used for spatial orientation in the following description. At the stages analysed the tissue of interest comprised three to five physical sections each of 200 μm thickness. For the earliest stages of endosperm development the confocal stacks were easy to interpret as 3D images. At later stages, the tissue became more complex so that it was necessary to make 3D models of the nuclei.

Since we scored anthesis as the emergence of the anthers from the flower, and pollination would have occurred earlier, i.e. after release of pollen from anthers but before emergence of anthers from the flower, the timings given as dpa are only approximations for the times of fertilization. Before or just after anthesis in addition to the antipodals the egg sac contained up to four large, weakly staining nuclei at the micropylar end. These corresponded to the egg cell, the two synergids and the central cell (Fig. 2a). Endosperm nuclei were identified by their elongated shape and were first seen 1 dpa. At the earliest stage we observed three different

populations of endosperm nuclei in different sections. These were found in three locations: a group of nuclei were located near the zygote, a further group of nuclei were located in the dorsal region of the egg sac and another in the ventral region (Fig. 2b, Fig. 3a). The zygote-associated nuclei formed a stem like structure that connected this population with the dorsal nuclei but not to the ventral nuclei (Fig. 2c,e). These groups may correspond to three distinct populations that are present within a single developing endosperm or they may illustrate variability in the spatial distribution of nuclei during early endosperm development. At this 1 dpa stage, mitoses were observed in two specimens. In these examples all endosperm nuclei had just undergone nuclear division and formed pairs of small nuclei suggesting that mitosis is synchronised at this early stage of endosperm development (Fig. 3a). Only nuclei near the antipodals were observed in these specimens.

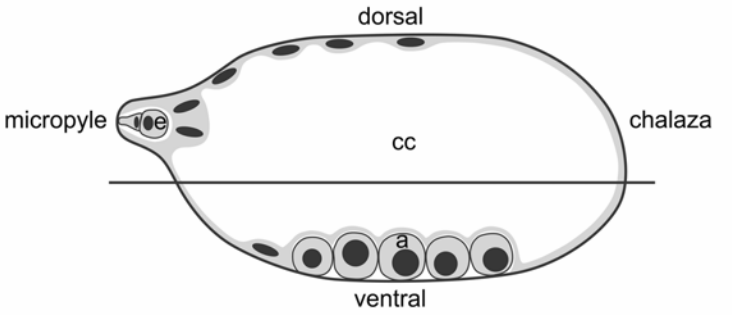

Figure 1. Diagram of young embryo sac with plane of sectioning
a antipodals, cc central cell, e embryo

Figure 2. Nuclear plate formation in early endosperm development
Projections of serial optical sections through immature seeds after staining with SYTOX Green. All sections are shown with the chalaza at the top and the micropyle at the bottom. (a) – (d) 1dpa, (e) and (f) 2dpa. (a) Two large nuclei are visible at the micropylar end (arrow head), presumably the zygote and one of the disintegrating synergids. (b) Two endosperm nuclei are seen in the centre of the section and two at the micropylar end (arrow head). (c) A stem of nuclei is formed around the zygote at the micropylar end and a small dorsal plate is attached to it. (d) In the same caryopsis the first nuclei of the ventral plate (arrow heads) are seen near the antipodals. (e) Caryopsis with a larger dorsal plate than in (c) but without endosperm nuclei near the antipodals (f). a antipodals, cc central cell, en endosperm nuclei, i integuments, n nucellus, p pericarp. Bar, 250 µm.

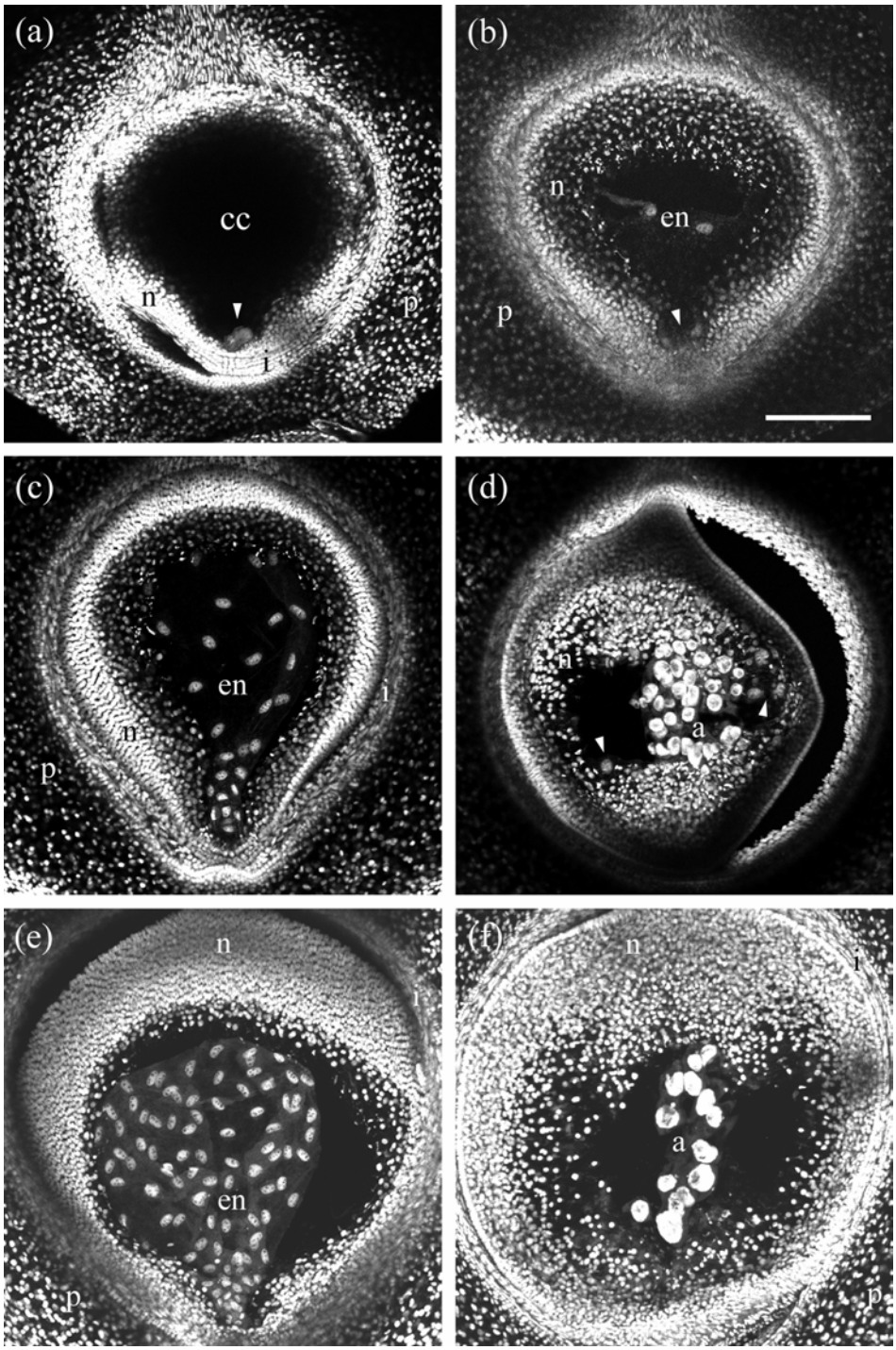

Figure 2

The dorsal and ventral groups of nuclei developed into plates of nuclei (Fig. 2c,e). Where early dorsal and ventral plates were seen in the same caryopsis, the dorsal plates were generally more developed than the ventral plates, but dorsal plates without ventral plates were occasionally found too. It is possible that some material was lost during sectioning. In, particular we observed occasional loss of the inner dorsal seed coat and nucellus layers and the adhering walls and cytoplasm of the central cell and the zygote. In embryo sacs with dorsal plates without the stem nuclei, which connect the dorsal plate to the zygote, neither zygote nor embryo was seen. This may indicate that material was lost during tissue processing. At the ventral side the presence of antipodal nuclei was a good indicator that this part of the central cell was complete as endosperm nuclei first appeared on either side of the antipodals (Fig. 2d,f). At 1 dpa complete dorsal plates plus stem contained on average 91 nuclei in central cells without ventral plate (counts from four central cells, s.d. 4). In central cells with both dorsal and ventral plates similar numbers of total endosperm nuclei were found (83, counts from four central cells, s.d. 7).

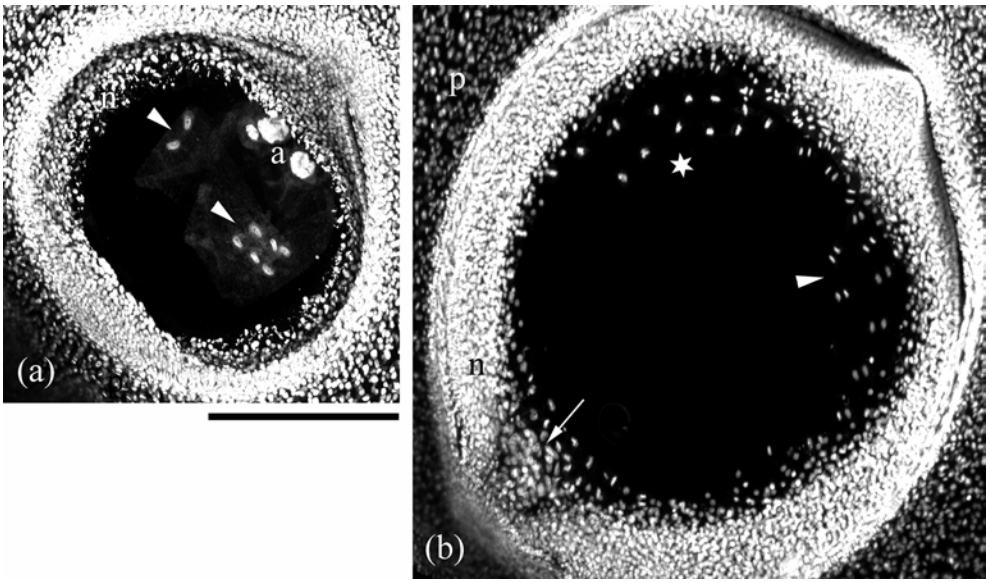

Figure 3. Coordinated nuclear divisions during syncytium formation
Projections of serial optical sections through immature caryopses after staining with Sytox Green. Sections are shown with the chalaza at the top right corner and the micropyle at the bottom left corner. (a) 1 dpa, eight endosperm nuclei, the products of the first three nuclear divisions, in the centre (arrow heads). (b) 2 dpa, metaphases (star) and telophases (arrow head) towards the chalazal end of the central cell and no nuclear divisions around the embryo at the micropylar end (arrow). a antipodals, n nucellus, p pericarp. Bar, 500 µm.

By 2 dpa both dorsal and ventral plates of nuclei were visible in the same central cell and the dorsal plate was connected to the embryo by a stem of nuclei. By this

stage, dorsal and ventral plates were beginning to coalesce and nuclear divisions were largely synchronous in all regions except near the embryo where few divisions were observed (Fig. 3b). The overall pattern of nuclei remained similar at 3 dpa (Fig. 4a). At 2 to 3 dpa central cells contained between 200 and 400 nuclei. At 4 dpa, the entire periphery of the central cell was surrounded by a layer of nuclei, making the syncytium complete, and no cell divisions were observed (Fig. 4c). Complete syncytia contained ca. 1000 nuclei. Movies of the models of both these stages can be viewed as supplementary data.

We conclude that syncytium formation starts generally with a dorsal plate of nuclei which is connected to the zygote. This is followed or in some cases preceded by the formation of a ventral plate either side of the antipodals. By 2 dpa further synchronous divisions connect the plates to form a complete syncytium by 4 dpa, where no nuclear divisions are visible.

3D modelling of changes in chromosome organisation related to increased C content in endosperm nuclei

After cellularisation, polyploidisation occurs in some endosperm nuclei. 3D modelling of nuclei with DNA contents of 3C, 6C and 12C allowed us to visualise changes in nuclear shape and chromosome positioning in developing endosperm. With increasing C content, nuclear volumes increase predominantly in two directions, thereby changing the shape of the nuclei (Fig. 5) into a disc-like structure. To determine if the disc shaped nuclei were artefacts of our fixation, sectioning, drying or imaging conditions we compared the shapes of nucleoli in nuclei lying at various angles to the focal plane and found no evidence of distortion (Fig. 6). In the majority of 3C and 6C nuclei and in all 12C nuclei, centromeres and telomeres were located on opposite, flat sides (Fig. 5, Table 1).

Table 1. Centromere/telomere and rye arm distribution along the long and short axes of endosperm nuclei

The positions of either centromeres and telomeres or rye arms were determined in 3D reconstructions and DNA content was estimated based on nuclear volume in combination with centromere number or number of rye chromatids.

	Centromeres/telomeres		Rye arm distribution		
	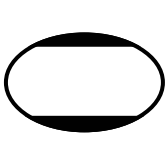	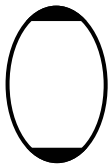	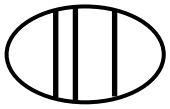		
3C	13 (76.5%)	4 (23.5%)	14 (63.6%)	6 (27.3%)	2 (9.1%)
6C	11 (91.7%)	1 (8.3%)	9 (69.2%)	0 (0%)	4 (30.8%)
12C	8 (100%)	0 (0%)	1 (14.3%)	0 (0%)	6 (85.7%)

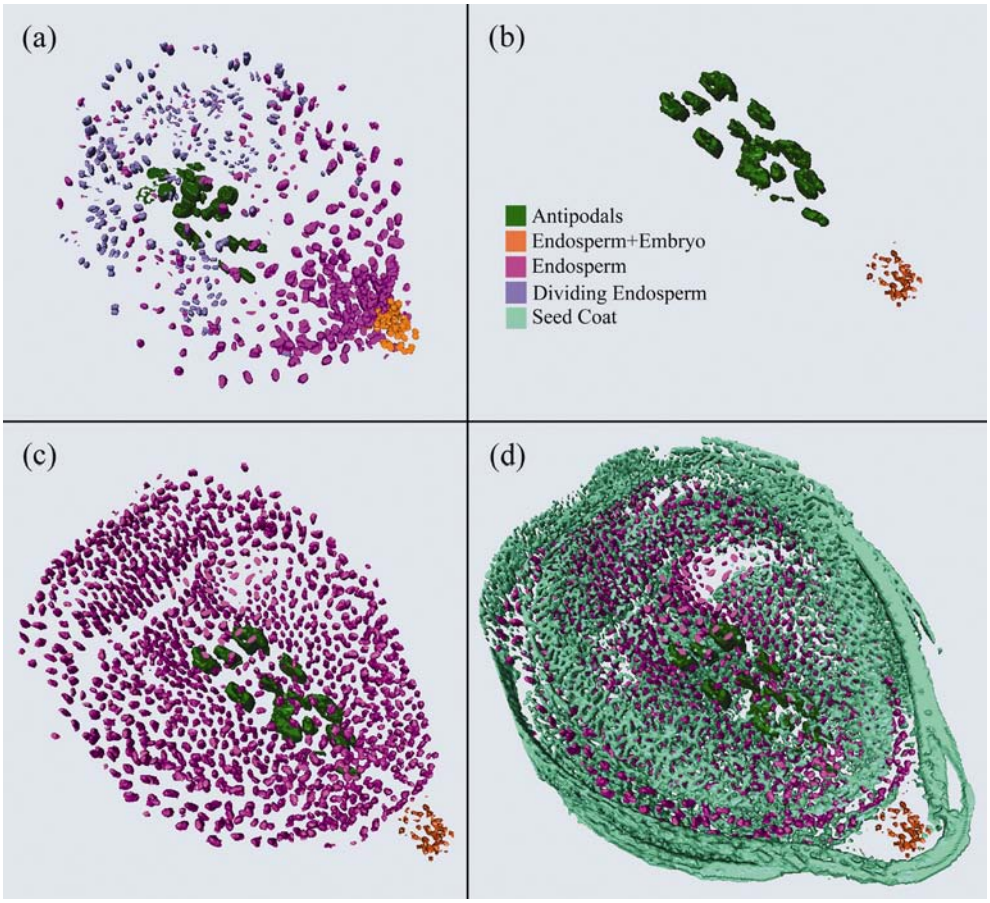

Figure 4. Models of syncytia at 3 and 4 dpa
(a) Incomplete syncytium with coordinated nuclear divisions at 3 dpa. (b – d) Tissue layers in complete syncytium and seed coat at 4 dpa

Movies of 3D reconstructions of nuclei with centromere and telomere labelling can be viewed as supplementary data. Orthogonal slices through 3D reconstructions showed that the majority of centromeres and telomeres are arranged at or close to the nuclear surface; crossovers to the other side were rare (Fig. 7d), but some centromeres and telomeres were also found in the nuclear interior (Fig. 5g). This means that centromeres and telomeres are not anchored, or are only transiently anchored, to the nuclear membrane.

Changes in chromosome structure during polyploidisation were revealed when we labelled the rye arm substitution: chromosomes were aligned in 3C nuclei and were positioned more randomly in nuclei of higher ploidy. Reconstructions of

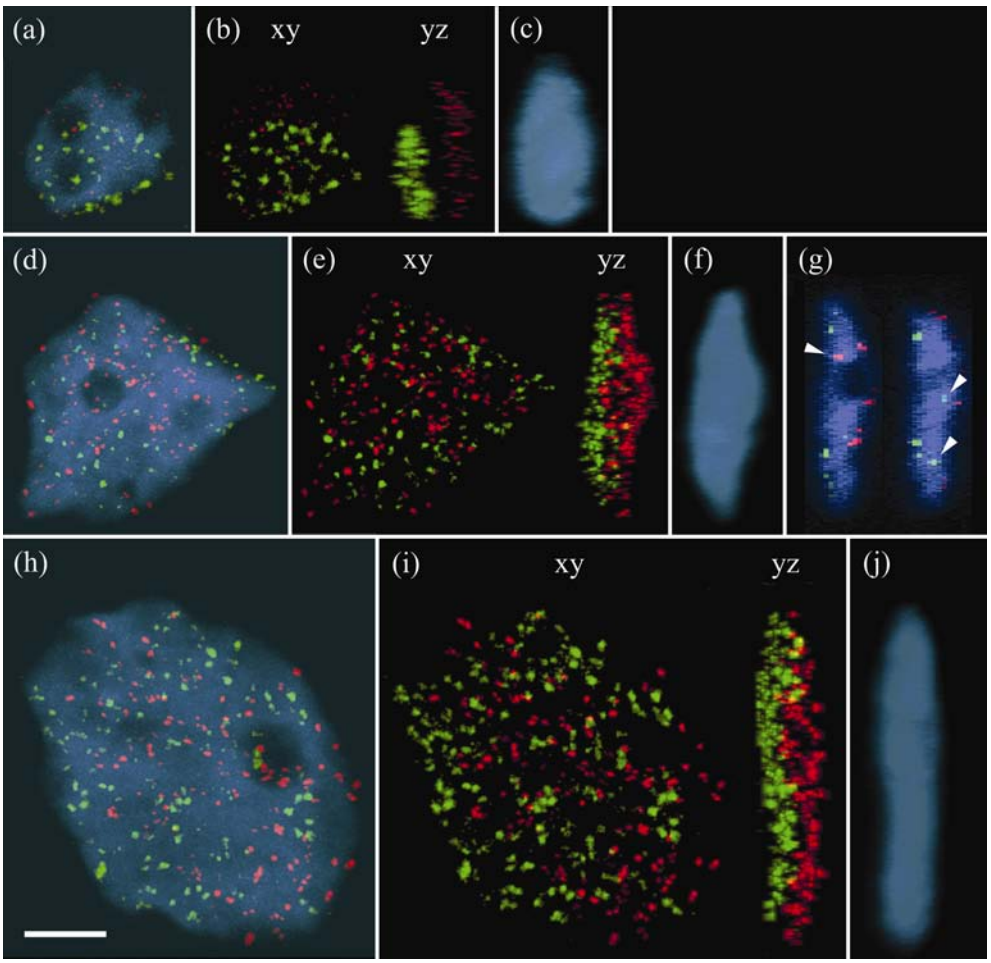

Figure 5. Centromere and telomere organisation in nuclei with increasing C content
(a) – (c) 3C nucleus, 7 dpa. (d) – (g) 6C nucleus, 16 dpa. (h) – (j) 12C nucleus, 16 dpa. (a), (d), (h) 3D reconstructions of nuclei with centromeres in green, telomeres in red and chromatin counterstained with DAPI (blue) in frontal view. (b), (e), (i) the same view without DAPI (xy) and turned 90° (yz) showing separation of telomere and centromere signals along the z axis of the nuclei. (c), (f), (j) side view of the nuclei showing DAPI staining only. With increasing C content, nuclear volumes increase predominantly in two directions and telomeres and centromeres are arranged on the flat sides. While the majority of telomeres and centromeres are close to the nuclear membrane some are found in the interior of the nucleus towards the opposite side as shown in two orthogonal sections (g, arrow heads). Bar, 10 μm.

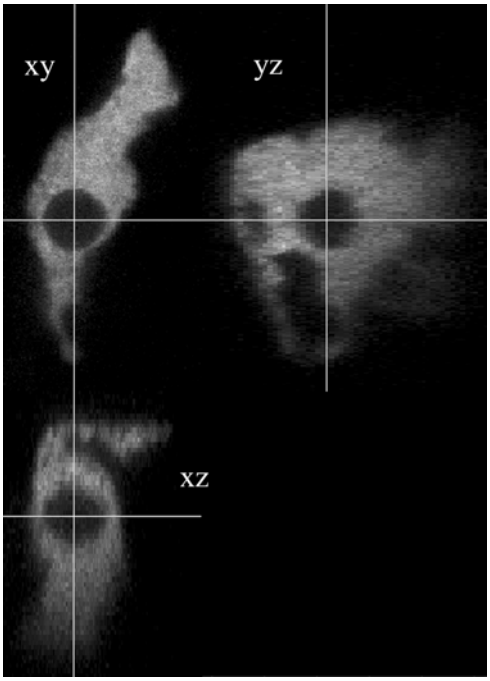

Figure 6. Orthogonal slices through a DAPI stained nucleus showing no distortion of the nucleolus after confocal imaging

Figure 7. Rye chromosome arm organisation 3D reconstructions of two nuclei with rye chromosome arms in white and chromatin counterstained with DAPI. A prominent subtelomeric knob identifies the telomeric end of the chromosome arms. (a), (b) 3C nucleus, 7 dpa in frontal view and tilted. (c), (d) 12C nucleus, 16 dpa in frontal view and tilted. Rye chromosome arms traverse the 3C nucleus, but in 12C nuclei they can be arranged almost horizontally (stars) or even flip over to the other side (arrow heads). Bar, 10 μm.

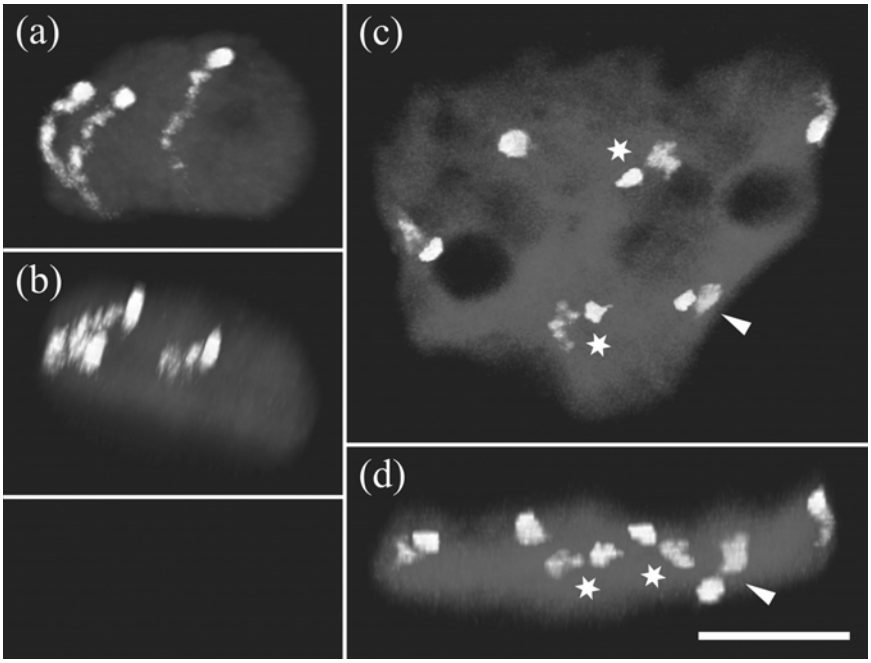

nuclei in which the rye chromosome arms were labelled showed that in most 3C nuclei the chromosome arms stretched from one flat side to the other, i.e. along the

short axis of the nucleus. In a minority of nuclei, the rye arms were aligned along the long axis of the nucleus (Fig. 7a,c, Table 1). In 12C nuclei, while the position of the heterochromatic knobs indicated preservation of the Rabl conformation, rye chromosome arms often lay diagonally or perpendicular to the general direction of the telomere/centromere axis (Fig. 7b,d). The organisation of chromosomes in 6C nuclei was intermediate between that found in 3C and 12 C nuclei. Movies of nuclei with rye chromosome arm labelling can be viewed as supplementary data.

A combination of calcofluor and DAPI staining of 16 dpa endosperm sections showed that in the majority of nuclei only part of the nuclear surface is pressed against the cell wall while the rest extends into the cell lumen, which is filled with starch. Being less rigid than starch, nuclei at this stage are mostly flattened between starch granules, and the direction in which the nucleus is squashed is perpendicular to the centromere/telomere axis (data not shown).

Discussion

Modelling of endosperm development

In this paper we have presented a new method for the histological analysis of the development of complex tissues. Precise description of development requires precise mapping of cells and nuclei. In large complex structures such as cereal endosperm, this presents severe technical challenges. In the past, complex tissues have been studied by making thin microtome sections, but this procedure necessarily only visualises a small part of the tissue and loses 3D information. Reconstruction of serial thin sections is possible in principle, but in practice becomes impossibly time-consuming and is therefore rarely used. Confocal microscopy offers a solution to the problem of 3D optical imaging, and the method we have developed combines confocal imaging with sectioning of unembedded plant material into a series of sections, each 200µm in thickness. The 3D stacks from each of the physical sections are then combined and aligned to form a complete 3D image, encompassing a greater thickness than confocal microscopy alone could achieve. In the early stages of endosperm development this 3D image can be interpreted and displayed directly. At stages older than 2 dpa, the endosperm organization is too complex to visualise through confocal sections alone and we therefore modelled the positions of nuclei and nuclear divisions in 3D to analyse endosperm development until the mature syncytial stage (4 dpa). To give an indication of the time involved: fixation and dehydration take two to three days and 15 seeds can be sectioned and scanned on the confocal microscope in two days. The segmentation analysis is the most time-consuming part and takes half a day to a day per seed. Amira was the only program we found that was capable of easily aligning the data within the composite stacks, which was vital since the stacks came from serial physical sections which could only be approximately aligned prior to confocal data collection. 3D imaging and modelling works best for objects with clearly defined surface boundaries. We used SYTOX Green as nucleic acid

stain for endosperm reconstructions because of its good penetration and defined fluorescent signal. In our context it proved superior to DAPI and other SYTOX stains. The differences in fluorescence intensity, shape and distribution density between endosperm, antipodal, embryo and seed coat nuclei enabled us to identify different tissues. The program has tools to aid segmentation, but most of the segmentation still has to be done manually depending on how well-defined different tissues are and how much they overlap within a section.

3D analysis of individual nuclei

We have shown here that the method we developed for the analysis and 3D reconstruction of complex tissues is equally applicable for the modelling of FISH signals in individual nuclei. Because of the diffuse distribution of chromatin in the interphase nucleus, clearly defined signals are difficult to obtain with FISH. However, reconstructions in Amira provided good positional information for rye chromosome arms, centromeres and telomeres. 3D models of individual nuclei were also made in ImageJ using a simpler volume projection algorithm. However, the results were not as easily interpreted and it was not possible to display several channels together or to rotate the reconstructions in arbitrary directions - a capability that was important in analysing these large and asymmetric nuclei. Counting of centromere and telomere numbers in a nucleus, on the other hand, was best done in ImageJ on raw data because signal thresholding in Amira to reduce background throughout the nucleus may lead to signal loss. In general it has to be said that the closer the size of a fluorescent signal gets to the resolution limit of the microscope the more difficult accurate modelling will be. We also made reconstructions of nuclei with large transgene loci after FISH of both the loci and their nascent transcript but found that the differentiation between actively transcribing and silent regions of the transgene locus, i.e. between regions that were associated with transcript and those that were not, was much clearer in overlays of several confocal sections of both channels in Photoshop.

Early development of cereal endosperm

In this paper we have described the early steps in wheat endosperm development. We were not able to identify the position of the initial endosperm nuclei. However, Huber & Grabe (1987a) showed the first two endosperm nuclei located next to the zygote in the embryo sac. Both Brenchley (1909) and Huber & Grabe (1987a) reported the formation of a syncytium but gave no details. Our own observations show the formation of a stem-like group of nuclei close to the zygote and joined to a dorsal plate, which then merges with a ventral plate. In most but not all cases, nuclei start filling the dorsal plate before the ventral plate. The endosperm nuclei at the embryo interface are the earliest to stop dividing, at 2 dpa (Fig. 3b, Fig. 4a), and to cellularise (Huber and Grabe, 1987a) while synchronous mitoses in other parts continue until the syncytium is complete. Maize is the only other cereal where syncytium development has been studied in any detail. There the first three endosperm cell divisions occur close to the zygote (Randolph, 1936). The products of these divisions are located at the cell periphery and concomitant with further,

largely synchronous nuclear divisions endosperm nuclei migrate to the opposite pole of the embryo sac resulting in the formation of a complete syncytium. Further studies of wheat should now address the exact mode of cell wall development at the embryo end and later in the rest of the central cell. For studies of caryopses older than 4 dpa this will require a motorised stage so that multiple images can be stitched together quickly and easily to visualize regions substantially larger than the field of view.

In summary, we have shown that 3D modelling allows accurate descriptions of nuclear structure and position during endosperm development. The method we have developed for large tissues makes use of the increased depth resolution in confocal microscopy in combination with serial physical sections. Finally, the information in the sections is simplified and condensed into 3D reconstructions, which can be rotated, assembled and disassembled on screen.

Acknowledgements
This work was supported by funding from the UK Biotechnology and Biological Science Research Council (BBSRC) and from Syngenta plc.

Supplementary material
Supplementary movies for figures 4, 5, 6 and 8 are available under the following links.
http://jicbio.bbsrc.ac.uk/fig4.mpg (40mb)
http://jicbio.bbsrc.ac.uk/fig4small.avi (7mb)
http://jicbio.bbsrc.ac.uk/fig5.mpg (70mb)
http://jicbio.bbsrc.ac.uk/fig5small.avi (8mb)
http://jicbio.bbsrc.ac.uk/fig6a.mpg (2-3mb)
http://jicbio.bbsrc.ac.uk/fig6b.mpg (2-3mb)
http://jicbio.bbsrc.ac.uk/fig6d.mpg (2-3mb)
http://jicbio.bbsrc.ac.uk/fig6e.mpg (2-3mb)
http://jicbio.bbsrc.ac.uk/fig6h.mpg (2-3mb)
http://jicbio.bbsrc.ac.uk/fig6i.mpg (2-3mb)
http://jicbio.bbsrc.ac.uk/fig8a.mpg (2-3mb)
http://jicbio.bbsrc.ac.uk/fig8c.mpg (2-3mb)

Chapter 4

Chromosome organisation in wheat endosperm and embryo

Eva Wegel and Peter Shaw*

Department of Cell and Developmental Biology, John Innes Centre, Norwich Research Park, Colney Lane, Norwich NR4 7UH, UK

Published in Cytogenetic and Genome Research (2005) 109, 175-180

Abstract

We have analysed the chromosome organisation in endosperm and embryo of bread wheat (*Triticum aestivum* L.), in order to compare these tissues with developing anthers, in which the centromeres associate, and the developing root xylem vessel cells, in which the chromosomes endoreduplicate to become polytene and associate via their centromeres. Both endosperm and embryo showed a typical Rabl configuration and a degree of non-homologous centromere association and the endosperm also showed extensive telomere association. Wheat endosperm is initially triploid and during its development a percentage of the nuclei increase their DNA-content to 6C and 12C. 6C nuclei showed twice as many centromeres as 3C nuclei and the centromere number increased further in 12C nuclei. The higher the C-content of a nucleus the more the telomeres associated in endosperm. The vast majority of 12 C nuclei showed six rye chromosome arms, although a few showed three associated groups of rye chromosome arms. This means that during endosperm development wheat nuclei show both polyploidisation and polytenisation.

Introduction

Bread wheat (*Triticum aestivum* L.) is a hexaploid species with more than 80 per cent of repetitive sequences, which are homogenised across all chromosomes (Flavell et al., 1977; Heslop-Harrison, 2000). Chromosome specific *in situ* paints, which are now used for the analysis of chromosome organisation in *Arabidpsis* (Lysak et al., 2003), are therefore still lacking in wheat. However, there are many wheat lines into which chromosomes or parts of chromosomes from other cereals such as rye have been introgressed and labelling of alien chromosomes or chromosome arms has proved a useful tool for the elucidation of chromosome organisation in this species. Wheat chromosomes span the width of the nucleus in rod-like structures with the two arms of each chromosome close together and in all *Triticeae* analysed so far centromeres and telomeres are located at opposite poles in a Rabl configuration (Abranches et al., 1998; 2001; Martínez-Pérez et al., 1999;

2000). In plants, Rabl configurations have also been found in rye, barley and oats, but not in rice or maize (Dong and Jiang, 1998). Outside the plant world Rabl configurations have been reported in yeast and in *Drosophila* (Hochstrasser et al., 1986; Jin et al., 2000).

Endosperm is derived from the fertilisation of the central cell in the megagametophyte of higher plants by a second haploid male gamete, the first one fertilising the egg cell to form the embryo. The central cell is diploid and the endosperm is therefore triploid, containing three sets of chromosomes, one paternal and two maternal. The first stage in endosperm development is characterised by nuclear divisions without cellularization. Cell wall formation starts from the periphery at day four after fertilization and is completed by day seven (van Lammeren, 1988). Subsequently some nuclei in the central starchy endosperm undergo two or three rounds of DNA replication taking the DNA content up to 12C or 24C (Brunori et al., 1989). An increase in DNA content outside the mitotic cycle can lead to polyteny (through endoreduplication, where the number of chromosomes remains constant while the number of chromatids increases) or polyploidy (an increase in number of chromosome sets) or both.

In hexaploid wheat, centromeres are associated in non-homologous pairs early in anther development. The non-homologous centromere associations become homologous premeiotically in both meiocytes and tapetal cells and the telomeres form a cluster (bouquet) at the onset of meiosis (Martínez-Pérez et al., 1999). In developing xylem vessel cells in roots chromosomes become polytene and homologues associate by their centromeres (Martínez-Pérez et al., 2001). In this study we describe the chromosome organisation in endosperm and compare it to that of the diploid embryo. We show that in contrast to xylem vessel cells polyploidisation in endosperm generally occurs through an increase in chromosome number without homologous centromere associations. A proportion of non-homologous centromere associations is found in both endosperm and embryo. Telomere associations in the endosperm increase with an increase in C-content while the percentage of centromere associations remains constant.

Materials and Methods

Plant material

The following wheat (*Triticum aestivum*) genotype was used: AABBDD, 2n=6x=42, cv. Pro INTA Federal with a 1RS (*Secale cereale*) chromosome arm substitution for the 1BS wheat chromosome arm ($1B^l/1R^s$). Plants were grown in a controlled environment room (15 ^oC, 16 h photoperiod, 70% humidity).

Seed sections

Immature seeds were harvested at 7, 16 and 24 dpa (days post-anthesis) and fixed for 6 h in 4% (w/v) formaldehyde, freshly made from paraformaldehyde, in PEM

(50 mM PIPES, 5 mM EGTA, 5 mM $MgSO_4$ pH 6.9). Endosperm tissue was analysed at 7 and 16 dpa, and embryo tissue (both root and shoot tissue) was analysed at 24 dpa. Fixed seeds were dehydrated through an ethanol:water series (10%, 20%, 40%, 60%, 80% and absolute ethanol for 4 to 12h per step) and stored in absolute ethanol at 4 ^oC. 100 μm sections were prepared under absolute ethanol using a Vibratome Series 1000plus (TAAB Laboratories Equipment Ltd., Aldermarston, UK) and rehydrated in water. They were allowed to dry on poly-lysine-coated slides (BDH, Poole, UK). Sections were incubated with 1% (w/v) driselase (Sigma, Poole, UK), 0.5% (w/v) Onozuka R10 cellulase (Yakult Pharmaceutical Ind. Co. Ltd., Tokyo, Japan), 0.025% pectolyase Y23 (Kikkoman, Tokyo, Japan) in PBS (1.6 mM NaH_2PO_4, 15 mM Na_2HPO_4, 150 mM NaCl pH 7.4) for 1 h at room temperature and washed in TBS (10 mM Tris, 140 mM NaCl pH 7.4) for 10 min. They were then treated with RNase A (Sigma, 100 μg mL^{-1} in 2x SSC (300 mM NaCl, 30 mM sodium citrate pH 7.0)) for 1h at 37 ^oC, washed in TBS for 10 min, dehydrated in an ethanol:water series (70% and absolute ethanol) and air-dried.

Probes and *in situ* hybridisation

Total rye genomic DNA was partly digested with *Taq*1 and the fragments were then labelled with biotin-16-dUTP (Roche) by nick translation. Telomeric probes labelled with biotin-16-dUTP (Roche) were prepared according to Cox et al. (1993). Centromeric probes labelled with digoxigenin-11-dUTP (Roche) were prepared according to Aragón-Alcaide (1996) using the following primers for the CCS1 repeat fragment: 5'CGCAATATCTTGATTGCATCTATATTC3' (positions 17 to 43) and 5'GCTGGTAGTGAAAAGGTGCCCGATCTT3' (positions 249 to 223). Sections were first treated with the avidin/biotin blocking kit (Vector Laboratories, Burlingame, California, US) according to the manufacturer's instructions using a biotin blocking step followed by avidin and biotin, respectively, to block biotin binding sites in the tissue. After a final wash in PBS, FISH was performed in a slightly modified version of Abranches et al. (2000) using 200 ng of each probe in a total volume of 30 μL per slide in a hybridisation buffer containing 20x excess salmon sperm DNA in 50% formamide, 10% dextran sulfate, 2x SSC and 0.1% SDS. The probe was denatured in the hybridisation mixture for 5 min at 95 ^oC. Sections were denatured at 75 ^oC for 8 min in a modified thermocycler (Omnislide, Hybaid, Ashford, UK), and hybridisation carried out overnight at 37 ^oC. Post-hybridisation washes were carried out in 0.1x SSC, 20% formamide at 42 ^oC.

Immunodetection

Biotin-labelled probes were detected with Extravidin-Cy3 (Sigma). Probe labelled with digoxigenin was detected with a mouse anti-digoxin antibody (Sigma) followed by a secondary goat anti mouse antibody conjugated to Alexa Fluor® 488 (Molecular Probes, Leiden, The Netherlands). Antibodies were diluted in 4x SSC, 0.2% Tween 20 according to the manufacturer's instructions. Antibody incubation was performed in a humid chamber for 1 h at 37 ^oC followed by 3x 5 min washes in

4x SSC, 0.2% Tween 20 at room temperature. Sections were counterstained in 1 μg mL^{-1} DAPI for 10 min. Slides were mounted in Vectashield (Vector Laboratories).

Image acquisition and analysis
Hybridised sections were analysed on a Leica TCS SP2 confocal microscope (Leica Microsystems GmbH, Heidelberg, Germany) equipped with two Argon lasers (351, 363 nm and 457, 488, 514 nm respectively) and two Helium/Neon lasers (543 nm and 633 nm respectively). Section spacing was 0.6 μm. The confocal data were then transferred to ImageJ (a public domain program by W. Rasband available from http://rsb.info.nih.gov/ij/). All images were composed using Adobe Photoshop 7.0 (Adobe Systems Inc., Mountain View, CA). C values were estimated for individual nuclei from nuclear volume and DAPI fluorescence intensity.

Flow cytometry
For each experiment six to eight isolated embryos from 24 dpa seeds were chopped up with a razor blade and extracted using a two-step disaggregation and DAPI staining kit (CyStain UV Precise P, Partec, Münster, Germany) according to the manufacturer's instructions. The extracts were passed through a 30 μm filter and stored on ice until measurement. The DNA content of nuclei (C value) was measured using a Ploidy Analyser PA-II (Partec) with UV excitation by a mercury arc lamp. Six independent experiments were carried out and between 18 000 and 20 000 nuclei were measured each time. Nuclei from young wheat leaves were used as a standard to determine the positions of 2C and 4C.

Results

We investigated chromosome territories in endosperm and embryo of wheat. For the endosperm we chose two time points: 7dpa (days post-anthesis) where 72% of the nuclei are 3C, 27% 6C and the rest greater than 6C and 16 dpa where 40% are 3C, 48% 6C and 12% 12C (as determined by flow cytometry – chapter 5). Both embryo and endosperm nuclei showed Rabl configurations with centromeres at one pole of the nucleus and the telomeres at the other (Fig. 1). In the embryo, centromere foci varied greatly in size even within a single nucleus indicating associations among centromeres - whereas telomere foci were more uniform. In the endosperm, centromere foci varied little in size irrespective of the C content of the nucleus. The size of the telomere foci was more variable: small nuclei showed small telomeres, but the telomere signal in larger nuclei ranged from small foci to much bigger ones. Also, in 12C nuclei the number of telomeres did not seem to have increased to the same extent as the number of centromeres.

To quantify our observations we counted the numbers of centromeres and telomeres in endosperm nuclei and centromere numbers in embryo nuclei. Since the density of nuclei in embryo tissue was very high and telomere signal was found on half the nuclear surface it was difficult to distinguish between telomeres

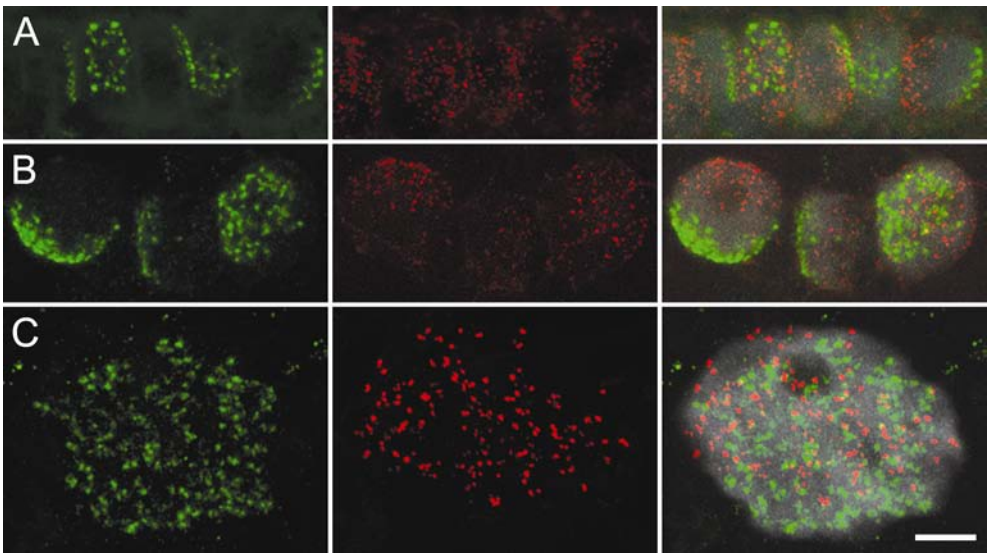

Figure 1. Centromeres and telomeres in embryo and endosperm of wheat show a Rabl configuration with telomeres at one pole and centromeres at the other.
Confocal stacks spanning the depth of the nuclei. Centromeres are shown in green, telomeres in red. Chromatin (grey) was counterstained with DAPI. (A) Embryo root. All embryo tissues show the same centromere and telomere conformation, but root nuclei are stacked in files and therefore easier to visualise. (B) to (C) endosperm. (B) 3C nuclei at 7 dpa. (C) 16 dpa. Frontal view of an endoreduplicated (12C) nucleus. Note the much greater variation in telomere size compared to (B). Bar, 10 μm.

from different nuclei and accurate counts could not be made. Centromere association was found in both endosperm and embryo nuclei (Table 1). In the embryo, 2C and 4C nuclei were difficult to tell apart by size and could not be distinguished by centromere counts, which averaged at 27 per nucleus. We determined the C-content in embryo nuclei by flow cytometry in six independent experiments and found 85% (± 3) 2C nuclei and 14% (± 2) 4C nuclei. In one experiment 5% 8C nuclei were found, while the other samples contained insignificant amounts. The centromere data for the endosperm therefore mainly reflected the numbers from 2C nuclei. In endosperm, 6C nuclei showed twice as many centromere signals as 3C ones (92 compared to 48) (Table 1). Based on a haploid chromosome number of 21 we would expect 63 chromatids for 3C nuclei and 126 for 6C nuclei. Thus, an average of 48% of the centromeres in 3C and 54% of the centromeres in 6C nuclei were associated (Table 1). Plotting centromere counts against telomere counts in 53 endosperm nuclei shows that the higher the C-content the more telomeres associate in endosperm: 50 centromeres corresponding to 95 telomeres, 100 centromeres corresponding to 139 telomeres and 200 centromeres to 225 telomeres (Fig. 2).

Table 1. Centromere numbers in endosperm and embryo

Tissue	age	centromeres	nuclei counted	% centromere association
Embryo	24 dpa	27.2 ± 6.0	41 (2C + 4C*)	35 ± 14
Endosperm	7 dpa	47.8 ± 7.5	39 (3C)	48 ± 24
Endosperm	16 dpa	92.3 ± 11.6	19 (6C)	54 ± 18

* A DNA content of 2C was measured in 85% of embryo nuclei.

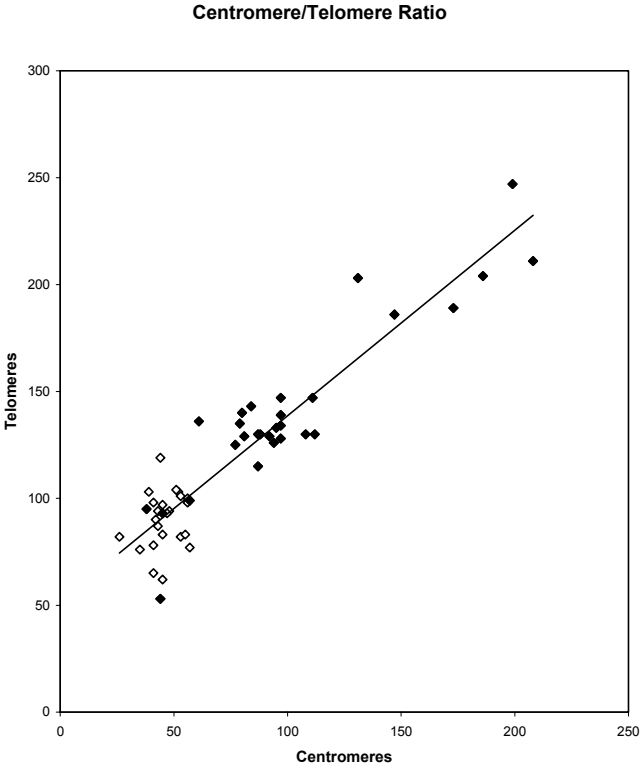

Figure 2.
Correlation between telomere/centromere ratio and C content in endosperm nuclei
Clusters corresponding to 3C and 6C are clearly distinguishable, but the numbers of telomeres and centromeres seen are lower than expected. There is a linear correlation between the number of telomeres and centromeres; the telomere/centromere ratio decreases as the number of centromeres increases. The slope of the trend line is y=0.87x+51.8. Open diamonds: 7dpa. Black diamonds: 16 dpa. The data from the two different timepoints follow the same overall trend.

Labelling of the rye chromosome arms showed that both centromere and telomere associations in embryo and endosperm are non-homologous, since the two or three labelled, homologous chromosome arms in embryo or endosperm respectively are clearly separated (Fig. 3). The three rye chromosome arms in 6C nuclei were broader than those in 3C nuclei and often separated towards the centromeres (Fig. 3 B, C). These observations provide an explanation for the results of the centromere and telomere counts in endosperm: after S-phase, the centromeres begin to dissociate, resulting in a doubling of the number of visible sites, while the telomeres have a strong tendency to remain associated, resulting in a significantly smaller number of visible sites than expected. Some medium sized nuclei, presumably with a DNA content of 6C, showed six separate rye chromosome arms, most notably a few cells at 6 dpa (Fig. 3 B). 12C nuclei usually contained six rye chromosome arms (Fig. 3 D). Occasionally nuclei with separating chromatids were

seen (Fig. 3 F), but we found only two 12C nuclei out of 14 examined where the chromosome arms remained associated in three groups (Fig 3 E).

Discussion

In this study we have shown that the DNA increase in wheat endosperm leads to both polyploidy and polyteny. Evidence for the former comes from the doubling of centromere numbers in 6C nuclei compared to 3C nuclei and the observation of six rye chromosome arms in these cells. Evidence for the latter comes from the frequent occurrence of 12C nuclei with six rye chromosome arms, which must each carry two chromatids and the occasional observation of 12C nuclei with three groups of rye chromosome arms, which must have four chromatids (Fig. 3 D, E). In contrast to this, in developing xylem vessel cells in wheat roots, two regions of labelled rye chromatin remained through successive rounds of endoreduplication producing polytene chromosomes (Martínez-Pérez et al., 2001). In the most extensively studied cereal, maize, evidence exists for both polyteny, which seems to play the major part, and polyploidy, which was found in some nuclei in younger, actively dividing endosperm tissue (for an overview see Kowles and Phillips, 1988). The latter corresponds to our findings of nuclei with six separated rye chromosome arms at 7 dpa. Our image data show that chromatids separate along their lengths and later assume widely separated positions within the nucleus (Fig. 3 F).

A process leading to the doubling of chromosomes within a nucleus was first described by Geitler (1939): in endomitosis chromosomes contract, the chromatids separate parallel to each other without the formation of a spindle apparatus and decondense again to their interphase conformation while the nuclear envelope remains intact throughout. Endomitosis occurs more frequently in animals and humans and has been studied intensively in megakaryocytes, which are a special case because the nuclear envelope breaks down in each cycle and a spindle is formed (Italiano and Shivdasani, 2003). In some plants, endomitosis has been found in the cells of the anther tapetum (D'Amato, 1984; Oksala and Therman, 1977). In wheat tapetal cells nuclei divide to form binucleate cells (Bennett et al., 1973). In contrast to the data presented for the tapetum, the separation of chromatids in wheat endosperm does not always happen simultaneously in all chromosomes (Fig. 3 F). Cell cycle regulators have been shown to be involved in megakaryocyte endomitosis (Italiano and Shivdasani, 2003) and in endoreduplication in maize endosperm (Grafi and Larkins, 1995). No data are available yet on the regulation of the spindle formation in megakaryocytes. Spindle formation during endomitosis in wheat endosperm is unlikely since chromatid separation is not synchronized, but as the six rye chromosomes are widely distributed, the microtubule network might play a role in the movement of the separated chromatids away from each other.

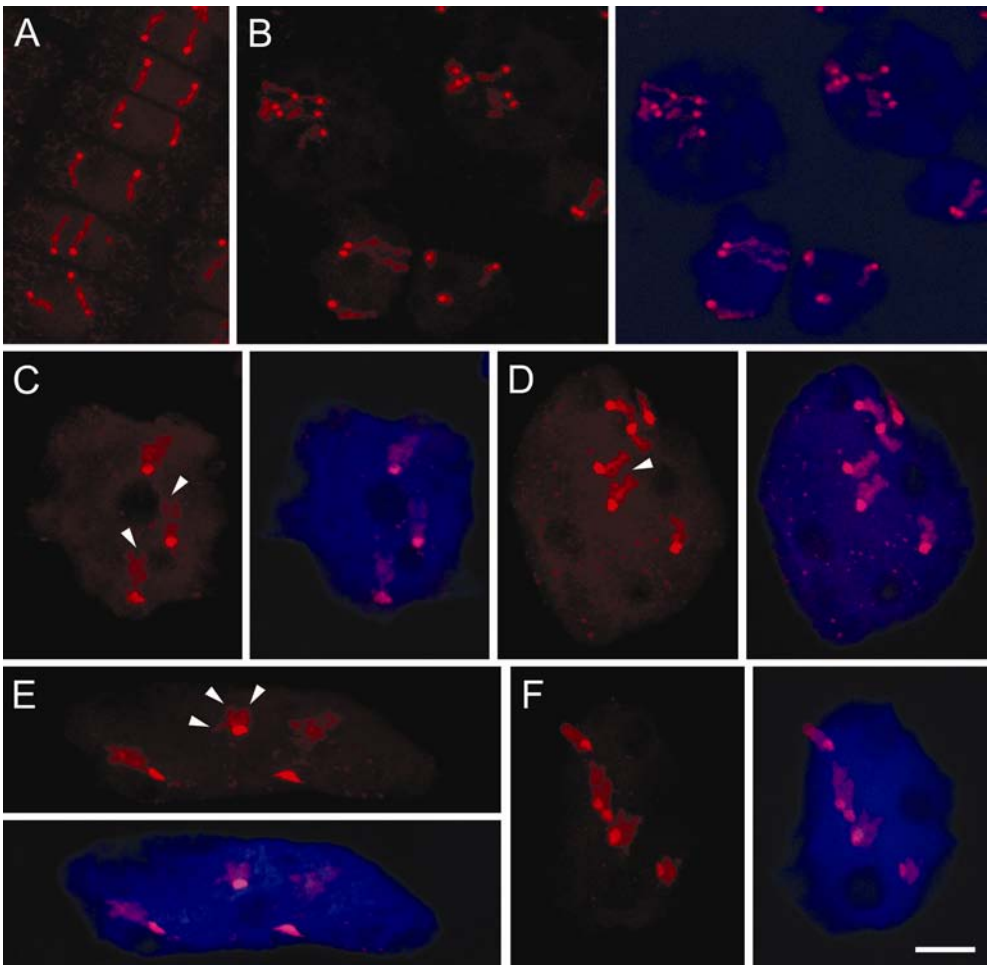

Figure 3. Rye chromosome arms in a wheat background span the whole of the nucleus in both embryo and endosperm and are not grouped together.
Confocal stacks spanning the depth of the nuclei. Rye arms in red with a bright subetelomeric heterochromatin knob, DAPI counterstaining of the nuclei in blue. (A) Embryo root showing two rye arms. (B) to (F) endosperm. (B) 7 dpa. The top two nuclei are bigger than other nuclei at this stage, show six separate rye arms and occur only occasionally in central parts of the endosperm. (C) to (F) 16 dpa. (C) 6C nucleus with three rye arms. Both chromatids overlap at the telomeres, but separate towards the centromeres (arrow heads). (D) 12C nucleus with six rye arms. Chromatids of two rye chromosome arms seem to separate towards the centromeres (arrow head). (E) 12C nucleus where several chromatids remain associated (arrow heads). (F) 6C nucleus with chromatids at different stages of separation: at the periphery two single chromatids, in the centre two chromatids that are splitting at the centromeres and two chromatids lying next to each other with two discernable telomeres. Bar, 10 μm.

Acknowledgements
E. Wegel was supported by the BBSRC Gene Flow Project. We thank Dr. Hans de Jong for critical reading of the manuscript.

Chapter 5

Large-scale chromatin decondensation induced in a developmentally activated transgene locus

Eva Wegel,[a] Ruben H. Vallejos,[b] Paul Christou,[c] Eva Stöger,[d] and Peter Shaw[a,]

[a] Department of Cell and Developmental Biology, John Innes Centre, Norwich Research Park, Colney Lane, Norwich NR4 7UH, UK
[b] Centro de Estudios Fotosintéticos y Bioquímicos (CEFOBI), CONICET-UNR-F-LILLO, Suipacha 531, S202LRK Rosario, Argentina
[c] Fraunhofer Institute for Molecular Biology and Applied Ecology, IME, Grafschaft, Auf dem Aberg 1, 57392 Schmallenberg, Germany
[d] Institute of Molecular Biotechnology, BiologieVII, RWTH Aachen, Worringerweg 1, 52074 Aachen, Germany

Published in Journal of Cell Science (2005) 118, 1021-1031

Summary

The High Molecular Weight (HMW) glutenin genes in wheat are developmentally activated in the endosperm at about 8 days post anthesis (dpa). We have investigated the physical changes that occur in these genes in two transgenic lines containing about 20 and 50 copies respectively of the HMW glutenin genes together with their promoters. By fluorescence in situ hybridisation (FISH) and confocal imaging, we demonstrate that in non-expressing tissue each transgene locus consists of one or two highly condensed sites, which decondense into many foci upon activation of transcription in endosperm nuclei. Initiation of transcription can precede decondensation but not vice versa. We show that in one of the lines, cytoplasmic transcript levels are high after onset of transcription, but disappear by 14 dpa, while siRNAs, indicative of post-transcriptional gene silencing (PTGS), are detected at this stage. However, the transcript levels remain high at the transcription sites, the great majority of the transgene copies are transcriptionally active and transcriptional activity in the nucleus ceases only with cell death at the end of endosperm development.

Introduction

In recent years, several studies using mammalian cell cultures have shown that chromatin decondenses when it becomes transcriptionally active. Employing the *lac* operator/repressor interaction, Tumbar et al. (1999) showed that targeting of the acidic activation domain of the herpes simplex virus transcriptional activator

VP16 to specific chromosomal sites resulted in the unfolding of the sites and their transcriptional activation. Tsukamoto et al. (2000) made use of the same *lac* operator/repressor sequence in a different environment and hormonally induced chromatin decondensation at the transgene locus. Müller et al. (2001) reported different degrees of decondensation depending on the level of transcription of their reporter genes after the activation of the mouse mammary tumour virus promoter by its cognate transcription factor. In plants, two studies on Arabidopsis have recently shown decondensation of a previously hypermethylated and silenced transgene locus in the background of a *decrease in DNA methylation1* (*ddm1*) mutant and looping out of a fraction of the rDNA loci correlated with an overall increase in rDNA transcript in the leaves of developing seedlings (Mathieu et al., 2003; Probst et al., 2003). In mammalian cell cultures, highly transcribed chromosomal regions have been found to extend away from chromosomal territories when they become transcriptionally active, which seems to be the result of chromatin decondensation over one to several megabases (Volpi et al., 2000; Williams et al., 2002) and recently looping out of genes from the chromosome territory has also been reported for a gene cluster of 90 Kb (Chambeyron and Bickmore, 2004). Transcript at the site of transcription has been localized in various animal and human cell lines (Custódio et al., 1999; Dirks et al., 1995; Müller et al., 2001; Tsukamoto et al., 2000; Xing et al., 1993). Different patterns of the main RNA signal inside the nucleus were observed ranging from dots to elongated dots and tracks. In plants, previously only ribosomal RNAs have been located with their gene loci (González-Melendi et al., 2001; Highett et al., 1993).

We have used the activation of storage protein expression in a transgenic bread wheat line to study changes in the physical organization of a transgene locus upon transcriptional activation. One group of these proteins are the high molecular weight (HMW) subunits of the glutenins, which account for up to 12% of the total grain protein content and are only expressed in the endosperm of developing wheat grain (for a review see Shewry et al., 2003). HMW glutenin genes are located on the long arms of the chromosomes 1A, 1B and 1D. Each locus contains two genes. One of the six genes is always silenced and cultivated wheat expresses three to five genes depending on the variety (Shewry et al., 2003). The HMW subunits are activated about 8 days post anthesis (dpa) and the transcripts disappear between 36 and 38 dpa (Altenbach et al., 2002). Previously, wheat genomic clones encoding the high molecular weight glutenin subunits 1Ax1 and 1Dx5, together with their promoter regions, had been introduced into the commercial wheat cultivar Federal which expresses the endogenous subunits 1Ax2*, 1Bx7, 1By9, 1Dx5 and 1Dy10. Two of the resulting transgenic lines containing an estimated 20 copies (line E) and 50 copies (line F) of the transgenes were substantially silenced resulting in a 60% (line F) to 90% reduction (line E) in total HMW glutenin protein compared to the wild-type (Alvarez et al., 2000).

Two types of silencing are known: transcriptional gene silencing (TGS) and post-transcriptional gene silencing (PTGS). TGS usually occurs via methylation of

promoter sequences, which causes transcription to cease. PTGS is characterized by ongoing transcription, subsequent transcript degradation, and the appearance of small interfering RNAs (siRNAs) of 21–25 bp lengths (Hamilton and Baulcombe, 1999; Zamore et al., 2000), which are produced by a double-stranded RNA-specific endonuclease (Dicer) that was first detected in *Drosophila* (Bernstein et al., 2001). Dicer-like enzyme activity has also been found in wheat germ extract (Tang et al., 2003). SiRNAs can guide heterochromatin formation and therefore TGS through RNA-directed methylation of homologous DNA and through methylation of histone H3 at lysine 9 (Finnegan and Matzke, 2003; Matzke et al., 2001; Schramke and Allshire, 2003).

Here we show that the transgene loci in both line E and line F are visible as condensed foci in tissues where they are not transcriptionally active and decondense in transcriptionally active tissue. A detailed analysis of line E reveals that decondensation starts upon transcriptional activation in the endosperm at 8 dpa, although the onset of transcription can precede any visible decondensation. The great majority of the transgene copies are transcriptionally active and transcriptional activity in the nucleus ceases only with cell death at the end of endosperm development. We also show that the transcript is absent from the cytoplasm by 14 dpa while siRNAs can be detected in RNA extracts from seeds of the same age, indicating that the silencing mechanism is PTGS. Transcripts at the loci remain high throughout the silenced period.

Materials and Methods

Plant material

Triticum aestivum L., cv Pro INTA Federal and the transgenic lines E and F, which had been generated from Federal by particle bombardment (Alvarez et al., 2000), were used for the experiments. The following plasmids had been used in equimolar concentrations for the transformation: pHMW1Dx5 (Halford et al., 1989) containing the complete coding sequence of the 1Dx5 gene, pHMW1Ax1 (Halford et al., 1992) containing the complete coding sequence of the 1Ax1 gene, pAHC25 (Christensen and Quail, 1996) containing the bar resistance gene and the gus marker gene. Line E and F contain ca. 20 and 50 copies respectively of pHMW1Ax1 and pHMW1Dx5. All plants were homozygous.

Preparation of wheat roots for FISH analysis in metaphase spreads and root sections

Seeds were germinated in a Petri dish lined with wet filter paper for three days and root tips approximately 5 mm long were excised. Metaphase spreads and tissue sections for the analysis of interphase nuclei were prepared according to Abranches et al. (2000) including pretreatments for in situ hybridisation. The protocol included RNase A treatment to remove transcript.

Preparation of wheat seeds for sectioning

Wheat plants were grown in a controlled environment room (15ºC, 16 hour photoperiod, 70% humidity). For preparation of tissue sections, immature seeds were harvested at different time points and fixed for 6 hours in 4% (w/v) formaldehyde in PEM (50mM PIPES, 5mM EGTA, 5 mM $MgSO_4$, pH 6.9). For wax sectioning, seeds were fixed as above and embedded in wax in a Sakura Tissue-Tek Vacuum Infiltration Processor (Bayer Diagnostics, Newbury, Berkshire, UK) using the manufacturer's recommended protocol. For unembedded vibratome sectioning, fixed seeds were dehydrated through an ethanol:water series (10%, 20%, 40%, 60%, 80% and absolute ethanol for 4 to 12 hours per step) and stored in absolute ethanol at 4ºC prior to sectioning.

Seed sections

30 μm wax sections from embedded seeds were cut on a Leica RM2055 microtome (Leica, Nussloch, Germany). Sections were allowed to dry on poly-lysine-coated slides (BDH). 100 μm sections from unembedded seeds were prepared under absolute ethanol using a Vibratome Series 1000plus (TAAB Laboratories Equipment Ltd., Aldermarston, UK) and rehydrated in water. Wax sections from embedded seeds for RNA in situ hybridisation were pretreated according to Jackson (1991) with the following modifications: Histoclear treatments were for 30 minutes each and no NaCl was included in the ethanol series. Also, before the pronase treatment the sections were treated with 2% (w/v) Onozuka R10 cellulase (Yakult Pharmaceutical Ind. Co. Ltd., Tokyo, Japan) in TBS (10 mM Tris, 140 mM NaCl, pH 7.4) for 30 minutes at room temperature. The final fixation step was omitted. After histoclear treatment and rehydration wax sections for DNA FISH were treated by incubation with cellulase for 1 hour and washed in TBS for 10 minutes. The slides were then incubated in 0.1 mg/mL RNase A (Sigma) in 2x SSC for 1h at 37 ºC prior to another wash in TBS. After dehydration in an ethanol:water series (70% and absolute ethanol) the slides were air-dried. Sections from unembedded seeds were treated with cellulase for 1 hour like the wax sections followed by RNase treatment when transcript detection was not required.

Probes and in situ hybridisation

Probes were made from the same plasmids that had been used for the transformation (Alvarez et al., 2000): pHMW1Dx5 (Halford et al., 1989) containing a 8.7-Kb *Eco*RI genomic fragment including the complete coding sequence of the 1Dx5 gene (Anderson et al., 1989, accession no. X12928), flanked by approximately 3.8 Kb and 2.2 Kb of 5′ and 3′ sequences, respectively; pHMW1Ax1 (Halford et al., 1992, accession no. TAGL1AX1) containing a 7.0-Kb *Eco*RI fragment including the complete coding sequence of the 1Ax1 gene, flanked by approximately 2.2 and 2.1 Kb of 5′ and 3′ sequences, respectively. For chromosome spreads, probes were made by nick translation of the *Eco*RI fragments of both genes labelled with digoxigenin-11-dUTP (Roche) and of PUC19 labelled with biotin-16-dUTP (Roche). For labelling of the locus on its own in sections, probes were prepared by nick translation of pHMW1Dx5 and pHMW1Ax1 labelled with digoxigenin-11-dUTP or

biotin-16-dUTP. For the RNA time-course experiment, digoxigenin-11-UTP labelled sense and antisense probes were prepared by in vitro transcription of the PCR-amplified 2.5-Kb coding region of 1Ax1 (forward primer: 5'TACGATTAACCCTCACTAAAGGAGATGACTAAGCGGTTGGTTC3', reverse primer: 5'TACGAATACGACTCACTATAGGAGCTGCAGAGAGTTCTATCAC3', both with overhanging primers for T3 polymerase and T7 polymerase, respectively). Biotin-16-UTP labelled probes using the same primers were prepared for transcript detection in double labelling experiments. In the same experiments, the loci were detected by digoxigenin-11-UTP labelled sense and antisense probes prepared by in vitro transcription of the PCR-amplified vector and gene flanking sequences of 1Ax1 and 1Dx5 of the sizes described above. The following primers were used for PCR:
5'TACGAATACGACTCACTATAGCGTTTTACAACGTCGTGACTGGG3',
5'TACGATTAACCCTCACTAAAGCCTGTGTGAAATTGTTATCCGCT3' (vector PUC19), 5'TACGAATACGACTCACTATAGGTGGACTGTCGGTGAATTGATC3',
5'TACGATTAACCCTCACTAAAGCCCAGTCACGACGTTGTAAAACG3' (left genomic flank of 1Ax1),
5'TACGAATACGACTCACTATAGCTTAGGCATGCATGCACCTTAG3',
5'TACGATTAACCCTCACTAAAGAGCGGATAACAATTTCACACAGG3' (right genomic flank of 1Ax1),
5'TACGAATACGACTCACTATAGCGGTGTTGTGGGTGATGATAAG3',
5'TACGATTAACCCTCACTAAAGCCCAGTCACGACGTTGTAAAACG3' (left genomic flank of 1Dx5),
5'TACGAATACGACTCACTATAGGCTTAGGCATGCATGCCTTTAG3',
5'TACGATTAACCCTCACTAAAGAGCGGATAACAATTTCACACAGG3' (right genomic flank of 1Dx5).

Fig. 1 illustrates the positions on the plasmids of the probes used for single and double labelling of interphase nuclei. Added on to the forward and reverse primers are the primers for T3 polymerase and T7 polymerase, respectively. 0.5 - 1 μg of template was used for the in vitro transcription reactions and all in vitro transcription probes were size reduced to an average of 75 bases using alkaline hydrolysis in a 100mM carbonate buffer (pH 10.2) at 60ºC. Approximately 2-4% of each in vitro transcription reaction was used alone (1Ax1 coding region) or in a probe mixture (flanking sequences and vector) in a total volume of 40 μL per slide in a modified hybridisation buffer according to Ingham et al. (1985). All probes were heat denatured and cooled on ice immediately before hybridisation. For the detection of the HMW glutenin genes on metaphase spreads, a mixture of the *Eco*RI fragments of 1Ax1 and 1Dx5 was used with the combined concentration of 100 ng and in addition 100 ng PUC19 probe per slide for the identification of the transgene loci. A mixture of HMW-1Ax1 and HMW-1Dx5 (200 ng probe per slide) was used for all experiments that did not include transcript detection. FISH on chromosome spreads and sections without transcript detection was performed according to Abranches et al. (2000). The hybridisation for the RNA expression time-course was carried out at 50ºC overnight. Slides were washed in 2x SSC, 50% formamide at 50ºC followed by 1x SSC, 50% formamide at 50ºC. For the

simultaneous detection of transgene loci and transcript unembedded sections of wheat seeds were first treated with the avidin/biotin blocking kit (Vector Laboratories, Burlingame, California, US) according to the manufacturer's instructions using a biotin blocking step followed by avidin followed by biotin to block biotin binding sites in the tissue. After a final wash in PBS they were immediately hybridised with the antisense or sense in vitro transcription probe for the coding region of 1Ax1 at 37°C for 7 hours. Post-hybridisation washes were carried out in 2x SSC, 50% formamide at 50°C followed by 1x SSC, 50% formamide at 50°C. After a short wash in 2x SSC the slides were fixed for 10 minutes in 4% formaldehyde in PEM followed by 3 short washes in 2x SSC. They were then immediately hybridised with the probe mixture for the locus detection in a modified Thermocycler (Omnislide, Hybaid, Ashford, UK) with a chromatin-denaturing step at 75°C for 8 minutes and hybridisation at 37 °C overnight. Post-hybridisation washes were carried out using 2x SSC, 50% formamide at 50°C followed by 1x SSC, 50% formamide at 50°C.

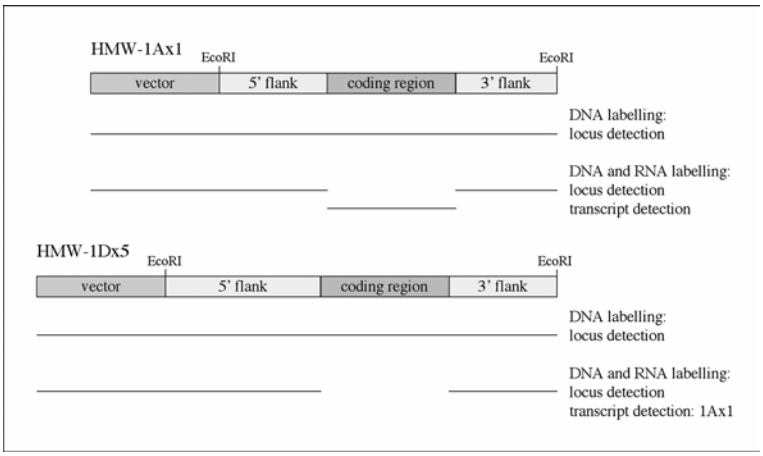

Figure 1. Probes used for locus and transcript detection in interphase nuclei

Immunodetection of DNA and RNA probes

Biotin-labelled probe for chromosome spreads was detected with Extravidin-Cy3 (Sigma). Biotin-labelled probe for the transcript in seed sections was detected with a streptavidin Alexa Fluor® 633 conjugate (Molecular Probes, Leiden, The Netherlands) to avoid overlap with the emission spectrum of Alexa Fluor® 488 used for the locus detection. For all FISH experiments, probes labelled with digoxigenin were detected with a mouse anti-digoxin antibody (Sigma) followed by a secondary goat anti mouse antibody conjugated to Alexa Fluor® 488 (Molecular Probes). Antibodies were diluted in 4x SSC, 0.2% Tween 20 according to the manufacturer's instructions. Antibody incubation was performed in a humid chamber for 1 h at 37°C followed by 3x 5 minute washes in 4x SSC, 0.2% Tween 20 at room temperature. Metaphase slides were counterstained with 6 μg mL^{-1} 4', 6-

diamidino-2-phenylindole (DAPI, Sigma) for 10 minutes. Sections were counterstained in 1 μg mL^{-1} DAPI for 4 minutes (root tips) or 10 minutes (seeds). For the RNA time-course experiments, digoxigenin-labelled probes were detected as described in the Roche digoxigenin–nucleic acid detection kit with modifications according to Coen et al. (1990). Alternatively they were detected with Alexa Fluor® 488 and the slides counterstained with DAPI as described above. All slides were mounted in Vectashield (Vector Laboratories).

Image acquisition, analysis and measurements

Chromosome spreads and the RNA time-course experiments were analysed with a Nikon E600 microscope. Photographs were either taken on Fujicolor 400 print film and digitalized with a Microtek ScanMaker 5 or they were taken on a Nikon Coolpix 990 digital camera. Vibratome tissue sections in FISH experiments were analysed on a Leica TCS SP2 confocal microscope (Leica Microsystems GmbH, Heidelberg, Germany) equipped with two Argon lasers (351, 363 nm and 457, 488, 514 nm respectively) and two Helium/Neon lasers (543 nm and 633 nm respectively). The confocal microscopy data were then transferred to ImageJ (a public domain program by W. Rasband available from http://rsb.info.nih.gov/ij/). Measurements of nuclear and locus volumes were done as follows. For each section the extent of fluorescence was determined either by thresholding and using a plug-in for ImageJ called 'voxel counter' (loci) or by tracing the edge of the fluorescent area by hand and measuring the area using one of the program tools (nuclei). Volumes were determined by multiplying the areas by the spacing of the optical sections or by multiplying the number of voxels counted by the voxel volume. We also made linear length measurements of the paths connecting fluorescent foci from the same locus. While the volume measurements only took fluorescent regions into account, the locus length measurements included the shortest distance in three dimensions between two fluorescent foci belonging to the same locus and the length of the foci themselves. The non-expressing locus in endosperm, which in metaphase chromosomes is often seen as two foci and therefore contains a large intervening portion of genomic DNA, could be composed of one focus or two at variable distance to each other. Likewise, the decondensed loci were measured in three dimensions from the first focus through to the last within the linear path including gaps between foci, but this measurement could only be done in nuclei where a clear linear path was discernable. Nuclei at 6dpa were never found to express the HMW glutenin genes and all nuclei at 10 dpa onwards did express them, as judged by transcript labelling. All images were composed using Adobe Photoshop 7.0 (Adobe Systems Inc., Mountain View, CA).

Detection of small interfering RNAs

RNA extraction and detection of small interfering RNAs were done according to Hamilton and Baulcombe (1999). The antisense probe for the small RNA gel was prepared by in vitro transcription of the PCR-amplified coding region of 1Ax1 using the primers described above and labelled with α^{32}P-UTP (Amersham).

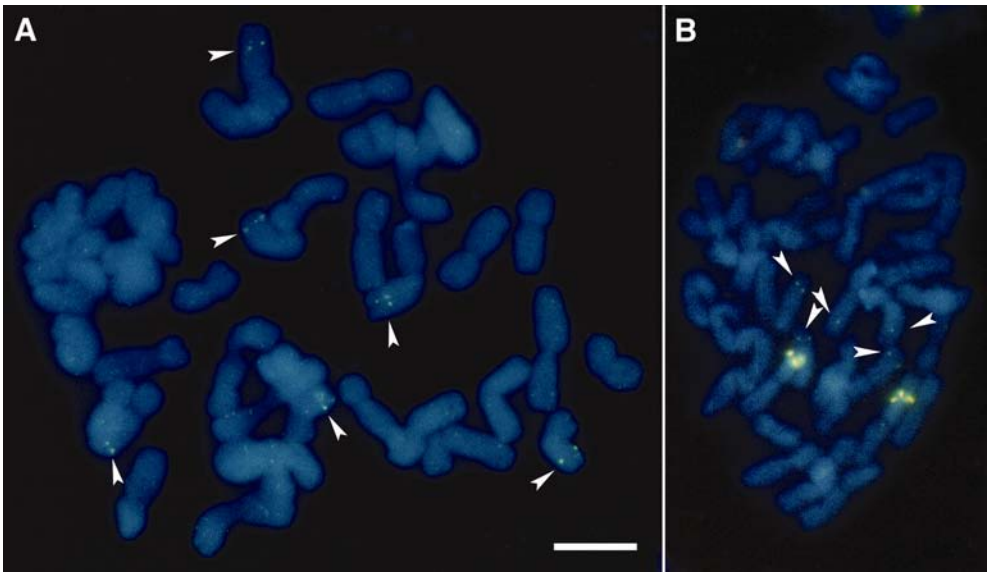

Figure 2. FISH analysis on metaphase chromosomes
Metaphase spreads were hybridised with probes detecting the genomic fragments (green) and the vector sequences (red). (A) HMW glutenin subunit loci in wild-type wheat (arrowheads); (B) Transgene loci (orange, hybridising with both genomic and vector sequences) and gene loci (green, arrowheads) of HMW glutenin subunits in line E; bar, 10 μm.

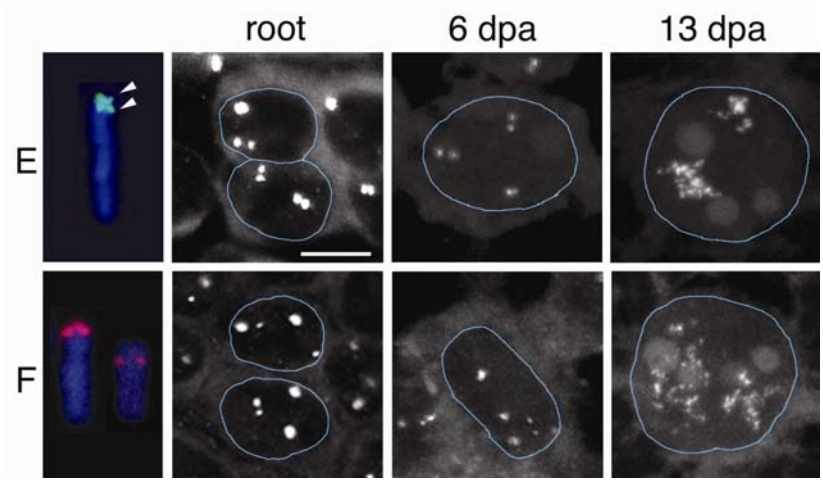

Figure 3

Flow cytometry

Isolated endosperms were chopped with a razor blade and extracted using a two-step disaggregation and DAPI staining kit (CyStain UV Precise P, Partec, Münster, Germany) according to the manufacturer's instructions. The extracts were passed through a 50 μm filter and stored on ice until measurement. The DNA content of nuclei (C value) was measured using a Ploidy Analyser PA-II (Partec) with UV excitation by a mercury arc lamp. For each sample between 6000 and 16 000 nuclei were measured. Nuclei from young wheat leaves were used as a standard to determine the positions of 2C and 4C. The results were presented in histograms in a logarithmic scale to avoid missing peaks of higher C values.

Results

Transgene integration pattern on metaphase chromosomes

The integration pattern of the transgene copies in lines E and F was analysed by FISH on metaphase spreads. The genomic fragments containing 1Ax1 (accession no. TAGL1AX1) and 1Dx5 (accession no. X12928) were labelled with digoxigenin as probes for the endogenous and transgenic HMW subunits, while biotin-labelled vector, pUC19, was used to identify the transgene sites. Both clones HMW-1Ax1 and HMW-1Dx5 labelled the transgene loci very strongly and hybridised with the endogenous loci strongly enough to just detect them. The vector probe labelled only the transgene integration sites. The FISH results for the two homozygous lines showed two integration sites close together on one chromosome arm in line E (Fig. 2 and 3) and one large locus and one small locus on two chromosomes in line F (Fig. 3). Co-hybridisation with a probe coding for repetitive sequences from *Aegilops squarrosa* resulted in a distinct banding pattern for each of the three chromosomes meaning that the insertions in line E and F are in different chromosomes (data not shown). The integration sites did not correspond to any of the group 1 chromosomes carrying the endogenous HMW glutenin genes (shown for line E in Fig. 2, data for line F not shown).

Figure 3. Transgene locus structure in non-expressing and expressing tissue
Top row: line E. bottom row: line F. Left: chromosomes with transgene loci. Two loci very close together are visible in line E (arrow heads), probe: genomic fragments of 1Ax1 and 1Dx5. Line F contains two chromosomes with transgene loci, probe: vector sequence. Tissue sections of line E and F were hybridised with HMW-1Ax1 and HMW-1Dx5 to detect the transgene loci in the diploid root as non-expressing tissue and in the triploid endosperm at 6 dpa, before the onset of expression, and at 13 dpa, after the onset of expression. The image shows projections of serial confocal sections through one layer of nuclei. A blue line is drawn around the edge of each nucleus. The insertion sites in E are visible as one or two foci in root tips and young endosperm, while each locus in line F is visible as one focus. In expressing endosperm tissue, the loci in both lines are decondensed into many foci. Bar, 10 μm, section spacing: 0.6 μm

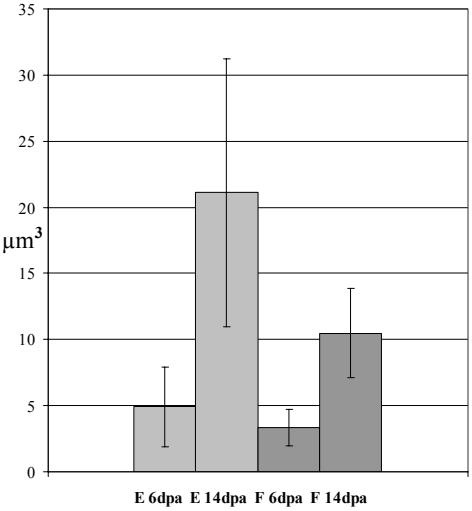

Figure 4. Locus decondensation in line E and F
After hybridisation with HMW-1Ax1 and HMW-1Dx5 to detect the transgene loci the fluorescent area per optical section was measured in 79 and 18 randomly selected nuclei of line E and F respectively at 6 dpa and in 59 and 18 nuclei of line E and F respectively at 14 dpa. The total number of voxels in the fluorescent region per nucleus was multiplied by the voxel volume and the resulting fluorescent volume is shown on the y-axis.

Expression-related changes in 3D gene organization I

In initial experiments, the 3D transgene locus structure in both lines was compared in expressing and non-expressing tissue. Root tips and endosperm at 6dpa, before the onset of expression, and at 13 dpa, after the onset of expression, were hybridised with HMW-1Ax1 and HMW-1Dx5 following RNase treatment. Root tips were vibratome-sectioned without embedding while seeds were wax-embedded. In non-expressing root tips, transgene loci were detected as one or two condensed foci per chromosome in line E, while the loci in line F appeared as a large focus and a small focus respectively (Fig. 3). In the triploid endosperm at 6 dpa, three large and three small foci were seen in line F and three to six foci in line E. In expressing endosperm at 13 dpa, the loci in both lines had decondensed into many foci. Two quantify the data we measured the volume occupied by locus fluorescence in nuclei of line E and F before and well into glutenin expression. Fig. 4 shows that the average increase in locus volume from 6 dpa to 14 dpa is ca. fourfold in Line E and threefold in line F.

When measuring fluorescence, thresholds have to be set to separate signal from background. This can introduce inaccuracies into the resulting volume calculations. In line E, decondensed loci were occasionally observed in a roughly linear path (Fig. 5B). This enabled us to reduce the measurement of chromatin compaction to one dimension with no need for thresholding. 42 non-expressing loci at 6 dpa were measured giving an average length of 2.84 µm (±0.73) per locus; this figure is an average over loci, which comprised two separated foci, and nuclei in which the loci show only a single, fused site. The average over loci where the locus was a single site was 2.17µm, and where there were 2 sites the individual sites were correspondingly smaller (1.0-1.5µm). We defined loci with a length of

>10 μm at 14 to 16 dpa as linearly expanded. The average length of ten of those linear loci was 13.66 μm (±3.34). In two nuclei of nearly identical volume (2426 μm^3 and 2412 μm^3) a decondensed locus at 16 dpa had a length of 16.25 μm and was 9.3 times as long as a condensed one at 6 dpa with a length of 1.75 μm (Fig. 5). The decondensed locus spanned more than half the nucleus. For a detailed analysis of locus decondensation in relation to transcription and gene silencing, we chose line E because it contains two closely linked insertion sites, which will be referred to as the locus below to simplify discussion.

Time course of HMW subunit silencing

In a time-course RNA in situ hybridisation experiment, HMW glutenin expression in the wild-type was compared with that of line E (Fig. 6). Seeds of line E and the wild-type were wax-embedded at different developmental stages. 30 μm sections were hybridised with digoxigenin-labelled 1Ax1 antisense probes. The inclusion of a probe for 1Dx5 was not necessary since in dot blot experiments, the antisense probes for the coding regions of both 1Ax1 and 1Dx5 hybridised equally well with both plasmids (data not shown). Both line E and the wild-type started expressing glutenin mRNA at 8 dpa. The level of mRNA signal seen in line E dropped dramatically at 12 dpa while the level of transcript in the wild-type increased steadily and was still high at 20 dpa (data not shown). The same results were obtained by detecting the transcripts with Alexa Fluor® 488 instead of the alkaline phosphatase reaction. In line E, fluorescence in and around the nuclei started in a few single cells. The cytoplasmic transcript signal spread to form sectors of fluorescence without ever comprising the entire endosperm and by 12 to 14 dpa was reduced again to a few isolated cells, disappearing completely at later stages (data not shown). In contrast, nuclear transcript in line E was detected in every endosperm nucleus one or two days after the onset of expression and persisted for weeks (Fig. 7). In the wild-type the entire endosperm was expressing by 10 dpa.

Detection of small interfering RNAs as a marker for PTGS

The early disappearance of cytoplasmic RNA signal in the transgenic line in combination with continuing nuclear transcription suggested post-transcriptional gene silencing. In order to confirm this, total seed RNA was extracted at 8 dpa, the beginning of HMW glutenin expression, and at 14 dpa, after the onset of silencing in line E. The RNA was separated by electrophoresis on a poly-acrylamide/urea gel, blotted and hybridised with an antisense probe for the 1Ax1 coding region. At 14 dpa siRNAs indicative of PTGS were detected in the transgenic line (Fig. 8).

Expression–related changes in 3D gene organisation II

In order to further characterise changes in the 3D structure of the transgene loci caused by their activation during endosperm development seeds of line E were harvested at different developmental stages from 6 dpa, before the onset of glutenin expression, through to 37 dpa, just before seed maturation. The wild-type was used as a negative control. Seeds were vibratome- sectioned without

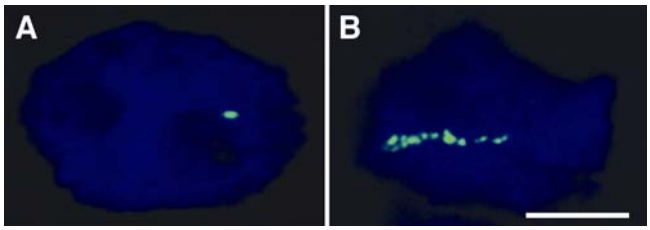

Figure 5. DNA decondensation in transcriptionally active loci
Endosperm nuclei of line E were hybridised with probes for HMW-1Ax1 and HMW-1Dx5 detecting the whole plasmids (green, A) or with probes detecting the flanking sequences and the vector (green, B) and counterstained with DAPI (blue). Overlay of several confocal sections showing only one of the three loci per nucleus. An overlay of all optical sections through the nucleus is shown for the DAPI staining in (A) and (B) to illustrate the similar sizes of the two nuclei. (A) 6 dpa, condensed locus before the start of expression. (B) 16 dpa, transcriptionally active locus in a rarely seen, linear comformation. In the straightened chromatin fibers the complex structure of the locus, which is broken up by genomic sequences, becomes visible. Section spacing 0.4 to 0.6 μm. Bar, 10 μm.

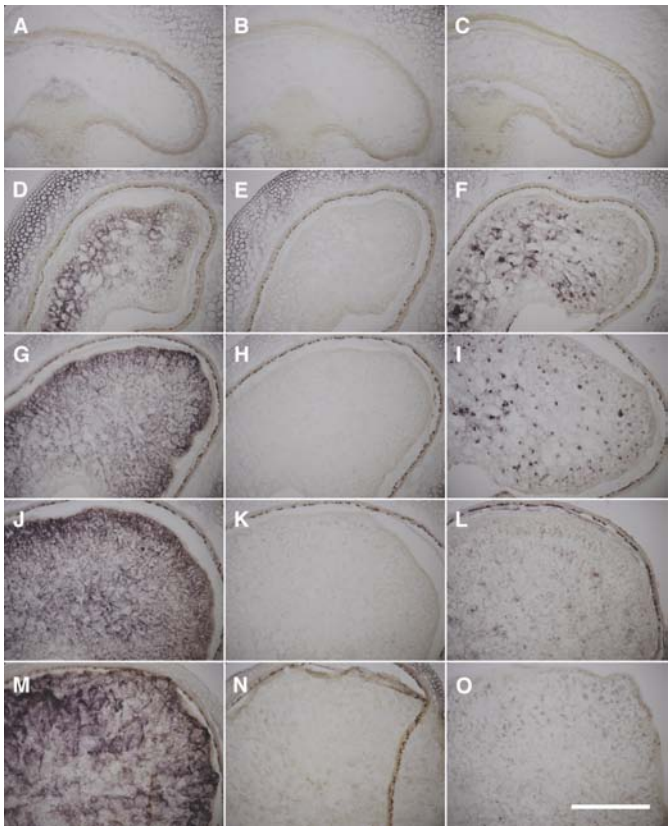

Figure 6. Time course of HMW glutenin subunit expression in endosperm
HMW glutenin transcript in seed sections of the wild-type and line E was detected with an antisense probe for the coding region of 1Ax1. The sense probe was used as control for unspecific labelling. (A-C) Before the onset of expression no RNA signal is visible in the endosperm. The pericarp and some aleurone cells show unspecific label. (D-F) Onset of expression in endosperm cells, unspecific label in the pericarp. (G-I) Strong expression in wild-type endosperm, while the RNA signal in line E is much weaker and mainly concentrated around the nuclei instead of the whole of the cytoplasm. (J-L) Very weak expression in line E in contrast to the wild-type. (M-O) The wild-type is still expressing strongly, while expression in line E has ceased. WT, wild type; bar, 0.5 mm.

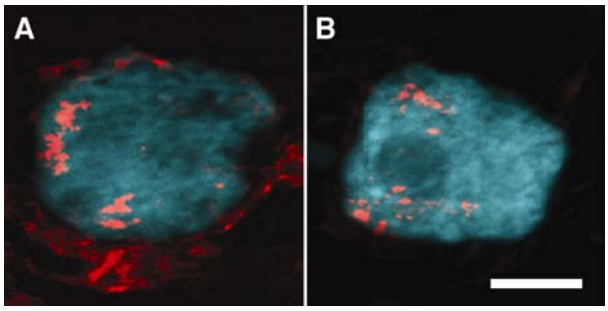

Figure 7. Disappearance of cytoplasmic HMW glutenin RNA at the onset of silencing
Sections from wax-embedded endosperm of line E were hybridised with an antisense probe for the coding region of 1Ax1 and detected with Cy3 (red). The nuclei were counter-stained with DAPI. The images comprise only the nucleus and the cytoplasm immediately around it. (A) 10 dpa. HMW glutenin RNA can be seen inside the nucleus and in the cytoplasm around it. (B) 14 dpa. RNA is still visible inside the nucleus, while it has disappeared from the cytoplasm. Bar, 10 μm.

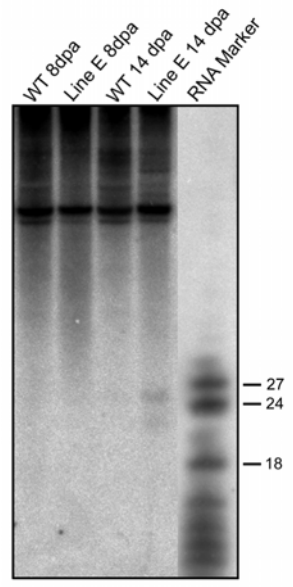

Figure 8. Detection of siRNAs corresponding to the 1Ax1 coding region
Total seed RNA of the wild-type (WT) and line E extracted before (8 dpa) and after (14 dpa) the onset of silencing was hybridised with an antisense probe for the coding region of 1Ax1. Two RNA bands of ca. 22 and 25 bp lengths, which are indicative of PTGS, are visible in line E at 14 dpa (lane 4).

embedding. For transcript detection, sections were hybridised with a biotin-labelled 2.5-Kb antisense RNA probe for the coding region of 1Ax1. After fixation and washes, a second hybridisation was carried out to detect the loci using the vector and sense and antisense RNA probes for the gene flanking sequences of both clones, but not the coding region itself in order to avoid cross-hybridisation with the transcript (illustrated in Fig. 1). Since no transcript was detected in tissue at 6 dpa and control experiments using a sense probe showed negligible labelling of the loci (data not shown) it can be concluded that the antisense probe for the transcript hybridised almost exclusively with the transcript and not with the locus.

Table 1. Locus structure and transcript detection in nuclei at the beginning of expression

Nuclei with detectable loci in endosperm sections of line E at 9 dpa were randomly selected and scored for the presence of nascent transcript.

	nuclei with	
	condensed loci	decondensing loci
no transcript	3.8% (2)	0.0% (0)
transcript	20.8% (11)	75.5% (40)

Before the onset of expression, each transgene locus was detected as one or two condensed foci (Fig. 9A). At around 7 dpa the first few nuclei in the centre of the lobes of the endosperm started showing transcript signal at the transgene loci. At 8 dpa nuclei transcribing the HMW subunits were found in all parts of the endosperm. Generally, all loci within a nucleus were expressing, but occasionally that was not the case (Fig. 9B). Expressing loci were condensed or slightly decondensed and both conformations could be found in the same nucleus. No decondensed, non-expressing loci were seen (Table 1). At 10 dpa all endosperm nuclei were transcriptionally active and the majority had decondensed loci. At subsequent time points (12, 14, 16 and 20 dpa), all nuclei had transcriptionally active, decondensed loci and increasing numbers of larger nuclei were found indicative of endoreduplication events (Fig. 9E,F). The latest time point investigated was 37 dpa. At that stage, the seeds were just about to turn from green to brown. Some nuclei were still expressing, though mostly at lower levels, and showed fully decondensed loci, while the chromatin of other nuclei was disintegrating (Fig. 9G,H). In interphase nuclei of both line E and the wild-type, the endogenous loci, which were barely visible on metaphase spreads, were rarely detected. In some experiments transcript was detected in a few small foci in the wild-type nuclei, which probably represented the endogenous loci (not shown). Co-localisation experiments using line F at 13 to 16 dpa also showed transcript on the transgene loci (data not shown).

For most parts of each locus, double labelling of the transgene DNA and the transcript showed a high degree of coincidence. However, smaller regions of gene label without any or with very faint RNA label were detected right from the beginning of HMW subunit expression (Fig. 9B-F). This suggests that most of the transgene copies at the locus are transcriptionally active. The transcriptionally inactive regions detected may comprise concatemers of flanking sequences and vector due to plasmid rearrangements or they may contain transcriptionally inactive or truncated transgene copies.

Table 2. Ploidy levels during endosperm development in line E

DNA content	7 dpa	9 dpa	16 dpa
3C	71.5% ± 3.7[a]	62.8% ± 3.5	40.3% ± 1.1
6C	26.6% ± 1.3	32.8% ± 3.8	47.9% ± 1.0
> 6C[b]	1.8% ± 2.5	4.4% ± 3.1	11.8% ± 0.7

[a] The percentages are averages over five experiments. For each experiment three isolated endosperms were pooled from 7 day old seeds and two from 9 and 16 day old ones.
[b] i.e. endoreplicated. For seeds 16 dpa this peak was always at 12C, but at 7 and 9 dpa an additional peak with a C-value between 6C and 12C appeared.

Locus decondensation at the beginning of expression is not linked to endoreduplication in endosperm nuclei

Nuclei in the developing wheat endosperm undergo one or two cycles of endoreduplication and an analysis of 97 varieties showed that the percentage of endoreplicated nuclei ranged from 3% to 32%, the most represented class being 12C, with the highest value 24C corresponding to two rounds of endoreduplication (Brunori et al., 1989). We wanted to know at what stage endoreduplication starts, what percentage of nuclei are affected and if the observed decondensation of the loci could be in part a reflection of endoreduplication. Therefore flow cytometric analyses of the DNA content of line E were carried out before and shortly after the onset of HMW subunit expression and at 16 dpa, well into glutenin expression when the tissue showed a fair number of large nuclei (Fig. 9, Table 2). The increase in DNA content at the beginning of transcription compared to two days earlier was small and could not account for the increase in foci size and number observed in so many nuclei at these early stages. By 16 dpa the balance had shifted from a majority of nuclei in G1 to a majority in G2 but still only about 12% of nuclei had completed one round of endoreduplication and none had a higher C content. In nuclei with a DNA content of 12C one would theoretically expect a maximum of eight foci per locus compared with the maximum of two foci per locus seen in nuclei in G1 (3C) before the onset of glutenin expression. The observed number of foci was, however, much higher (Fig. 9). Therefore, even at 16 dpa the increased DNA content could only partly contribute to the observed locus size.

Discussion

Transcriptional activation precedes observable locus decondensation

We have studied transcriptionally induced chromatin decondensation in two wheat lines with large, developmentally activated arrays of transgenes, which could easily be detected by FISH. The loci contain endogenous genes under the control of their own promoters, which were transferred as genomic clones containing a few Kb of flanking sequences on either side so that at least the micro-environment is a natural one if the chromosomal position and the tandem arrays are not. The fact that decondensation was observed in both lines with transgene

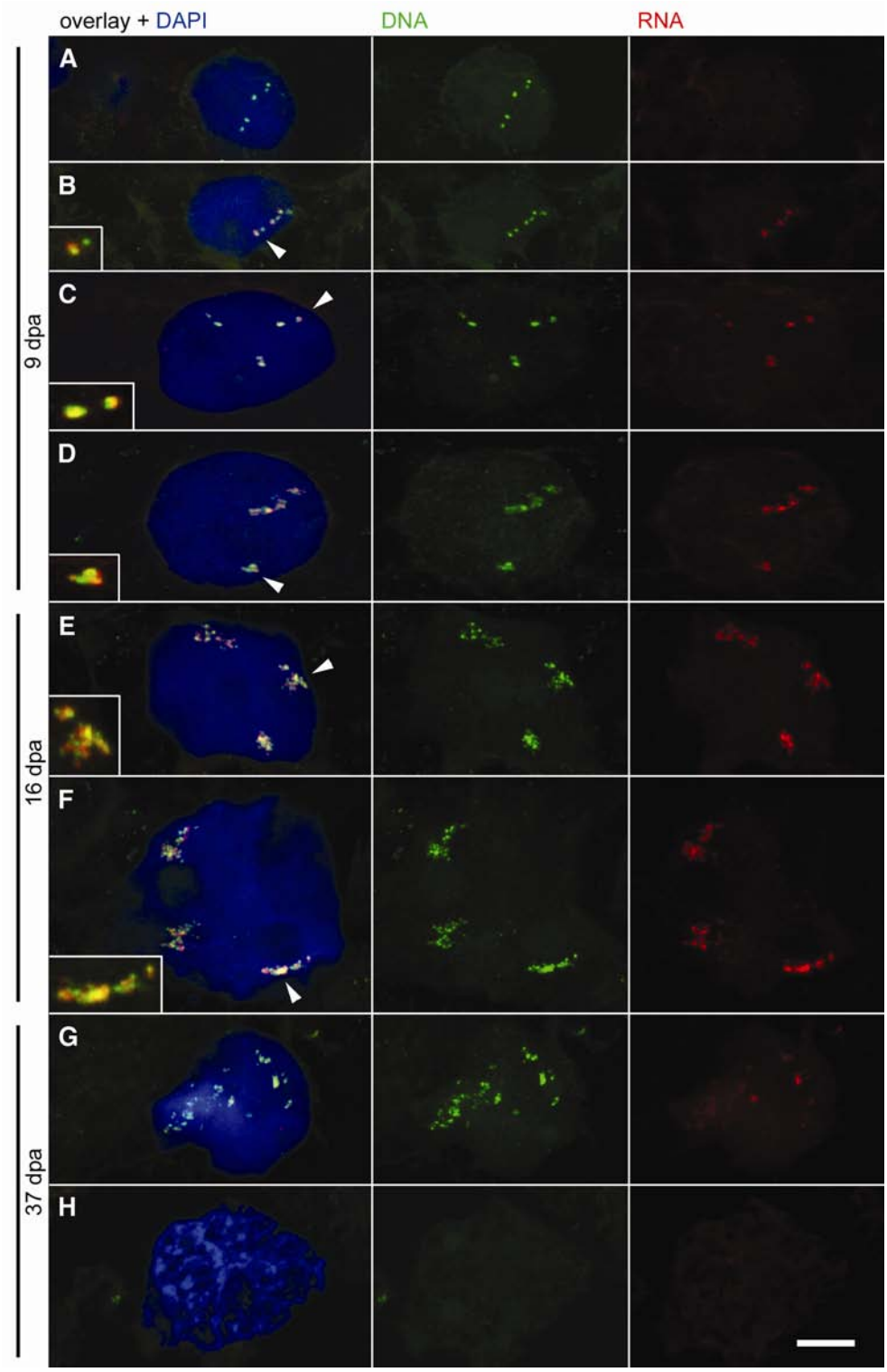
overlay + DAPI
DNA
RNA
A
B
C
D
E
F
G
H
9 dpa
16 dpa
37 dpa

insertions into different chromosomes shows that the effect is independent of the surrounding chromatin.

At the beginning of expression, 22 per cent of the transcriptionally active loci in line E were condensed and we therefore conclude that transcriptional activation can precede any significant loosening of the chromatin structure. Similar observations have recently been published for an inducible transgene array in a mammalian cell line where an increase in RNA levels preceded noticeable changes in higher order chromatin structure (Janicki et al., 2004). The endoreduplication data show that the observed chromatin decondensation upon gene activation is not caused by an increase in ploidy during endosperm development. Further evidence comes from the DNA compaction measurements where two nuclei of almost identical volume exhibit very different degrees of locus decondensation. In the example given, the condensed locus was 9 times as linearly compacted as the transcriptionally active one. Similar decondensation ratios were reported by Müller et al. (2001) where the 2 Mb long MMTV array decondensed from ca. 0.5 μm to an average of 6 μm and a maximum of 10 μm after hormonal activation. In two hormonally inducible transgene arrays the first changes in chromatin organization were visible 30 minutes or less after the addition of the activator and the chromatin was fully extended after two or four hours (Janicki et al., 2004; Tsukamoto et al., 2000). Fully decondensed loci in wheat endosperm were first detected ca. one to two days after the start of transcription.

Figure 9. Localization of transgene loci and their transcript during endosperm development
Endosperm nuclei counterstained with DAPI (blue) were hybridised with probes for the gene flanking regions and vector sequences of HMW-1Ax1 and HMW-1Dx5 to detect the locus (green) and with an antisense probe for the 1Ax1 coding region to detect the transcript (red). The insets are 2x enlargements of the loci marked by an arrowhead in the overlay. The sizes of the nuclei vary considerably due to the cell cycle phase they are in and because of endoreduplication at later stages. A and B are probably G1 nuclei, C, D, E and G G2 nuclei. F shows an endoreplicated nucleus. Each image is a projection of serial confocal sections. (A) Non-expressing nucleus in tissue starting to express. One locus is seen as one focus in the centre of the nucleus while the two loci above and below are seen as two foci each. (B) Nucleus starting to transcribe the transgene in the same tissue as in A. All three loci are seen as two foci. Only the left part of the locus denoted by the arrowhead is transcribing. (C) Nucleus in which all three loci are transcribing and condensed. The inset shows that some areas of the transgene locus are not transcriptionally active. (D) Transcriptionally active nucleus in the centre of the endosperm starting to decondense. One region in the locus in the inset shows no transcript. (E, F) Nuclei with fully decondensed loci, which are largely but not completely transcriptionally active. (G) Dying nucleus with dispersed transgene DNA and very weak RNA labelling. (H) Nucleus with degrading chromatin and no hybridisation signal for the transgenes and their transcripts. Bar, 10 μm, section spacing: 0.4 to 0.6 μm.

The analysis of wheat chromosome structure has so far been based on the observation of selectively labelled rye chromosome additions and introgressed rye chromosome arms in wheat roots and anthers, where chromosomes span the width of the nucleus in flexible, rod-like structures with the two arms of each chromosome close together and centromeres and telomeres located at opposite poles in a Rabl configuration (Abranches et al., 1998; Martínez-Pérez et al., 1999). We have made essentially the same observations in endosperm (chapter 4). The shape of the active loci in line E was highly variable (Fig. 5, Fig. 9) and the majority of the decondensed transgene loci are too big to fit into the structure predicted for wheat chromosomes based on the findings above. If the assumed chromosome shape is correct then the transgene loci must extend beyond it. Using mammalian cell cultures several groups have produced evidence for chromatin decondensation outside the chromosome territory in regions where densely packed endogenous genes are actively transcribed (Chambeyron and Bickmore, 2004; Mahy et al., 2002; Volpi et al., 2000; Williams et al., 2002). The same is happening in our highly transcribed and gene dense locus. A recent extensive mapping study estimated that only 1.2 to 2.4% of the wheat genome consists of genes and the authors showed that wheat genes are organised into gene-rich regions with a range of one gene per 78 Kb to 5500 Kb. Based on the sequence for selected wheat and barley regions the authors concluded that gene density might average at one per 10 to 20 Kb when the gene-rich regions were further partitioned (Erayman et al., 2004). The latter corresponds to the gene density in our transgene locus with 10 to 12Kb per plasmid and if the estimates of Erayman et al. are correct then visible decondensation should also occur in gene-rich regions in wheat provided the genes are transcribed at the same time in the same nucleus. Our results show that in plants, gene sequences undergo considerable decompaction upon activation. Some of the loci extended in more or less a straight line (Fig. 5). If they reflect the direction in which the chromosome spans the nucleus they are extended to at least one third of the total chromosome length. In summary, this demonstrates that transcription is maintained in very variable three-dimensional chromatin structures in which the chromatin is decondensed beyond the boundaries of the chromosome territory. A chromatin territory therefore seems to be constantly remodelled with the onset and cessation of transcriptional activity. The question remains where the chromatin loops that extend away from the chromosomal territory intermingle with other chromosome territories or are found in the interchromatin space. The latter is supported by electron microscopy studies suggesting that chromosomal territories are mostly separated into non-overlapping spaces surrounded by interchromatin space (Visser and Aten, 1999; Visser et al., 2000). This could be tested by looking for overlaps between the transgene loci and the rye chromosome arm present in Federal, which carries a 1RS (*Secale cereale*) chromosome arm substitution for the 1BS wheat chromosome arm ($1B^l/1R^s$).

Transcript localization within the nucleus

In our experiments, the main RNA signal in the nucleus was always restricted to the close vicinity of the locus. Dirks et al. (1995) looked at transgene loci and

reported RNA tracks at the site of transcription of two highly spliced viral sequences and elongated dots at the site of transcription of the luciferase gene with an artificial intron. For one of the viral sequences and the luciferase gene they also saw halo-like signal distribution around the main RNA signal radiating towards the nuclear periphery. Xing et al. (1993) found the RNA for the fibronectin gene frequently in tracks emanating from the gene while the transcript of the neurotensin gene was seen as a focus overlapping the gene. Both groups suggest that the shape of the RNA signal at the transcription site depends largely on how much the pre-mRNA is processed, i.e. on the number of introns that have to be removed. This view is supported by the fact that splicing factors (reviewed in Spector, 1996) as well as polyadenylated transcripts (Dirks et al., 1997; Xing et al., 1993) have been detected at the site of transcription. It has been shown that polyadenylation and transcription are coupled via the carboxy-terminal domain (CTD) of the large subunit of RNA polymerase II which forms a functional complex on the pre-mRNA with polyadenylation factors to catalyse endonucleolytic cleavage (for review see Hirose and Manley, 2000). HMW glutenin genes have no introns and so are likely to leave the site of transcription soon after they have been released from the RNA polymerase complex. Therefore only relatively small pools of transcript are detected around the locus (red areas in the insets of Fig. 9) while the majority of the signal co-localizes with the locus as nascent transcript.

PTGS in wheat endosperm

So far, mainly biochemical techniques have been employed to study PTGS. In this report, we have used in situ hybridization to show PTGS at the cellular level. From the start of expression until cell death HMW glutenin transcript was detected by FISH on top of the transgene locus. The fluorescence in the cytoplasm was strong at the beginning of HMW subunit expression and had disappeared almost completely in line E by 14 dpa while it remained strong in the wild-type. At the biochemical level, PTGS was confirmed by the detection of siRNAs. The siRNA lengths seen in wheat endosperm correspond to the lengths of the long (25 nt) and short (21-22 nt) siRNAs reported by Hamilton et al. (2002) for transgene silencing in *Nicotiana benthamiana*. Recently Tang et al. (2003) showed Dicer activity in wheat germ extracts, which are essentially cytoplasm, and found a similar distribution of both RNA classes to ours when double-stranded RNA was digested into double-stranded siRNA. PTGS can be caused by highly transcribed transgenes or by an inverted transgene repeat in both cases leading to the production of a double-stranded transcript, that is the substrate for Dicer and causes silencing (Béclin et al., 2002; Fagard and Vaucheret, 2000; Ketting et al., 2001). We tested the presence of an inverted repeat in line E using single PCR primers at several positions in and around the coding sequences but the results were negative (data not shown). In *Arabidopsis* sequences for four Dicer-like genes have been found, two with a nuclear targeting signal and two that are probably cytoplasmic (Finnegan et al., 2003). While we have shown that the mostly nascent transcript at the locus remains throughout the life span of the nucleus, the method employed was not sensitive

enough to detect single RNA molecules on their way through the nucleus. It is most likely that the transcript is digested by a Dicer-like enzyme in the cytoplasm as shown by Tang et al. (2003) but we cannot exclude that a proportion is cleaved in the nucleus after it has left the proximity of the locus. Hamilton et al. (2002) propose that the longer siRNAs could mediate nucleotide-specific methylation of DNA and thus transcriptional silencing. In the two generations of line E that were analysed we did not find any perceptible decrease in transcriptionally active parts of the locus. Our own unpublished data also show no changes in cytosine methylation levels in the transgenes among leaves, endosperm before and shortly after the onset of expression and after the onset of PTGS.

In summary, we have followed the onset and spread of PTGS by tracking the disappearance of cytoplasmic but not nuclear mRNA and supported our findings with the biochemical detection of small siRNAs. It is clear from our results that even after a sustained period of PTGS, there is no consequent transcriptional silencing in this system. In the future, it will be interesting to correlate the transcription-related changes in higher chromatin order seen in the transgene locus with possible changes in DNA methylation state and histone modifications (Chambeyron and Bickmore, 2004; Mathieu et al., 2003).

Acknowledgements
E. Wegel was supported by the UK Biotechnology and Biological Science Research Council (BBSRC) Gene Flow Initiative and E. Stöger was supported by the Sofia-Kovalevskaja Award of the Alexander von Humboldt Foundation. R.H.Vallejos is a member of the Research Career from CONICET, Argentina. We thank Dr. Fabian Vaistij for technical assistance with the detection of siRNAs. Dr. Nigel Halford from Rothamsted Research (Harpenden, Hertfordshire) kindly provided plasmids pHMW1Ax1 and pHMW1Dx5.

Chapter 6
GENERAL DISCUSSION

In this chapter I want to combine the results of the previous chapters and look at the general conclusions that can be drawn with respect to chromosome and nuclear structure in wheat endosperm and at questions that are still open.

Why does endosperm have extra S-phase cycles?
The biological significance of polyploidisation is poorly understood and three possible functions have been suggested (Larkins et al., 2001). A higher C-content could increase transcription and translation, which in the case of endosperm would allow higher storage protein accumulation, or it could increase cell size. A higher C-content could also provide a means of storing nucleotides for the embryo. A study of a transgenic maize line with half the level of endosperm endoreduplication of the wild-type showed little difference in starch and storage protein transcription and protein accumulation between the transgenic plant and the wild-type (Leiva-Neto et al., 2004). Cell size did not differ and the transgenic line showed only a 6.5 % reduction in average seed weight compared to the wild-type. These data imply that endoreduplicaton is not needed for an increase in cell size nor for the accumulation of sufficient storage protein. The authors therefore draw the conclusion that an increased endosperm C-content might be primarily a source of nucleotides during embryogenesis and germination. What supports this argument is the fact that in both wheat and maize endosperm nuclei start undergoing apoptosis in mid to late development (Young and Gallie, 1999; Young et al., 1997). In the case of wheat this means that the first cells die ca. 20 days before the end of glutenin transcription (Altenbach et al., 2002). However tempting this hypothesis may be, evidence for nucleotide transport (presumably through the symplast) from endosperm to embryo has yet to be found.

How much freedom of movement do wheat chromosomes have in interphase nuclei?
We know that wheat chromosomes have a Rabl configuration with telomeres at one pole and centromeres at the other. It is generally argued that the Rabl configuration is a remnant of the anaphase chromosome conformation. Newly divided nuclei are almost mirror images of each other and DAPI staining shows that in frequently dividing nuclei in young endosperm chromosome territories are visibly separated and chromosomes are aligned like sausages in a tin. Assuming that the 1RS (*Secale cereale*) chromosome arm substitution ($1B^{l}/1R^{s}$) we labelled behaves like a wheat chromosome arm we could follow the development of this initially very regular chromosome structure through two rounds of DNA synthesis without mitosis. We have shown that the majority of centromeres and telomeres in wheat endosperm nuclei reside close to the nuclear envelope (Chapter 3). More interior localisations are also frequently found which might reflect differences in chromosome length and which shows that telomeres and centromeres are only transiently or not at all anchored to the nuclear envelope. The Rabl configuration

starts to deteriorate in some 3C and 6C nuclei where diagonally or horizontally lying rye chromosome arms are visible (Table 1, Chapter 3). In 12C nuclei the chromosome arrangement becomes even more irregular and occasionally 'flipped' chromosome arms can be seen that seem to have turned over inside the nucleus (Fig. 7, Chapter 3). 12C nuclei are very flat with the chromosomes stretching along the shortest axis, which might make it easier for them to flip over. That chromosomes move parallel to the centromere/telomere axis becomes apparent during endomitosis where the daughter chromatids separate and drift apart (Chapter 4). I conclude from these observations that during endosperm development chromosomes are able to change their position in all three dimensions and as the C-content increases in nuclei that have stopped dividing chromosome arrangements become progressively distorted. However, chromosomes still retain an approximate rod shape. In contrast in *Drosophila* nuclei of the larval central nervous system, the Rabl configuration seems to break down within two hours of mitosis, as the median distance between a proximal and a distal locus on chromosome 2 ceases to fit the simulation of a randomly oriented rod at this stage (Csink and Henikoff, 1998).

Apart from wheat chromosome movement has only been analysed in human interphase nuclei. There the analysis is actually far more difficult because chromosome territories are irregularly shaped and have a radial organisation (for example Bolzer et al., 2005; Stadler et al., 2004). In cycling human cells, gene-rich chromosome 19 is located in the nuclear interior while gene-poor chromosome 18 is located at the periphery (Croft et al., 1999). This nuclear architecture is established within two to four hours at the beginning of G1 and then maintained throughout the cell cycle (Bridger et al., 2000; Croft et al., 1999). Upon cell cycle exit either through starvation or senescence chromosome 19 moves to a more internal site in the nucleus (Bridger et al., 2000). Why this happens is unknown. As far as wheat endosperm is concerned I believe that chromosome movement and the weakening of the Rabl conformation have a large accidental component. The infrequently observed misalignment of chromosomes in 3C nuclei might already have happened during telophase and subsequent formation of the nuclear envelope. Nuclear envelope enlargement and DNA synthesis during S-phase might not be perfectly co-ordinated and some chromosomes might be moved to irregular positions in the process. Later growing amyloplasts might slowly squash and flatten nuclei and in the process distort nuclear structure.

During endomitosis sister chromatids detach from each other. Whether they are actively separated or passively drift apart remains to be shown. So far no microtubules have been found inside plant interphase nuclei (Dr. Jordi Chan, personal communication). Which other proteins could facilitate chromatid movement? Animal nuclei contain a nuclear lamina, a meshwork of intermediate filaments (lamins) some of which are perinuclear while others traverse the nucleus. Lamins are linked via other proteins to the nuclear envelope, to chromatin and to the cytoskeleton (Taddei et al., 2004). As far as plants are concerned no proteins have been found yet with close sequence similarity to animal lamins but other plant coiled-coil proteins have been proposed to replace lamins in plants among

them proteins binding to matrix/scaffold attachments regions (M/SARs) (Blumenthal et al., 2004). What ever form a nuclear matrix or structural protein complex in the nucleus might have, wheat shows that as far as plants are concerned it is no rigid corset forcing chromosomes into particular positions.
In Chapter 5 we have shown that considerable chromatin movement also happens at the subchromosomal level when genes undergo decompaction upon activation. Some of the analysed active transgene loci extended in various conformations beyond the confines of their chromosome territories, which led us to conclude that a chromatin territory seems to be constantly remodelled with the onset and cessation of transcriptional activity. The molecular processes underlying chromatin movement, condensation and decondensation, i.e. gene activation and gene silencing, were discussed in Chapter 2.

Future Research

We have shown that a transgene cluster visibly decondenses when it becomes transcriptionally active. The next step is to analyse endogenous chromosomal regions in plants to prove that the same processes happen there as well. Since the resolution of a fluorescence microscope does not allow the analysis of changes in the chromatin structure of a single gene, areas of the genome will have to be used that contain several genes that are active in the same tissue. Decondensation upon coordinated gene activation has been shown in animals for the step-wise activated mouse *hox* gene cluster (Chambeyron and Bickmore, 2004). A coordinately regulated gene cluster in plants would be the ideal candidate. Comprising a number of different genes this would allow the identification of chromatin and DNA modifications occurring in the cluster before activation and after developmental shut-down. It would then also be possible to analyse whether all genes in the cluster are active in the same nucleus at the same time, which would be expected if they had similar promoter elements (Levsky et al., 2002). These experiments are under way at the moment.

REFERENCES

Abranches, R., Beven, A. F., Aragón-Alcaide, L. and Shaw, P. J. (1998). Transcription sites are not correlated with chromosome territories in wheat nuclei. *J Cell Biol* **143**, 5-12.

Abranches, R., Santos, A. P., Wegel, E., Williams, S., Castilho, A., Christou, P., Shaw, P. and Stoger, E. (2000). Widely separated multiple transgene integration sites in wheat chromosomes are brought together at interphase. *Plant J* **24**, 713-23.

Altenbach, S. B., Kothari, K. M. and Lieu, D. (2002). Environmental conditions during wheat grain development alter temporal regulation of major gluten protein genes. *Cereal Chem.* **79**, 279-285.

Alvarez, M. L., Guelman, S., Halford, N. G., Lustig, S., Reggiardo, M. I., Ryabushkina, N., Shewry, P., Stein, J. and Vallejos, R. H. (2000). Silencing of HMW glutenins in transgenic wheat expressing extra HMW subunits. *Theor. Appl. Genet.* **100**, 319-327.

Anderson, O. D., Greene, F. C., Yip, R. E., Halford, N. G., Shewry, P. R. and Malpica-Romero, J. M. (1989). Nucleotide sequences of the two high-molecular-weight glutenin genes from the D-genome of a hexaploid bread wheat, Triticum aestivum L. cv Cheyenne. *Nucleic Acids Res.* **17**, 461-2.

Aragón-Alcaide, L., Miller, T., Schwarzacher, T., Reader, S. and Moore, G. (1996). A cereal centromeric sequence. *Chromosoma* **105**, 261-8.

Bannister, A. J., Zegerman, P., Partridge, J. F., Miska, E. A., Thomas, J. O., Allshire, R. C. and Kouzarides, T. (2001). Selective recognition of methylated lysine 9 on histone H3 by the HP1 chromo domain. *Nature* **410**, 120-4.

Béclin, C., Boutet, S., Waterhouse, P. and Vaucheret, H. (2002). A branched pathway for transgene-induced RNA silencing in plants. *Curr. Biol.* **12**, 684-8.

Bednar, J., Horowitz, R. A., Grigoryev, S. A., Carruthers, L. M., Hansen, J. C., Koster, A. J. and Woodcock, C. L. (1998). Nucleosomes, linker DNA, and linker histone form a unique structural motif that directs the higher-order folding and compaction of chromatin. *Proc Natl Acad Sci U S A* **95**, 14173-8.

Belmont, A. S. and Bruce, K. (1994). Visualization of G1 chromosomes: a folded, twisted, supercoiled chromonema model of interphase chromatid structure. *J Cell Biol* **127**, 287-302.

Bennett, M. D., Rao, M. K., Smith, J. B. and Bayliss, M. W. (1973). Cell development in the anther, the ovule, and the young seed of *Triticum aestivum* L. var. Chinese Spring. *Philosophical Transactions and Proceedings of the Royal Society* **266**, 39-81.

Bernstein, E., Caudy, A. A., Hammond, S. M. and Hannon, G. J. (2001). Role for a bidentate ribonuclease in the initiation step of RNA interference. *Nature* **409**, 363-6.

Blumenthal, S. S., Clark, G. B. and Roux, S. J. (2004). Biochemical and immunological characterization of pea nuclear intermediate filament proteins. *Planta* **218**, 965-75.

Bode, J., Goetze, S., Heng, H., Krawetz, S. A. and Benham, C. (2003). From DNA structure to gene expression: mediators of nuclear compartmentalization and dynamics. *Chromosome Res* **11**, 435-45.

Boisnard-Lorig, C., Colon-Carmona, A., Bauch, M., Hodge, S., Doerner, P., Bancharel, E., Dumas, C., Haseloff, J. and Berger, F. (2001). Dynamic analyses of the expression of the HISTONE::YFP fusion protein in arabidopsis show that syncytial endosperm is divided in mitotic domains. *The Plant Cell* **13**, 495-509.

Bolzer, A., Kreth, G., Solovei, I., Koehler, D., Saracoglu, K., Fauth, C., Muller, S., Eils, R., Cremer, C., Speicher, M. R. et al. (2005). Three-dimensional maps of all chromosomes in human male fibroblast nuclei and prometaphase rosettes. *PLoS Biol* **3**, e157.

Brenchley, W. E. (1909). On the strength and development of the grain of wheat (Triticum vulgare). *Annals of Botany* **23**, 117-142.

Bridger, J. M., Boyle, S., Kill, I. R. and Bickmore, W. A. (2000). Re-modelling of nuclear architecture in quiescent and senescent human fibroblasts. *Curr Biol* **10**, 149-52.

Brown, R. C., Lemmon, B. E. and Nguyen, H. (2003). Events during the first four rounds of mitosis establish three developmental domains in the syncytial endosperm of Arabidopsis thaliana. *Protoplasma* **222**, 167-74.

Brunori, A., Forino, L. M. C. and Frediani, M. (1989). Polyploid DNA contents in the starchy endosperm nuclei and seed weight in *Triticum aestivum*. *J Genetics and Breeding* **43**, 131-134.

Chambeyron, S. and Bickmore, W. A. (2004). Chromatin decondensation and nuclear reorganization of the HoxB locus upon induction of transcription. *Genes Dev* **18**, 1119-30.

Christensen, A. H. and Quail, P. H. (1996). Ubiquitin promoter-based vectors for high-level expression of selectable and/or screenable marker genes in monocotyledonous plants. *Transgenic Res.* **5**, 213-218.

Chua, Y. L., Watson, L. A. and Gray, J. C. (2003). The transcriptional enhancer of the pea plastocyanin gene associates with the nuclear matrix and regulates gene expression through histone acetylation. *Plant Cell* **15**, 1468-79.

Cmarko, D., Verschure, P. J., Martin, T. E., Dahmus, M. E., Krause, S., Fu, X. D., van Driel, R. and Fakan, S. (1999). Ultrastructural analysis of transcription and splicing in the cell nucleus after bromo-UTP microinjection. *Mol Biol Cell* **10**, 211-23.

Coen, E. S., Romero, J. M., Doyle, S., Elliott, R., Murphy, G. and Carpenter, R. (1990). floricaula: a homeotic gene required for flower development in antirrhinum majus. *Cell* **63**, 1311-22.

Cook, P. R. (1999). The organization of replication and transcription. *Science* **284**, 1790-5.

Cox, A. V., Bennett, S. T., Parokonny, A. S., Kenton, A., Callimassia, M. A. and Bennett, M. D. (1993). Comparison of Plant Telomere Locations Using a PCR-Generated Synthetic Probe. *Ann Bot* **72**, 239-247.

Craig, J. M. (2005). Heterochromatin--many flavours, common themes. *Bioessays* **27**, 17-28.

Cremer, T. and Cremer, C. (2001). Chromosome territories, nuclear architecture and gene regulation in mammalian cells. *Nat Rev Genet* **2**, 292-301.

Cremer, T., Cremer, C., Schneider, T., Baumann, H., Hens, L. and Kirsch-Volders, M. (1982). Analysis of chromosome positions in the interphase nucleus of Chinese hamster cells by laser-UV-microirradiation experiments. *Hum Genet* **62**, 201-9.

Cremer, T., Lichter, P., Borden, J., Ward, D. C. and Manuelidis, L. (1988). Detection of chromosome aberrations in metaphase and interphase tumor cells by in situ hybridization using chromosome-specific library probes. *Hum Genet* **80**, 235-46.

Croft, J. A., Bridger, J. M., Boyle, S., Perry, P., Teague, P. and Bickmore, W. A. (1999). Differences in the localization and morphology of chromosomes in the human nucleus. *J Cell Biol* **145**, 1119-31.

Csink, A. K. and Henikoff, S. (1998). Large-scale chromosomal movements during interphase progression in Drosophila. *J Cell Biol* **143**, 13-22.

Curtis, B. C. (2002). Wheat in the world. In *Bead wheat improvement and production*, (eds B. C. Curtis S. Rajaram and H. Gómez Macpherson). Rome: Food and Agriculture Organization of the United Nations.

Custódio, N., Carmo-Fonseca, M., Geraghty, F., Pereira, H. S., Grosveld, F. and Antoniou, M. (1999). Inefficient processing impairs release of RNA from the site of transcription. *EMBO J.* **18**, 2855-66.

D'Amato, F. (1984). Role of polyploidy in reproductive organs and tissues. In *Embryology of Angiosperms*, (ed. B. M. Johri), pp. 519-566. New York: Springer-Verlag.

Daneholt, B., Andersson, K., Bjorkroth, B. and Lamb, M. M. (1982). Visualization of active 75 S RNA genes in the Balbiani rings of Chironomus tentans. *Eur J Cell Biol* **26**, 325-32.

Danzer, J. R. and Wallrath, L. L. (2004). Mechanisms of HP1-mediated gene silencing in Drosophila. *Development* **131**, 3571-80.

de Laat, W. and Grosveld, F. (2003). Spatial organization of gene expression: the active chromatin hub. *Chromosome Res* **11**, 447-59.

De Lucia, F., Ni, J. Q., Vaillant, C. and Sun, F. L. (2005). HP1 modulates the transcription of cell-cycle regulators in Drosophila melanogaster. *Nucleic Acids Res* **33**, 2852-8.

Dernburg, A. F., Broman, K. W., Fung, J. C., Marshall, W. F., Philips, J., Agard, D. A. and Sedat, J. W. (1996). Perturbation of nuclear architecture by long-distance chromosome interactions. *Cell* **85**, 745-59.

Dirks, R. W., Daniël, K. C. and Raap, A. K. (1995). RNAs radiate from gene to cytoplasm as revealed by fluorescence in situ hybridization. *J. Cell Sci.* **108 (Pt 7)**, 2565-72.

Dirks, R. W., de Pauw, E. S. and Raap, A. K. (1997). Splicing factors associate with nuclear HCMV-IE transcripts after transcriptional activation of the gene, but dissociate upon transcription inhibition: evidence for a dynamic organization of splicing factors. *J. Cell Sci.* **110 (Pt 4)**, 515-22.

Dong, F. and Jiang, J. (1998). Non-Rabl patterns of centromere and telomere distribution in the interphase nuclei of plant cells. *Chromosome Res* **6**, 551-8.

Dorigo, B., Schalch, T., Kulangara, A., Duda, S., Schroeder, R. R. and Richmond, T. J. (2004). Nucleosome arrays reveal the two-start organization of the chromatin fiber. *Science* **306**, 1571-3.

Elgin, S. C. and Grewal, S. I. (2003). Heterochromatin: silence is golden. *Curr Biol* **13**, R895-8.

Erayman, M., Sandhu, D., Sidhu, D., Dilbirligi, M., Baenziger, P. S. and Gill, K. S. (2004). Demarcating the gene-rich regions of the wheat genome. *Nucleic Acids Res.* **32**, 3546-65.

Fagard, M. and Vaucheret, H. (2000). (TRANS)GENE SILENCING IN PLANTS: How Many Mechanisms? *Annu. Rev. Plant Physiol. Plant Mol. Biol.* **51**, 167-194.

Finnegan, E. J., Margis, R. and Waterhouse, P. M. (2003). Posttranscriptional gene silencing is not compromised in the Arabidopsis CARPEL FACTORY (DICER-LIKE1) mutant, a homolog of dicer-1 from Drosophila. *Curr. Biol.* **13**, 236-240.

Finnegan, E. J. and Matzke, M. A. (2003). The small RNA world. *J. Cell Sci.* **116**, 4689-93.

Fischle, W., Wang, Y. and Allis, C. D. (2003). Histone and chromatin cross-talk. *Curr Opin Cell Biol* **15**, 172-83.

Fisher, A. G. and Merkenschlager, M. (2002). Gene silencing, cell fate and nuclear organisation. *Curr Opin Genet Dev* **12**, 193-7.

Flavell, R. B., Rimpau, J. and Smith, D. B. (1977). Repeated sequence DNA relationships in four cereal genomes. *Chromosoma* **63**, 205-222.

Francastel, C., Walters, M. C., Groudine, M. and Martin, D. I. (1999). A functional enhancer suppresses silencing of a transgene and prevents its localization close to centrometric heterochromatin. *Cell* **99**, 259-69.

Francis, N. J., Kingston, R. E. and Woodcock, C. L. (2004). Chromatin compaction by a polycomb group protein complex. *Science* **306**, 1574-7.

Fransz, P., De Jong, J. H., Lysak, M., Castiglione, M. R. and Schubert, I. (2002). Interphase chromosomes in Arabidopsis are organized as well defined chromocenters from which euchromatin loops emanate. *Proc Natl Acad Sci U S A* **99**, 14584-9.

Garcia, D., Fitz Gerald, J. N. and Berger, F. (2005). Maternal control of integument cell elongation and zygotic control of endosperm growth are coordinated to determine seed size in arabidopsis. *The Plant Cell* **17**, 52-60.

Gaudin, V., Libault, M., Pouteau, S., Juul, T., Zhao, G., Lefebvre, D. and Grandjean, O. (2001). Mutations in LIKE HETEROCHROMATIN PROTEIN 1 affect flowering time and plant architecture in Arabidopsis. *Development* **128**, 4847-58.

Geitler, L. (1939). Die Entstehung der polyploiden Somakerne der Heteropteren durch Chromosomenteilung ohne Kernteilung. *Chromosoma* **1**, 1-22.

Gilbert, N., Boyle, S., Fiegler, H., Woodfine, K., Carter, N. P. and Bickmore, W. A. (2004). Chromatin architecture of the human genome: gene-rich domains are enriched in open chromatin fibers. *Cell* **118**, 555-66.

Gill, B. S. and Friebe, B. (2002). Cytogenetics, phylogeny and evolution of cultivated wheats. In *Bead wheat improvement and production*, (eds B. C. Curtis S. Rajaram and H. Gómez Macpherson). Rome: Food and Agriculture Organization of the United Nations.

González-Melendi, P., Wells, B., Beven, A. F. and Shaw, P. J. (2001). Single ribosomal transcription units are linear, compacted Christmas trees in plant nucleoli. *Plant J* **27**, 223-33.

Goodrich, J. and Tweedie, S. (2002). Remembrance of things past: chromatin remodeling in plant development. *Annu Rev Cell Dev Biol* **18**, 707-46.

Grafi, G. and Larkins, B. A. (1995). Endoreduplication in Maize Endosperm - Involvement of M-Phase- Promoting Factor Inhibition and Induction of S-Phase-Related Kinases. *Science* **269**, 1262-1264.

Grewal, S. I. and Moazed, D. (2003). Heterochromatin and epigenetic control of gene expression. *Science* **301**, 798-802.

Gribnau, J., Diderich, K., Pruzina, S., Calzolari, R. and Fraser, P. (2000). Intergenic transcription and developmental remodeling of chromatin subdomains in the human beta-globin locus. *Mol Cell* **5**, 377-86.

Halford, N. G., Field, J. M., Blair, H., Urwin, P., Moore, K., Robert, L., Thompson, R., Flavell, R. B., Tatham, A. S. and Shewry, P. R. (1992). Analysis of HMW glutenin subunits encoded by chromosome1a of bread wheat (Triticum aestivum L) indicates quantitative effects on grain quality. *Theor. Appl. Genet.* **83**, 373-378.

Halford, N. G., Forde, J., Shewry, P. R. and Kreis, M. (1989). Functional analysis of the upstream regions of a silent and an expressed member of a family of wheat seed protein genes in transgenic tobacco. *Plant Sci.* **62**, 207-216.

Hamilton, A., Voinnet, O., Chappell, L. and Baulcombe, D. (2002). Two classes of short interfering RNA in RNA silencing. *EMBO J.* **21**, 4671-9.

Hamilton, A. J. and Baulcombe, D. C. (1999). A species of small antisense RNA in posttranscriptional gene silencing in plants. *Science* **286**, 950-2.

Heitz, E. (1928). Das Heterochromatin der Moose. In *Jahrb. Wiss. Botanik*, vol. 69, pp. 762-818.

Heng, H. H., Goetze, S., Ye, C. J., Liu, G., Stevens, J. B., Bremer, S. W., Wykes, S. M., Bode, J. and Krawetz, S. A. (2004). Chromatin loops are selectively anchored using scaffold/matrix-attachment regions. *J Cell Sci* **117**, 999-1008.

Heslop-Harrison, J. S. (2000). Comparative genome organization in plants: from sequence and markers to chromatin and chromosomes. *Plant Cell* **12**, 617-36.

Highett, M. I., Beven, A. F. and Shaw, P. J. (1993). Localization of 5S genes and transcripts in Pisum sativum nuclei. *J. Cell Sci.* **105**, 1151-1158.

Hirose, Y. and Manley, J. L. (2000). RNA polymerase II and the integration of nuclear events. *Genes Dev.* **14**, 1415-29.

Hochstrasser, M., Mathog, D., Gruenbaum, Y., Saumweber, H. and Sedat, J. W. (1986). Spatial organization of chromosomes in the salivary gland nuclei of *Drosophila melanogaster*. *J Cell Biol* **102**, 112-23.

Horn, P. J. and Peterson, C. L. (2002). Molecular biology. Chromatin higher order folding - wrapping up transcription. *Science* **297**, 1824-7.

Huber, A. G. and Grabe, D. F. (1987a). Endosperm morphogenesis in wheat: transfer of nutrients from the antipodals to the lower endosperm. *Crop Science* **27**, 1248-1252.

Huber, A. G. and Grabe, D. F. (1987b). Endosperm morphogenesis in wheat: termination of nuclear division. *Crop Science* **27**, 1252-1256.

Ingham, P. W., Howard, K. R. and Ishhorowicz, D. (1985). Transcription Pattern of the Drosophila Segmentation Gene Hairy. *Nature* **318**, 439-445.

Italiano, J. E., Jr. and Shivdasani, R. A. (2003). Megakaryocytes and beyond: the birth of platelets. *J Thromb Haemost* **1**, 1174-82.

Jackson, D. P. (1991). *In situ* hybridization in plants. In *Molecular Plant Pathology: A practical Approach*, vol. 1 (eds S. J. Gurr M. J. McPherson and D. J. Bowles), pp. 163-174. Oxford: Oxford University Press.

Janicki, S. M., Tsukamoto, T., Salghetti, S. E., Tansey, W. P., Sachidanandam, R., Prasanth, K. V., Ried, T., Shav-Tal, Y., Bertrand, E., Singer, R. H. et al. (2004). From silencing to gene expression: real-time analysis in single cells. *Cell* **116**, 683-98.

Jenuwein, T. and Allis, C. D. (2001). Translating the histone code. *Science* **293**, 1074-80.

Jin, Q. W., Fuchs, J. and Loidl, J. (2000). Centromere clustering is a major determinant of yeast interphase nuclear organization. *J Cell Sci* **113 (Pt 11)**, 1903-12.

Kato, Y. and Sasaki, H. (2005). Imprinting and looping: epigenetic marks control interactions between regulatory elements. *Bioessays* **27**, 1-4.

Ketting, R. F., Fischer, S. E., Bernstein, E., Sijen, T., Hannon, G. J. and Plasterk, R. H. (2001). Dicer functions in RNA interference and in synthesis of small RNA involved in developmental timing in C. elegans. *Genes Dev.* **15**, 2654-9.

Kim, J. H., Durrett, T. P., Last, R. L. and Jander, G. (2004). Characterization of the Arabidopsis TU8 glucosinolate mutation, an allele of TERMINAL FLOWER2. *Plant Mol Biol* **54**, 671-82.

Kotake, T., Takada, S., Nakahigashi, K., Ohto, M. and Goto, K. (2003). Arabidopsis TERMINAL FLOWER 2 gene encodes a heterochromatin protein 1 homolog and represses both FLOWERING LOCUS T to regulate flowering time and several floral homeotic genes. *Plant Cell Physiol* **44**, 555-64.

Kowles, R. V. and Phillips, R. L. (1988). Endosperm development in maize. *International Review of Cytology* **112**, 97-136.

Larkins, B. A., Dilkes, B. P., Dante, R. A., Coelho, C. M., Woo, Y. M. and Liu, Y. (2001). Investigating the hows and whys of DNA endoreduplication. *J Exp Bot* **52**, 183-92.

Leiva-Neto, J. T., Grafi, G., Sabelli, P. A., Dante, R. A., Woo, Y. M., Maddock, S., Gordon-Kamm, W. J. and Larkins, B. A. (2004). A dominant negative mutant of cyclin-

dependent kinase A reduces endoreduplication but not cell size or gene expression in maize endosperm. *Plant Cell* **16**, 1854-69.

Lemon, B. and Tjian, R. (2000). Orchestrated response: a symphony of transcription factors for gene control. *Genes Dev* **14**, 2551-69.

Levsky, J. M., Shenoy, S. M., Pezo, R. C. and Singer, R. H. (2002). Single-cell gene expression profiling. *Science* **297**, 836-40.

Li, Y., Danzer, J. R., Alvarez, P., Belmont, A. S. and Wallrath, L. L. (2003). Effects of tethering HP1 to euchromatic regions of the Drosophila genome. *Development* **130**, 1817-24.

Li, Y. J., Fu, X. H., Liu, D. P. and Liang, C. C. (2004). Opening the chromatin for transcription. *Int J Biochem Cell Biol* **36**, 1411-23.

Lindroth, A. M., Shultis, D., Jasencakova, Z., Fuchs, J., Johnson, L., Schubert, D., Patnaik, D., Pradhan, S., Goodrich, J., Schubert, I. et al. (2004). Dual histone H3 methylation marks at lysines 9 and 27 required for interaction with CHROMOMETHYLASE3. *Embo J* **23**, 4286-96.

Lysak, M. A., Pecinka, A. and Schubert, I. (2003). Recent progress in chromosome painting of Arabidopsis and related species. *Chromosome Res* **11**, 195-204.

Mahy, N. L., Perry, P. E. and Bickmore, W. A. (2002). Gene density and transcription influence the localization of chromatin outside of chromosome territories detectable by FISH. *J. Cell Biol.* **159**, 753-63.

Mares, D. J., Norstog, K. and Stone, B. A. (1975). Early stages in the development of wheat endosperm. I The change from free nuclear to cellular endosperm. *Australian Journal of Botany* **23**, 311-326.

Martínez-Pérez, E., Shaw, P. and Moore, G. (2001). The Ph1 locus is needed to ensure specific somatic and meiotic centromere association. *Nature* **411**, 204-7.

Martínez-Pérez, E., Shaw, P., Reader, S., Aragón-Alcaide, L., Miller, T. and Moore, G. (1999). Homologous chromosome pairing in wheat. *J. Cell Sci.* **112 (Pt 11)**, 1761-9.

Martínez-Pérez, E., Shaw, P. J. and Moore, G. (2000). Polyploidy induces centromere association. *J Cell Biol* **148**, 233-8.

Mathieu, O., Jasencakova, Z., Vaillant, I., Gendrel, A. V., Colot, V., Schubert, I. and Tourmente, S. (2003). Changes in 5S rDNA chromatin organization and transcription during heterochromatin establishment in Arabidopsis. *Plant Cell* **15**, 2929-39.

Matzke, M., Aufsatz, W., Kanno, T., Daxinger, L., Papp, I., Mette, M. F. and Matzke, A. J. (2004). Genetic analysis of RNA-mediated transcriptional gene silencing. *Biochim Biophys Acta* **1677**, 129-41.

Matzke, M., Matzke, A. J. and Kooter, J. M. (2001). RNA: guiding gene silencing. *Science* **293**, 1080-3.

Matzke, M. A. and Birchler, J. A. (2005). RNAi-mediated pathways in the nucleus. *Nat Rev Genet* **6**, 24-35.

Müller, W. G., Rieder, D., Kreth, G., Cremer, C., Trajanoski, Z. and McNally, J. G. (2004). Generic features of tertiary chromatin structure as detected in natural chromosomes. *Mol Cell Biol* **24**, 9359-70.

Müller, W. G., Walker, D., Hager, G. L. and McNally, J. G. (2001). Large-scale chromatin decondensation and recondensation regulated by transcription from a natural promoter. *J. Cell Biol.* **154**, 33-48.

Oksala, T. and Therman, E. (1977). Endomitosis in tapetal cells of *Eremurus* (Liliaceae). *American Journal of Botany* **64**, 866-872.

Olsen, O. A. (2004). Nuclear endosperm development in cereals and Arabidopsis thaliana. *The Plant Cell* **16 Suppl**, S214-27.

Olsen, O. A., Potter, R. H. and Kalla, R. (1992). Histo-differentiation and molecular biology of developing cereal endosperm. *Seed Science Research* **2**, 117-131.

Osborne, C. S., Chakalova, L., Brown, K. E., Carter, D., Horton, A., Debrand, E., Goyenechea, B., Mitchell, J. A., Lopes, S., Reik, W. et al. (2004). Active genes dynamically colocalize to shared sites of ongoing transcription. *Nat Genet* **36**, 1065-71.

Percival, J. (1921). The wheat plant. London, UK: Duckworth and Co.

Plant, K. E., Routledge, S. J. and Proudfoot, N. J. (2001). Intergenic transcription in the human beta-globin gene cluster. *Mol Cell Biol* **21**, 6507-14.

Probst, A. V., Fransz, P. F., Paszkowski, J. and Scheid, O. M. (2003). Two means of transcriptional reactivation within heterochromatin. *Plant J.* **33**, 743-9.

Ragoczy, T., Telling, A., Sawado, T., Groudine, M. and Kosak, S. T. (2003). A genetic analysis of chromosome territory looping: diverse roles for distal regulatory elements. *Chromosome Res* **11**, 513-25.

Randolph, L. F. (1936). Developmental morphology of the caryopsis in maize. *Journal of Agricultural Research* **53**, 881-916.

Sadoni, N. and Zink, D. (2004). Nascent RNA synthesis in the context of chromatin architecture. *Chromosome Res* **12**, 439-51.

Schramke, V. and Allshire, R. (2003). Hairpin RNAs and retrotransposon LTRs effect RNAi and chromatin-based gene silencing. *Science* **301**, 1069-74.

Shewry, P. R., Halford, N. G., Tatham, A. S., Popineau, Y., Lafiandra, D. and Belton, P. S. (2003). The high molecular weight subunits of wheat glutenin and their role in determining wheat processing properties. *Adv. Food Nutr. Res.* **45**, 219-302.

Spector, D. L. (1996). Nuclear organization and gene expression. *Exp. Cell Res.* **229**, 189-197.

Springhetti, E. M., Istomina, N. E., Whisstock, J. C., Nikitina, T., Woodcock, C. L. and Grigoryev, S. A. (2003). Role of the M-loop and reactive center loop domains in the folding and bridging of nucleosome arrays by MENT. *J Biol Chem* **278**, 43384-93.

Stadler, S., Schnapp, V., Mayer, R., Stein, S., Cremer, C., Bonifer, C., Cremer, T. and Dietzel, S. (2004). The architecture of chicken chromosome territories changes during differentiation. *BMC Cell Biol* **5**, 44.

Su, R. C., Brown, K. E., Saaber, S., Fisher, A. G., Merkenschlager, M. and Smale, S. T. (2004). Dynamic assembly of silent chromatin during thymocyte maturation. *Nat Genet* **36**, 502-6.

Szentirmay, M. N. and Sawadogo, M. (2000). Spatial organization of RNA polymerase II transcription in the nucleus. *Nucleic Acids Res* **28**, 2019-25.

Taddei, A., Hediger, F., Neumann, F. R. and Gasser, S. M. (2004). The function of nuclear architecture: a genetic approach. *Annu Rev Genet* **38**, 305-45.

Tang, G., Reinhart, B. J., Bartel, D. P. and Zamore, P. D. (2003). A biochemical framework for RNA silencing in plants. *Genes Dev.* **17**, 49-63.

Tsukamoto, T., Hashiguchi, N., Janicki, S. M., Tumbar, T., Belmont, A. S. and Spector, D. L. (2000). Visualization of gene activity in living cells. *Nat. Cell Biol.* **2**, 871-8.

Tumbar, T., Sudlow, G. and Belmont, A. S. (1999). Large-scale chromatin unfolding and remodeling induced by VP16 acidic activation domain. *J. Cell Biol.* **145**, 1341-54.

van Driel, R. and Fransz, P. (2004). Nuclear architecture and genome functioning in plants and animals: what can we learn from both? *Exp Cell Res* **296**, 86-90.

van Lammeren, A. A. M. (1988). Structure and function of the microtubular cytoskeleton during endosperm development in wheat: an immunofluorescence study. *Protoplasma* **146**, 18-27.

Verschure, P. J., van der Kraan, I., de Leeuw, W., van der Vlag, J., Carpenter, A. E., Belmont, A. S. and van Driel, R. (2005). In vivo HP1 targeting causes large-scale chromatin condensation and enhanced histone lysine methylation. *Mol Cell Biol* **25**, 4552-64.

Visser, A. E. and Aten, J. A. (1999). Chromosomes as well as chromosomal subdomains constitute distinct units in interphase nuclei. *J. Cell Sci.* **112 (Pt 19)**, 3353-60.

Visser, A. E., Jaunin, F., Fakan, S. and Aten, J. A. (2000). High resolution analysis of interphase chromosome domains. *J. Cell Sci.* **113 (Pt 14)**, 2585-93.

Volpi, E. V., Chevret, E., Jones, T., Vatcheva, R., Williamson, J., Beck, S., Campbell, R. D., Goldsworthy, M., Powis, S. H., Ragoussis, J. et al. (2000). Large-scale chromatin organization of the major histocompatibility complex and other regions of human chromosome 6 and its response to interferon in interphase nuclei. *J. Cell Sci.* **113 (Pt 9)**, 1565-76.

Watson, J. D. and Crick, F. H. C. (1953). The structure of DNA. *Cold Spring Harbor Symposium on Quantum Biology* **18**, 123-131.

Wegel, E. and Shaw, P. (2005). Chromosome organisation in wheat endosperm and embryo. *Cytogenet. Genome Res.* **109**, 175-180.

Wegel, E., Vallejos, R. H., Christou, P., Stoger, E. and Shaw, P. (2005). Large-scale chromatin decondensation induced in a developmentally activated transgene locus. *J Cell Sci* **118**, 1021-31.

Weiler, K. S. and Wakimoto, B. T. (1995). Heterochromatin and gene expression in Drosophila. *Annu Rev Genet* **29**, 577-605.

Williams, R. R., Broad, S., Sheer, D. and Ragoussis, J. (2002). Subchromosomal positioning of the epidermal differentiation complex (EDC) in keratinocyte and lymphoblast interphase nuclei. *Exp. Cell Res.* **272**, 163-75.

Woodcock, C. L. and Dimitrov, S. (2001). Higher-order structure of chromatin and chromosomes. *Curr Opin Genet Dev* **11**, 130-5.

Wu, R., Terry, A. V., Singh, P. B. and Gilbert, D. M. (2005). Differential subnuclear localization and replication timing of histone H3 lysine 9 methylation states. *Mol Biol Cell* **16**, 2872-81.

Xing, Y., Johnson, C. V., Dobner, P. R. and Lawrence, J. B. (1993). Higher level organization of individual gene transcription and RNA splicing. *Science* **259**, 1326-30.

Young, T. E. and Gallie, D. R. (1999). Analysis of programmed cell death in wheat endosperm reveals differences in endosperm development between cereals. *Plant Mol Biol* **39**, 915-26.

Young, T. E., Gallie, D. R. and DeMason, D. A. (1997). Ethylene-Mediated Programmed Cell Death during Maize Endosperm Development of Wild-Type and shrunken2 Genotypes. *Plant Physiol* **115**, 737-751.

Zamore, P. D., Tuschl, T., Sharp, P. A. and Bartel, D. P. (2000). RNAi: double-stranded RNA directs the ATP-dependent cleavage of mRNA at 21 to 23 nucleotide intervals. *Cell* **101**, 25-33.

SUMMARY

This thesis is an investigation into the structure of wheat endosperm nuclei starting with nuclear divisions and migration during syncytium formation followed by the development of nuclear shape and positioning of chromosome territories and ending with changes in subchromosomal structure during the activation of a transgene locus.

At the level of the whole endosperm we have developed a method for modelling in 3D the formation of the syncytium that characterises early endosperm development. After the initial nuclear division of the first endosperm nucleus three groups of nuclei form in the original central cell: a stem-like group of nuclei close to the zygote and connected to a single layer of nuclei in the dorsal periphery and another, unconnected single layer in the ventral periphery. By two days post anthesis (dpa) both the ventral and dorsal groups of nuclei have developed into plates of nuclei. The dorsal plate then merges with the ventral plate through synchronous nuclear divisions. By 4 dpa the entire periphery of the central cell is surrounded by a layer of nuclei and the syncytium is complete.

Wheat endosperm is initially triploid and during its development a percentage of the nuclei increase their DNA-content to 6C and 12C. 3D modelling of nuclei with DNA contents of 3C, 6C and 12C allowed us to visualise progressive changes in nuclear shape and chromosome positioning. With increasing C content, nuclear volumes increase predominantly in two directions, thereby changing the shape of the nuclei into a disc-like structure. Wheat chromosomes in interphase nuclei have a typical Rabl configuration with centromeres and telomeres arranged at opposite poles. The majority of centromeres and telomeres are found at or close to the nuclear membrane, some also in the middle of the nucleus and in rare instances a telomere can be observed at the centromere pole and vice versa. This means that centromeres and telomeres are not or only transiently anchored to the nuclear membrane. Both centromeres and telomeres show a degree of non-homologous associations, which for centromeres remains constant through increases in ploidy, while telomere associations increase with higher C-values.

The wheat line we used has a 1RS / 1BS (*Secale cereale*) chromosome arm substitution. Fluorescence in situ hybridisation detection of the rye arm substitution with total genomic DNA as probe revealed the following: during endosperm development chromosomes are able to change their position in all three dimensions and as the C-content increases in nuclei that have stopped dividing chromosome arrangements become progressively distorted. The vast majority of 12 C nuclei show six rye chromosome arms, but a few show three groups of associated rye chromosome arms. This means that during endosperm development wheat nuclei increase their ploidy through both polyploidisation and polytenisation.

The final part analyses the chromatin structure of active and inactive gene loci. The High Molecular Weight (HMW) glutenin genes in wheat are developmentally activated in the endosperm at about 8 dpa. I have investigated the physical changes that occur in these genes in two transgenic lines containing about 20 and 50 copies respectively of the HMW glutenin genes together with their promoters. Fluorescence *in situ* hybridisation (FISH) and confocal imaging data show that in non-expressing tissue each transgene locus consists of one or two highly condensed sites that decondense into many foci upon activation of transcription in endosperm nuclei. Initiation of transcription can precede decondensation but not vice versa. In one of the lines, cytoplasmic transcript levels are high after onset of transcription, but disappear by 14 dpa, while siRNAs, indicative of post-transcriptional gene silencing (PTGS), are detected at this stage. However, the transcript levels remain high at the transcription sites, the great majority of the transgene copies are transcriptionally active and transcriptional activity in the nucleus ceases only with cell death at the end of endosperm development.

SAMENVATTING

Dit proefschrift beschrijft een onderzoek naar de structuur van endospermkernen van tarwe, beginnend bij kerndelingen en kernmigratie tijdens de vorming van het syncytium, gevolgd door de ontwikkeling van de kernvorm en positionering van de chromosoomgebieden, en eindigend met veranderingen in de subchromosomale structuur gedurende de activering van een transgeen locus.

Allereerst wordt een methode beschreven die de vorming van het syncytium, dat de vroege endospermontwikkeling karakteriseert, in drie dimensies modelleert. Na de initiële kerndeling van de eerste endospermkern vormen zich drie groepen kernen in de oorspronkelijke centrale cel: a stamachtige groep kernen dicht bij de zygote en verbonden met een enkele laag kernen in de dorsale periferie en een andere, vrijliggende enkele laag in de ventrale periferie. Omstreeks 2 dagen na anthese (het opengaan van de bloem, dpa) hebben de ventrale en dorsale groep kernen zich ontwikkeld in kernplaten. De dorsale plaat verenigt zich met de ventrale plaat via een aantal synchroon verlopende kerndelingen. Omstreeks 4 dpa is de hele periferie van de centrale cel omgeven door een laag kernen en is het syncytium compleet.

Aanvankelijk is het endosperm van tarwe triploïd. Gedurende de ontwikkeling neemt het DNA gehalte van een deel van de kernen toe tot 6 – 12 C. Ruimtelijke modellen van kernen met 3C, 6C en 12C DNA maakten het mogelijk om de progressieve veranderingen in kernvorm en chromosoompositionering zichtbaar te maken. Bij kernen met hogere C waarden, vergroten de kernvolumina zich in twee richtingen, waarbij tegelijkertijd de kern de vorm van een schijf aanneemt. Tarwechromosomen in interfasekernen hebben een typische Rabl configuratie met centromeren en telomeren gerangschikt naar tegenoverelkaar liggen polen. De meerderheid van de centromeren en telomeren liggen tegen of vlak bij de kernmembraan, maar soms liggen ze in het midden van de kern, en zelden wordt een telomeer in de centromeerpool waargenomen en omgekeerd. Dit betekent dat centromeren en telomeren niet of slechts tijdelijk aan het kernmembraan zijn verankerd. Zowel centromeren als telomeren vertonen enige mate van non-homologe associaties, die in het geval van de centromeren gelijk blijft bij toenemende ploïdie, terwijl telomeerassociaties bij hogere C waarden juist toenemen.

De tarwelijn die voor het onderzoek gebruikt is, heeft een 1RS / 1BS (van rogge, *Secale cereale*) chromosoomarmsubstitutie. Detectie van de roggearm door middel van fluorescente *in situ* hybridisatie met totaal-genomisch rogge DNA als probe toonde aan dat tijdens endospermontwikkeling de chromosomen in staat zijn hun positie in drie richtingen te kunnen veranderen. Bij de toename van het C gehalte blijken in de kernen die niet verder delen, de chromosoomposities in toenemende mate verstoord te raken. De zes losse rogge chromosoomarmen blijven in het overgrote deel van de 12C kernen ongeassocieerd; in een minderheid van de

kernen echter zien we drie groepen van geassocieerde chromosoomarmen, hetgeen wijst op zowel polyploïsatie als polytenie.

In het laatste deel van het proefschrift wordt de analyse van de chromatinestruktuur van actieve en inactieve loci beschreven aan de hand van de hoogmoleculaire (HMW) glutenine-genen in tarwe die in de ontwikkeling van het endosperm ongeveer 8 dpa worden aangeschakeld. Het onderzoek richtte zich op de fysische veranderingen in het plaatselijke chromatine van deze genen in twee transgene lijnen die ongeveer 20 en 50 kopieën van het HMW glutenine-gen en hun promotor bezitten. Beelden verkregen door middel van Fluorescente *in situ* Hybridisatie en confocale microscopie toonden aan dat in weefsel waarin gluteninegenen niet tot expressie komen, elk trangeen locus bestaat uit een of twee sterk gecondenseerde gebieden, die na activering van de transcriptie decondenseren in een groot aantal kleine chromatinestrukturen.

Initiatie van de transcriptie kan aan de decondensatie voorafgaan, maar dit gebeurt niet in de omgekeerde volgorde. In een van de lijnen zijn na aanschakeling van de transcriptie de niveaus van de transcriptie in het cytoplasma direct hoog, maar verdwijnt omstreeks 14 dpa, wanneer siRNAs, die indicatief zijn posttranscriptionele gene silencing (PTGS) kunnen worden aangetoond. De transcriptieniveaus blijven echter hoog op de plaats van transcriptie. Bovendien is het grote deel van de transgene kopieën transcriptioneel actief en neemt de transcriptionele activiteit in de kern alleen af met de celdood aan einde van de endospermontwikkeling.

ACKNOWLEDGEMENTS

I thank Prof. Peter Shaw for taking me on in a postdoc position when I did not have a PhD. He might have had his doubts in the beginning and I have to say that I was scared of failing to rise to the challenge. I have learned a lot and enjoyed our scientific discussions and am grateful for the support, his ideas and the space I have been given to develop my own. I am grateful to the Shaw lab and especially Ali Pendle and Dr. Sinéad Drea for having been such good colleagues. Grant Calder has been a great help with the (extremely capricious) confocal microscope and with image analysis. Thanks go to Dr. Eva Stöger for initiating the project. I am indebted to Dr. Hans de Jong for becoming my co-supervisor out of the goodness of his heart and his willingness to support me and the time and effort he has put into guiding me through this thesis. I also thank Prof. Maarten Koornneef for agreeing to become my promoter and Wageningen University (or should that be the Dutch educational system?) for allowing me to do an external doctorate there. I thank Dr. Tobias Knoch for planting the idea in my head that I could do a PhD by publication. I am grateful to Dr. Ajay Kohli for suggesting Hans de Jong and for his friendship and help over the years. I am grateful to my parents for the way they brought me up and for their love and continued interest in what I do. Last not least I thank Kevin, my husband, for his patience, reassurance and practical help at home and for building us a wonderful house while I was doing this.

CURRICULUM VITAE

Eva Wegel was born on 13 October 1965 in Bergisch Gladbach, Germany. She completed her secondary school education at the Otto-Hahn-Gymnasium in Bergisch Gladbach in 1985. She studied chemistry for one semester at the Universität Köln and then switched to biology at the Philipps-Universität Marburg in 1986 where she gained a degree (Diplom) in 1992. Her first attempt at a PhD on arbuscular mycorrhiza in parsley at the Max-Planck Institut für Züchtungsforschung in Cologne had to be abandoned after three years. She then moved to Norwich, England, completed two part-time horticultural courses at a local college, worked on a paper on arbuscular mycorrhiza in *Lotus japonicus* with Dr. Martin Parniske at the Sainsbury Laboratory and painted murals on commission with a professional painter abroad and on her own in Norwich. In 1998 she got a position at the John Innes Centre in Norwich as research assistant in the molecular biotechnology unit under Dr. Eva Stöger in the group of Dr. Paul Christou where she started working on the characterisation of transgenic wheat lines by fluorescence *in situ* hybridisation (FISH). In 2001 after two promotions she began the project that is described in this thesis, as the equivalent of a postdoc in the group of Prof. Peter Shaw. In 2002 she got in contact with Dr. Hans de Jong and Prof. Maarten Koornneef at Wageningen University who agreed to supervise her for an external PhD. The contract with Prof. Shaw finished in January 2005 and she started a new (postdoc) position with Dr. Anne Osbourn at the Sainsbury Laboratory in Norwich extending her previous analysis of activity related changes in three-dimensional gene structure to an endogenous gene cluster. The Osbourn group has now moved to the Metabolic Biology Department at the John Innes Centre.